

Investigation of SECISBP2 mutations and potential viral SECIS element recruitment

Inaugural-Dissertation
zur Erlangung des Doktorgrades
der Hohen Medizinischen Fakultät
der Rheinischen Friedrich-Wilhelms-Universität
Bonn

Henrik Johannes Schmidt
aus Münster
2021

Angefertigt mit der Genehmigung
der Medizinischen Fakultät der Universität Bonn

1. Gutachter : Prof. Dr. Ulrich Schweizer

2. Gutachter : Prof. Dr. Martin Schlee

Tag der Mündlichen Prüfung: 30.06.2021

Aus dem Institut für Biochemie und Molekularbiologie
Direktor: Prof. Dr. Thomas Becker

Table of contents

| | |
|--|-----------|
| List of abbreviations | 8 |
| 1. Introduction | 12 |
| 1.1 The role of selenium for life..... | 12 |
| 1.2 Selenoproteins in humans..... | 13 |
| 1.2.1 Glutathione-peroxidases (GPX)..... | 13 |
| 1.2.2 Thyroid Hormone Deiodinases..... | 14 |
| 1.2.3 Thioredoxinreductases..... | 15 |
| 1.2.4 Methionine-R-Sulfoxide Reductase 1 (MSRB1)..... | 16 |
| 1.2.5 Selenophosphate Synthetase 2 (SEPHS2)..... | 16 |
| 1.2.6 Selenoproteins H, T, V and W (SELENOH, SELENOT, SELENOV, SELENOW)..... | 16 |
| 1.2.7 Selenoprotein I (SELENOI)..... | 17 |
| 1.2.8 Selenoproteins F and M (SELENOF, SELENOM)..... | 17 |
| 1.2.9 Selenoproteins K and S (SELENOK, SELENOS)..... | 18 |
| 1.2.10 Selenoprotein O (SELENOO)..... | 18 |
| 1.2.11 Selenoprotein N (SELENON)..... | 18 |
| 1.2.12 Selenoprotein P (SELENOP)..... | 19 |
| 1.3 Eukaryotic mechanism of selenocysteine incorporation into proteins..... | 19 |
| 1.3.1 Selenocysteine insertion sequence (SECIS) elements..... | 20 |
| 1.3.2 SECIS binding protein 2 (SECISBP2)..... | 21 |
| 1.3.3 Sec-specific eukaryotic elongation factor (eEFSec)..... | 22 |
| 1.3.4 Ribosomal protein L30 (RPL30)..... | 23 |
| 1.3.5 Nucleolin..... | 23 |
| 1.3.6 Eukaryotic translation initiation factor 4a3 (eIF4a3)..... | 23 |
| 1.4. Hierarchy of selenoproteins..... | 24 |
| 1.5 Mutations in SECISBP2..... | 24 |
| 1.5.1 The R540Q mutation..... | 24 |
| 1.5.2 The C691R mutation..... | 26 |
| 1.6 Selenoproteins in viruses..... | 27 |
| 1.7 In-vitro assay to measure Sec-incorporation..... | 29 |

| | |
|--|-----------|
| 1.8 Aims of the thesis..... | 30 |
| 1.8.1 Effects of SECISBP2 mutations in regard to different SECIS elements..... | 30 |
| 1.8.2 Viral SECIS element recruitment..... | 31 |
| 1.9. Experimental outlines..... | 31 |
| 1.9.1 Investigation of SECISBP2 mutations..... | 31 |
| 1.9.2 Investigation of potential viral SECIS element recruitment..... | 32 |
| 2. Materials and Methods..... | 33 |
| 2.1 Supplementary list..... | 33 |
| 2.1.1 Technical equipment..... | 33 |
| 2.1.2 Chemicals..... | 35 |
| 2.1.3 Primers used in different experiments..... | 36 |
| 2.2 Cloning and amplification of recombinant DNA plasmids..... | 40 |
| 2.2.1 Cloning and amplification of pTrcHis2 with <i>CSecisbp2</i> inserts..... | 40 |
| 2.2.1.1 Site-directed mutagenesis..... | 41 |
| 2.2.1.2 Transformation of plasmids into <i>E.coli</i> DH5 α bacteria..... | 41 |
| 2.2.1.3 Plasmid isolation through alkaline lysis (Mini-Prep and Midi-Prep)..... | 42 |
| 2.2.2 Cloning and amplification of pcDNA3.1_Luciferase with SECIS element inserts... | 43 |
| 2.2.2.1 RNA extraction from mouse liver..... | 44 |
| 2.2.2.2 cDNA synthesis..... | 45 |
| 2.2.2.3 Genomic DNA extraction from mouse liver..... | 45 |
| 2.2.2.4 PCR amplification of <i>Gpx1</i> -, <i>Gpx4</i> -, <i>Txnrd1</i> -, <i>Dio1</i> SECIS elements from mouse cDNA and <i>Dio2</i> SECIS element from mouse genomic DNA..... | 45 |
| 2.2.2.5 Preparation of <i>Dio3</i> SECIS element from primer sequences..... | 46 |
| 2.2.2.6 Restriction digest of <i>Gpx1</i> , <i>Gpx4</i> , <i>Txnrd1</i> , <i>Dio1</i> and <i>Dio2</i> SECIS element fragments, gel electrophoresis and gel-extraction..... | 47 |
| 2.2.2.7 Dephosphorylation of the digested pcDNA3.1_Luc_1 vector and ligation of the vector with the SECIS element inserts..... | 47 |
| 2.2.2.8 Transformation of the ligated plasmids into <i>E.coli</i> DH5 α | 48 |
| 2.2.2.9 Plasmid isolation of transformed bacteria..... | 48 |
| 2.2.3 Cloning and amplification of pcDNA3.1_Luc_1 with viral inserts..... | 48 |
| 2.2.3.1 Preparation of Ebola_1976 and Ebola_2014 sequences..... | 49 |

| | |
|--|-----------|
| 2.2.3.2 Preparation of the HIV sequence..... | 49 |
| 2.2.3.3 Plasmid DNA isolation from transformed bacteria..... | 50 |
| 2.2.4 Acquisition of human Txnrd1 and Txnrd3 full length sequences..... | 51 |
| 2.3 Expression and purification of recombinant CSECISBP2 ^{WT} , CSECISBP2 ^{RQ} and CSECISBP2 ^{CR} from bacterial culture..... | 54 |
| 2.3.1 Expression of recombinant CSECISBP2 in E.coli BL21 star..... | 55 |
| 2.3.2 Ni-NTA-affinity-chromatography of recombinant CSECISBP2..... | 55 |
| 2.3.3 SDS-PAGE and Coomassie Staining..... | 56 |
| 2.3.4 Western-Blot analysis..... | 58 |
| 2.3.5 Concentration and quantification of purified CSECISBP2..... | 60 |
| 2.4 <i>In-vitro</i> transcription from plasmid DNA..... | 61 |
| 2.4.1 Plasmid linearisation..... | 61 |
| 2.4.2 Phenol-chloroform extraction of digested plasmids..... | 61 |
| 2.4.3 <i>In-vitro</i> transcription reaction..... | 62 |
| 2.4.4 Phenol-chloroform extraction of mRNA..... | 62 |
| 2.5 Luciferase assay comparing mouse SECIS elements using different SECISBP2 proteins..... | 63 |
| 2.6 Luciferase assay comparing CSECISBP2 ^{WT} and CSECISBP2 ^{RQ} by titrating luciferase reporter mRNA..... | 65 |
| 2.7 Luciferase assay comparing the temperature stability of CSECISBP2 ^{WT} and CSECISBP2 ^{RQ} | 66 |
| 2.8 Luciferase assays investigating potential viral SECIS element recruitment..... | 67 |
| 2.9 Agarose gel-shift assay with luciferase mRNAs with viral inserts and full length Txnrd1 and Txnrd3 mRNAs..... | 69 |
| 3. Results..... | 72 |
| 3.1 Results of protein purification..... | 72 |
| 3.1.1 Results for purification of CSECISBP2 ^{RQ} | 72 |
| 3.1.2 Results for purification of CSECISBP2 ^{CR} | 74 |
| 3.1.3 Results for purification of CSECISBP2 ^{WT} | 75 |
| 3.2 Results from luciferase assay comparing CSECISBP2 ^{WT} , CSECISBP2 ^{RQ} and CSECISBP2 ^{CR} in regard to different SECIS elements..... | 77 |

| | |
|--|------------|
| 3.3 Results from luciferase assays comparing CSECISBP2 ^{WT} and CSECISBP2 ^{RQ} by titration of mRNA reporters..... | 81 |
| 3.4 Results from luciferase assays comparing thermostability of CSECISBP2 ^{WT} and CSECISBP2 ^{RQ} | 84 |
| 3.5 Results of luciferase assay investigating possible viral SECIS recruitment..... | 85 |
| 3.6 Results of agarose gel-shift assays with luciferase reporters with viral inserts and Txnrd1 and Txnrd3 mRNAs..... | 86 |
| 4. Discussion..... | 89 |
| 4.1 Purification and quantification of heterologously expressed CSECISBP2..... | 89 |
| 4.2 Luciferase assay comparing effects of CSECISBP2 mutations in regard to different SECIS elements..... | 90 |
| 4.2.1 CSECISBP2 ^{CR} does not support Sec-incorporation..... | 90 |
| 4.2.2 CSECISBP2 ^{RQ} does not show any significant differences in Sec-incorporation activity compared to CSECISBP2 ^{WT} | 91 |
| 4.2.3 Significant readthrough of the UGA codon occurs even without CSECISBP2 and with a mutated SECIS element..... | 93 |
| 4.3 Titration experiments investigating CSECISBP2 kinetics independent of protein concentration..... | 93 |
| 4.4 Increased temperature impairs protein stability of CSECISBP2 ^{RQ} | 94 |
| 4.5 Conclusions to analysis of mutant SECISBP2..... | 98 |
| 4.5.1 SECISBP2 ^{CR} shows decreased function in Sec-incorporation and might also be unstable..... | 98 |
| 4.5.2 SECISBP2 ^{RQ} shows almost no impairment in Sec-incorporation but reduced protein stability possibly depending on the tissue..... | 99 |
| 4.6 Viral SECIS element recruitment cannot be shown in <i>in-vitro</i> assay despite compelling supporting evidence..... | 100 |
| 4.6.1 Data that supports the hypothesis of viral selenoproteins..... | 100 |
| 4.6.2 <i>In-vitro</i> assay fails to show Sec-incorporation by means of “hijacked” SECIS element..... | 103 |
| 5. Summary..... | 105 |
| 6. List of figures..... | 106 |

| | |
|---------------------------------|------------|
| 7. List of tables..... | 108 |
| 8. References..... | 110 |
| 9. Acknowledgements..... | 122 |

List of abbreviations

| | |
|-----------------|--|
| 3' UTR | 3' untranslated region |
| AA | amino acid |
| Amp | ampicillin |
| APS | ammonium persulfate |
| ATI | antisense-tethering-interaction |
| bp | basepair |
| cDNA | complementary DNA |
| CSECISBP2 | C-terminal part of SECIS binding protein 2 |
| Cys | cysteine |
| dATP | deoxyadenosine triphosphate |
| dCTP | deoxycytosine triphosphate |
| dGTP | deoxyguanosine triphosphate |
| Dio1 | deiodinase 1 |
| Dio2 | deiodinase 2 |
| Dio3 | deiodinase 3 |
| DNA | deoxyribonucleic acid |
| dNTPs | deoxynucleoside triphosphates |
| DTT | dithiothreitol |
| dTTP | deoxythymidine triphosphate |
| EDTA | ethylenediaminetetraacetic acid |
| eEFSec | Sec-specific eukaryotic elongation factor |
| eIF4a3 | eukaryotic translation initiation factor 4a3 |
| EMSA | electrophoretic-mobility-shift-assay |
| env | envelope |
| ER | endoplasmic reticulum |
| ERAD | ER associated degradation |
| EtOH | ethanol |
| fT ₃ | free T ₃ |
| fT ₄ | free T ₄ |

| | |
|-------------------|---|
| Fw/fw | forward |
| gDNA | genomic DNA |
| gp120 | glycoprotein 120 |
| Gpx | glutathione peroxidase |
| Grx | glutaredoxin |
| His-tag | histidine-tag |
| IPTG | Isopropyl- β -D-thiogalactopyranosid |
| IVT | <i>in-vitro</i> translation |
| kb | kilobasepair |
| kDa | kilo dalton |
| LAR | luciferase assay reagent |
| Mn-SOD | Mn-dependent superoxide dismutase |
| MSRB1 | methionine-R-sulfoxide reductase 1 |
| NADPH | nicotinamide adenine dinucleotide phosphate |
| NES | nuclear export signal |
| Ni-NTA | nickel-nitroltriacetic acid |
| NLS | nuclear localisation sequence |
| NMD | nonsense-mediated-decay |
| OD ₆₀₀ | optical density at 600 nm wavelength |
| PA | polyacrylamide |
| PBS | phosphate buffered saline |
| PCR | polymerase chain reaction |
| RBD | RNA-binding domain |
| rEMSA | RNA-electrophoretic-mobility-shift-assay |
| RiboSeq | ribosomal profiling |
| RNA | ribonucleic acid |
| ROS | reactive oxygen species |
| RPL30 | ribosomal protein L30 |
| rpm | rounds per minute |
| RRL | rabbit reticulocyte lysate |
| RT | room temperature |
| rT ₃ | reverse-triiodothyronine |

| | |
|------------------------|---|
| Rv/rv | reverse |
| Sbp2 | SECIS binding protein 2 |
| SD | standard deviation |
| SDS | sodium dodecyl sulfate |
| SDS-PAGE | sodium dodecyl sulfate polyacrylamide gel electrophoresis |
| Se | selenium |
| Sec | selenocysteine |
| SECIS | selenocysteine insertion sequence |
| SECISBP2 | SECIS binding protein 2 |
| SECISBP2 ^{CR} | SECISBP2 protein that has a mutation which represents the SECISBP2 p.Cys691Arg mutation in humans |
| SECISBP2 ^{RQ} | SECISBP2 protein that has a mutation which represents the SECISBP2 p.Arg540Gln mutation in humans |
| SELENOF | selenoprotein F |
| SELENOH | selenoprotein H |
| SELENOI | selenoprotein I |
| SELENOK | selenoprotein K |
| SELENOM | selenoprotein M |
| SELENON | selenoprotein N |
| SELENOP | selenoprotein P |
| SELENOS | selenoprotein S |
| SELENOT | selenoprotein T |
| SELENOV | selenoprotein V |
| SELENOW | selenoprotein W |
| SEPHS2 | selenophosphate synthetase 2 |
| SERCA2 | sarcoplasmic/endoplasmic reticulum calcium ATPase 2 |
| SID | Sec-incorporation domain |

| | |
|----------------|------------------------------------|
| T ₂ | diiodothyronine |
| T ₃ | triiodothyronine |
| T ₄ | thyroxine |
| TBST | tris buffered saline with Tween 20 |
| TEMED | tetramethylethylenediamin |
| TRIS | tris(hydroxymethyl)aminomethane |
| tRNA | transfer RNA |
| Trx | thioredoxin |
| Trx1 | cytosolic thioredoxin |
| Trx2 | mitochondrial thioredoxin |
| TSH | thyroid stimulating hormone |
| TXNRD | thioredoxinreductase |
| TXNRD1 | thioredoxinreductase 1 |
| TXNRD3 | thioredoxinreductase 3 |

1. Introduction

Throughout this thesis the new nomenclature of selenoproteins is used (Gladyshev et al., 2016)

1.1 The role of selenium for life

The element selenium (Se) was discovered in 1817 by Jacob Berzelius, a Swedish chemist. In 1934 it was reported that the so called alkali disease and blind staggers disease are caused by the uptake of Se-accumulating plants by livestock (Franke, 1934). The fact that Se can also be essential for life was found later when Pinsent (1954) found that Se is required for the synthesis of formate dehydrogenase in *E.coli*. In 1957 Se became first known as an essential trace element in mammals when Schwartz and Foltz (1957) reported that it protects against necrotic liver degeneration in rats. Moreover, certain diseases like Keshan's disease (a cardiomyopathy found in China) were later associated with Se deficiency (Yang, 1988).

The first characterisation of Selenocysteine (Sec) as the active compound of Se in bacterial proteins known to be dependent on Se-presence happened in 1976 (Cone et al., 1976). Finally, Sec became known as the 21st proteinogenic amino acid when it was shown that it was attached to its tRNA in both mammals (Lee et al., 1989) and bacteria (Leinfelder et al., 1989).

Specifically into protein inserted Sec is the most important factor of Se in all three domains of life (eukaryotes, bacteria, archaea). Se which is posttranslationally inserted as a dissociable cofactor in some molybdoproteins, selenomethionine and unspecifically inserted Sec (misincorporation of Se instead of sulphur) are less important (Hatfield and Gladyshev, 2002). However, there are also forms of life that do not express selenoproteins such as fungi, some insect species and higher land plants (Lobanov et al. 2008).

1.2 Selenoproteins in humans

Until now twentyfive selenoproteins are known in humans (Kryukov et al., 2003). Sec is probably only incorporated into proteins when it is essential for their function unlike the other twenty proteinogenic amino acids. This leads to the fact that Sec is often an important functional group within the protein (Gladyshev, 2016). Concerning the selenoproteins that have so far been characterised the Sec residue is always involved in redox-active functions (Labunskyy et al., 2014).

1.2.1 Glutathione-peroxidases (GPX)

Of the eight different GPX enzymes in humans five are selenoproteins, namely the GPX 1, 2, 3, 4 and 6 while the other three contain a cysteine (Cys) residue in their active site (Labunskyy et al., 2014). In the following only the selenoproteins are discussed in more detail.

Except for GPX4 which is a monomeric enzyme, GPX1, 2, 3 and possibly also GPX6 form tetramers (Labunskyy et al., 2014). The main functions of GPX enzymes are the detoxification of hydroperoxides and thereby influencing the H₂O₂ signalling as well as keeping up the cellular redox homeostasis.

GPX1 is the most abundant GPX and is expressed in all human cell types as a cytosolic enzyme which catalyses the glutathione-dependent reduction of H₂O₂ to water (Lubos et al., 2011). The expression of GPX1 is highly regulated by Se availability (Baker et al., 1993; Sunde et al., 2009). GPX1 knockout mice are viable but do show an increased susceptibility to oxidative stress (Cheng et al., 1998; Fu et al., 1999).

GPX2 is most notably expressed in gastrointestinal epithelium, whereas the GPX3 is primarily expressed in the kidneys and secreted into the blood (Labunskyy et al., 2014)

The mRNA of GPX6 can only be found in olfactory epithelium and in embryos (Kryukov et al., 2003).

GPX4 is expressed in many cell types and tissues. GPX4 has a broader substrate specificity, probably due to the fact that it is a monomeric enzyme. Its major function in most cell types is the reduction of membrane bound hydroperoxy-lipids (Schnurr et al.,

1996). In testis GPX4 is initially catalytically active in spermatids but is later inactivated in order to become a part of a polymer with structural function (Maiorino et al., 2005; Ursini et al., 1999). Due to the fact that knockout of GPX4 in mice was shown to lead to embryonic lethality, the function of GPX4 in reducing hydroperoxy-lipids was hypothesised to be essential during embryonic development (Imai et al., 2003; Yant et al., 2003).

GPX4 is a key player in the mechanism of ferroptosis. Both the depletion of the GPX4-substrate glutathione and direct inhibition of GPX4 leads to ferroptosis (Cao and Dixon, 2016).

1.2.2 Thyroid Hormone Deiodinases

The three types of deiodinases (DIO) known in mammals, DIO1, 2, and 3, are all selenoproteins. They all function in the reductive deiodination of thyroid hormone but differ in their subcellular localisation, tissue expression and the definite site of deiodination (inner or outer ring).

DIO1 is localised on the cell membrane and is both able to catalyse the activation of thyroxine (T_4) to triiodothyronine (T_3) by outer ring deiodination as well as the inactivation of T_4 - and T_3 -conjugates by inner ring deiodination. DIO1 is the deiodinase that primarily processes sulphated iodothyronines and does in part influence the circulating plasma levels of T_3 (Gereben et al., 2008, figure 1).

DIO2 is localised on the endoplasmic-reticulum(ER)-membrane and is also able to catalyse the activation of T_4 to T_3 or the degradation of reverse T_3 (rT3) to diiodothyronine (3,3'- T_2) by outer ring deiodination (figure 1). Together with DIO1 the DIO2 primarily regulates the circulating levels of plasma T_3 in humans (Gereben et al., 2008; Saberi et al., 1975).

DIO3 is localised on the cell membrane and catalyses the inactivation of T_4 to rT₃ and T_3 to T_2 by inner ring deiodination (figure 1).

Both DIO2 and DIO3 are able to locally increase or decrease, respectively, cellular levels of T_3 without changing the overall plasma level of T_3 (Dentice et al., 2013).

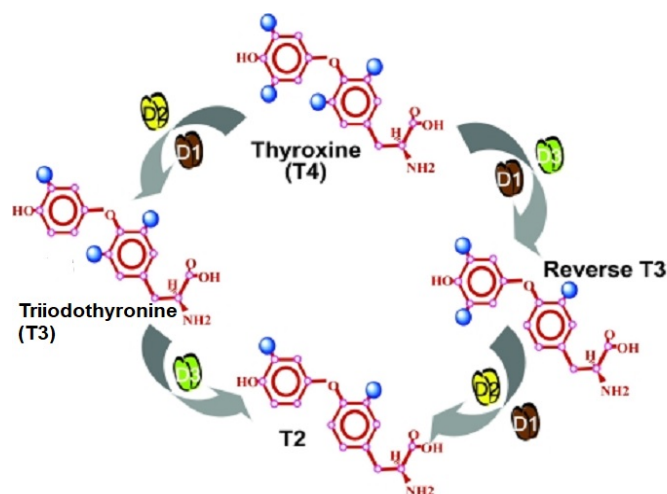


Fig. 1: Scheme showing the metabolism of iodothyronines as catalysed by deiodinases. D1, D2 and D3 represent the deiodinases 1, 2 and 3. Blue dots represent iodine-atoms, modified after Gereben et al, (2008).

1.2.3 Thioredoxinreductases

Similar to the deiodinases three thioredoxinreductases (TXNRD) are known in humans, all of which are selenoproteins. All three are oxidoreductases that are important for the disulfide reduction system of the cell (Labunskyy et al., 2014).

TXNRD1 is localised in both the cytosol and nucleus. It primarily reduces cytosolic thioredoxin (Trx1), but it can also reduce some other low-molecular-weight compounds (Arner and Holmgren, 2000). The major function of TXNRD1 lies in the Nicotinamide adenine dinucleotide phosphate (NADPH)-dependent reduction of Trx1. Trx1 is in turn an important electron donor within the cell for example for the ribonucleotide reductase and other proteins (Arner and Holmgren, 2000). Furthermore, together with Trx1, TXNRD1 is involved in the regulation of cell signaling but its complete function therein is not entirely understood (Labunskyy et al., 2014; Saitoh et al, 1998). It may play a part in cancer development (Labunskyy et al., 2014).

TXNRD2 is localised within mitochondria and acts there as a reductase of mitochondrial thioredoxin (Trx2) and glutaredoxin 2 (Grx2) (Labunskyy et al., 2014). Knockout of either *Txnrd1* or *Txnrd2* in mice leads to embryonic lethality (Bondareva et al., 2007; Conrad et al., 2004).

TXNRD3 differs from the other two TXNRDs in that it has an additional glutaredoxin domain (Sun et al., 2001) suggesting that it is involved in the reduction of both Trx and glutathion disulfide (GSSG). The physiological role of TXNRD3 is so far not known (Labunskyy et al., 2014) but it was found to be highly expressed in testes after puberty. TXNRD3 is able to catalyse the formation of disulfide bonds within and between proteins. Therefore, TXNRD3 was hypothesised to be involved in the formation of structural proteins in spermatids via the formation or isomerisation of disulfide bonds (Su et al., 2005).

1.2.4 Methionine-R-Sulfoxide Reductase 1 (MSRB1)

MSRB1 is a non-essential selenoprotein in mice since *Msrb1* knockout mice are viable (Fomenko et al., 2009). It reduces oxidised methionine-R-sulfoxides back to methionine in proteins. MSRB1 plays a central role in the formation of filamentous actin by reducing methionine-R-sulfoxide residues that have prior been oxidised by Mical proteins. Furthermore, bone-marrow-derived macrophages from *Msrb1* knockout mice show impairments in actin-polymerisation dependent processes and the release of proinflammatory cytokines (Lee et al., 2013).

1.2.5 Selenophosphate Synthetase 2 (SEPHS2)

SEPHS2 catalyses the production of monoselenophosphate from selenide in an ATP dependent manner (Xu et al., 2007a). It is essential for the synthesis of selenocysteine (Xu et al., 2007b). Due to the fact that SEPHS2 is a selenoprotein in vertebrates, it was suggested that it serves an autoregulatory purpose (Guimarães et al., 1996).

1.2.6 Selenoproteins H, T, V and W (SELENOH, SELENOT, SELENOV, SELENOW)

SELENOH, SELENOT, SELENOV and SELENOW all belong to the Rdx family of selenoproteins and are characterised by a thioredoxin-like fold and a conserved CXXU motif (Dikiy et al., 2007). This suggests a function in redox-activities (Dikiy et al., 2007).

Knockout of *Selenow* in mice using transcription activator-like effector nucleases led to an embryonic lethality of 92.8 %. However, it cannot be concluded that this lethality is all caused by the knockout of *Selenow* since the knockout procedure itself may contribute to the lethality (Sung et al., 2013).

Knockout of *Selenot* in mice causes embryonic lethality. Furthermore, SELENOT plays an important role in protecting dopaminergic neurons from oxidative stress and therefore, seems to be associated with Parkinson's disease (Boukhzar et al., 2016). SELENOT was identified as a subunit of the oligosaccharyltransferase complex and is important for both hormone synthesis and ER homeostasis (Hamieh et al., 2017).

Knockout of *Selenov* in mice affected the expression of *Gpx1*, *Txnrd1* and *Selenop* as well as Se concentrations (Chen et al., 2020).

Studies of *selenoh* mutants in zebrafish showed that *Selenoh* is involved in redox homeostasis, organ development and tumor suppression (Cox et al., 2016).

1.2.7 Selenoprotein I (SELENOI)

SELENOI is a transmembrane protein which contains a conserved CDP-alcohol-phosphatidyltransferase domain. It transfers phosphoethanolamine to diacylglycerol (Horibata and Hirabayashi, 2007). A patient known to have a mutation in the SELENOI gene shows neurological symptoms such as spastic paraplegia, blindness and seizures. MRI studies from the brain showed hypomyelination as well as brain atrophy suggesting an important role of SELENOI for myelination and development of the brain (Horibata et al., 2018).

1.2.8 Selenoproteins F and M (SELENOF, SELENOM)

SELENOF and SELENOM are two selenoproteins belonging to the same family that are localised in the ER (Labunskyy et al., 2014). They both possess redox active motifs and therefore may be involved in the reduction of disulfide bonds in ER-localised or secretory proteins (Labunskyy et al., 2007).

SELENOM is involved in leptin signalling in the hypothalamus and possesses a Trx

activity (Gong et al., 2019).

Abnormal function of SELENOF has been associated with various diseases including several cancers (Ren et al., 2018).

1.2.9 Selenoproteins K and S (SELENOK, SELENOS)

SELENOK and SELENOS are similar in that they both share a single transmembrane domain and are localised in the ER-membrane (Shchedrina et al., 2011). They are probably involved in the ER-associated degradation (ERAD) of misfolded proteins (Shchedrina et al., 2011; Ye et al., 2004) but their exact function remains unknown. Reduced expression of SELENOS has been shown to cause increased production of proinflammatory cytokines (Curran et al., 2005) and certain gene polymorphisms in *SELENOS* are associated with diabetic nephropathy (Li et al., 2019).

1.2.10 Selenoprotein O (SELENOO)

Very little is known about SELENOO. So far it has only been shown to be a redox-active protein that is localised in mitochondria (Han et al., 2014).

1.2.11 Selenoprotein N (SELENON)

SELENON is a transmembrane glycoprotein which is localised in the ER membrane. It is highly expressed in fetal tissues and to lesser extent also in adult tissues, for example in skeletal muscle (Petit et al., 2003). Exact functions of SELENON are not known but it is suggested to be involved in regeneration of skeletal muscle after stress or injury (Castets et al., 2011) supported by the fact that mutations in SELENON lead to so called SEPN1 (an earlier name of SELENON)-related myopathies (Arbogast and Ferreira, 2010). SELENON is required for normal function of the ryanodine receptor (Jurynek et al., 2008) and reduces isoforms of sarcoplasmic/endoplasmic reticulum calcium ATPase 2 (SERCA2) (Marino et al., 2015).

1.2.12 Selenoprotein P (SELENOP)

SELENOP is a unique selenoprotein because it contains ten Sec residues. It is thought to play an important role in the transport of Se from the liver to peripheral tissues, especially the brain, kidney and testes (Schomburg et al., 2003).

1.3 Eukaryotic mechanism of selenocysteine incorporation into proteins

Sec is incorporated into growing polypeptides when an in-frame UGA codon is recoded to Sec. This recoding mechanism requires a complex machinery that is so far not completely understood. Known factors involved in the Sec incorporation are the Selenocysteine insertion sequence (SECIS) element, the SECIS binding protein 2 (SECISBP2), the Sec-specific eukaryotic elongation factor (eEFSec), the ribosomal protein L30 (RPL30), the eukaryotic translation initiation factor 4a3 (eIF4a3) and the protein nucleolin (Labunsky et al., 2014, fig. 2). These factors are now discussed in more detail.

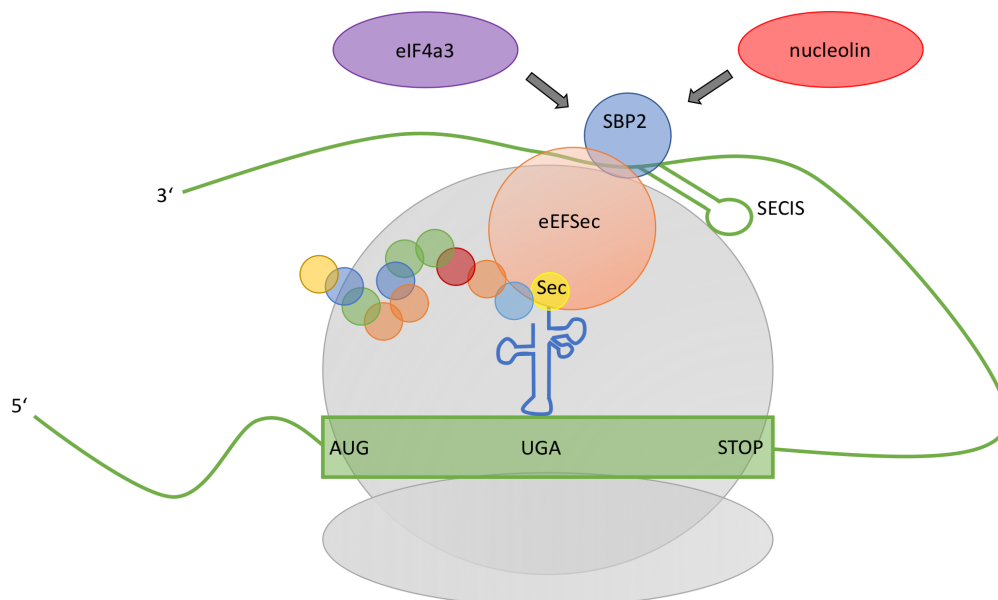


Fig. 2: Scheme of mammalian Sec incorporation showing a selenoprotein mRNA (green) with the essential factors SBP2 (blue), SECIS element, eEFSec (orange) and tRNA[Ser]Sec (blue with yellow Sec) as well as non-essential factors eIF4a3 (purple) and nucleolin (red). RPL30 is not shown.

1.3.1 Selenocysteine insertion sequence (SECIS) elements

The SECIS element is the major cis-acting factor of the Sec-incorporation machinery (Schweizer and Fradejas-Villar, 2016). Each selenoprotein mRNA contains one SECIS element within its 3' untranslated region (3' UTR) except for the SELENOP mRNA which contains two SECIS elements (Berry et al., 1993).

The SECIS element is an RNA stem-loop structure which is formed by two helices, an internal and an apical loop (Berry et al., 1991; Walczak et al., 1996). The junction of the internal loop to the 5' side of helix II is formed by a conserved AUGA motif of which the latter two bases form a GA/AG quartet (Walczak et al., 1996, figure 3). This GA/AG quartet is called SECIS core and is responsible for the kink-turn of SECIS elements (Matsumura et al., 2003; Walczak et al., 1996). Furthermore, nearly all human SECIS elements share a conserved AAR motif in the apical loop, the exception being the mRNAs of SELEONOM and SELENOO which contain a CCN motif (Korotkov et al., 2002, Kryukov et al. 2003). The AAR motif was shown to be required for Sec-incorporation in cell culture experiments (Berry et al., 1993) although its function remains unknown.

SECIS elements can be classified in type I and type II elements based on the existence of an additional bulge and ministem between the internal and apical loop (Grundner-Culemann et al., 1999, figure 3).

SECISBP2 was shown to primarily bind to the GA/AG quartet as well as the upper part of helix I and the 5' side of the internal loop (Fletcher et al., 2001).

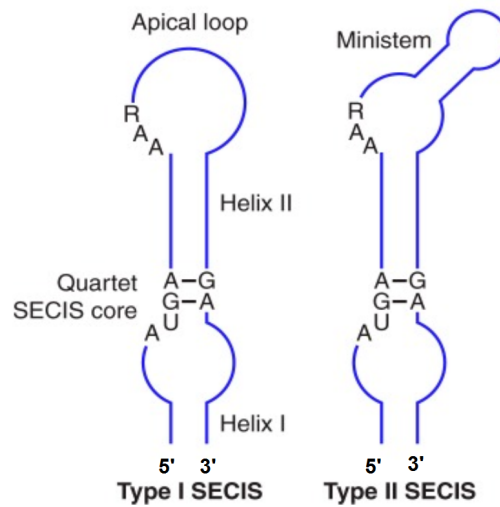


Fig. 3: Scheme of type I and type II SECIS elements. On the left a type I SECIS element is shown with its two helices, the internal and apical loop. On the right a type II SECIS element is shown, which has an additional bulge and ministem compared to type I SECIS elements. At the junction of the internal loop to helix 2 one can see the AUGA quartet for both type I and type II SECIS elements. The conserved AAR motif lies in the apical loop in type I SECIS elements. In type II SECIS elements the conserved AAR motif lies within the bulge between helix 2 and the ministem, modified from Labunskyy et al., (2014).

1.3.2 SECIS binding protein 2 (SECISBP2)

SECISBP2 is a protein that can be divided into three domains: the N-terminal domain, the Sec-incorporation domain (SID) and the RNA-binding domain (RBD) with the latter two domains forming the C-terminal domain (see figure 4). Four different functions are ascribed to SECISBP2 namely binding of the SECIS element, binding of the ribosome, interaction with eEFSec and Sec-incorporation (Copeland et al., 2001; Tujebajeva et al., 2000).

The function of the N-terminal domain is unknown. It roughly extends until amino acid (AA) 407 in murine SECISBP2 and is not required for Sec-incorporation *in-vitro* (Copeland et al., 2000). The N-terminal domain contains a putative nuclear localisation sequence (NLS) which is probably involved in the shuttling of SECISBP2 between the nucleus and cytoplasm (Papp et al., 2006, figure 4).

The C-terminal domain consists of the SID (AA 442-549 in murine SECISBP2) and the RBD (AA 628-789 in murine SECISBP2) and is *in-vitro* both essential and sufficient for Sec-incorporation (Donovan and Copeland, 2010). The SID enhances the binding of the RBD to the SECIS element and it also contributes to Sec-incorporation in a way that is independent of binding to the SECIS element (Donovan et al., 2008). Moreover, the SID transiently interacts with the ribosome (Donovan et al., 2008) but the function of this interaction is not yet known. The RBD contains an L7Ae RNA-binding motif (AA 662-762) which is required for SECIS binding but is also involved in stable binding to the ribosome (Caban et al., 2007). Just in front of the L7Ae motif there is a predicted nuclear export signal (NES) (Papp et al., 2006, figure 4).

Finally, SECISBP2 does also interact with eEFSec. This was shown in co-immunoprecipitation experiments of mammalian transfected cells (Tujebajeva et al., 2000) and in *in-vitro* electrophoretic-mobility-shift-assay (EMSA) experiments (Donovan et al., 2008).

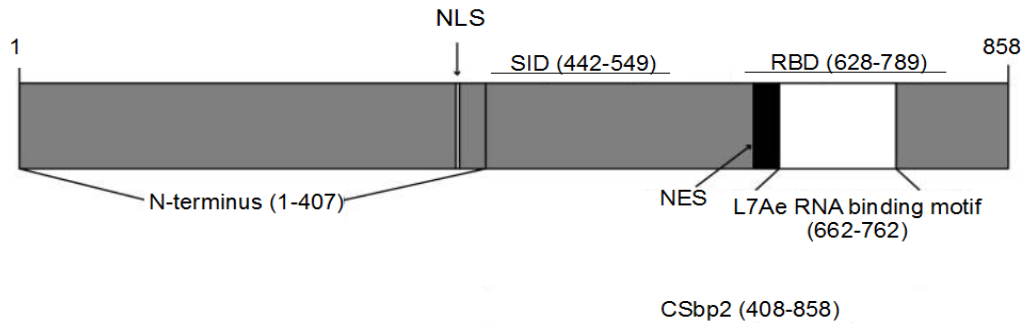


Fig. 4: Scheme of SECISBP2 domains in murine SECISBP2, NLS = nuclear localisation sequence, NES = nuclear export signal, CSbp2 = C-terminal SECISBP2, SID = Sec-incorporation domain, RBD = RNA-binding domain, modified after Donovan and Copeland (2010).

1.3.3 Sec-specific eukaryotic elongation factor (eEFSec)

eEFSec is a specific elongation factor for the tRNA^{[Ser]^{Sec}} and does not bind any other tRNA. Similarly, tRNA^{[Ser]^{Sec}} cannot be bound to other elongation factors. Compared to

other mammalian elongation factors the eEFSec has a fourth domain which is essential for both binding of SECISBP2 and tRNA^{[Ser]^{Sec}} (Gonzales-Flores et al., 2012). eEFSec also interacts with SECISBP2 as already described above.

1.3.4 Ribosomal protein L30 (RPL30)

RPL30 was shown to bind the SECIS element both *in-vitro* and *in-vivo* and is able to compete with SECISBP2 for SECIS-binding. Furthermore, overexpression of RPL30 stimulates Sec-incorporation in rat-hepatoma cells (Chavatte et al., 2005). It has therefore been hypothesised that RPL30 is involved in Sec-incorporation. The exact function remains, however, unclear.

1.3.5 Nucleolin

Nucleolin was initially identified when it was found to bind a GPX1 SECIS probe (Wu et al., 2000). In further experiments by different research groups conflicting results concerning the affinity of nucleolin towards different SECIS elements were published (Miniard et al., 2010; Squires et al., 2007). Overall, nucleolin seems to be involved in Sec-incorporation but its exact function remains unclear, too.

1.3.6 Eukaryotic translation initiation factor 4a3 (eIF4a3)

The eIF4a3 does also bind SECIS elements and has been shown to have a negative effect on Sec-incorporation. Moreover, it was shown that eIF4a3 is more highly expressed under conditions of limiting Se (Budiman et al., 2009). It has been proposed that under conditions of limiting Se eIF4a3 could reduce the expression of a subset of selenoproteins by binding to the SECIS elements of the corresponding mRNAs (Labunskyy et al., 2014).

1.4. Hierarchy of selenoproteins

A “hierarchy” of selenoproteins was first described when rats were fed diets of low Se. It was observed that the expression of some selenoproteins significantly decreased whilst others are less affected (Hill et al., 1992; Lei et al., 1995). This led to a differentiation of selenoproteins in so called “housekeeping” selenoproteins (such as TXNRD1, TXNRD3, GPX4) that are less dependent on Se-availability and stress-related selenoproteins that are more highly dependent on Se-availability (such as GPX1 and SELENOW) (Labunskyy et al., 2014).

The complete mechanism behind this hierarchy is not fully understood but several possible influencing pathways and factors are being discussed. This includes the susceptibility of selenoprotein mRNAs to nonsense-mediated-decay (NMD), the affinity of SECISBP2 towards different SECIS elements, its ability to stabilise mRNAs and the influence of factors like eIF4a3 and nucleolin (Fradejas-Villar et al., 2017; Sunde et al., 2011). In addition, post-transcriptional modifications of the tRNA^{[Ser]^{Sec} affect the expression of selenoproteins in a selenoprotein-dependent manner (Schweizer et al., 2017).}

1.5 Mutations in SECISBP2

Several mutations in SECISBP2 have been described in humans (Fradejas-Villar, 2018, Schoenmakers and Chatterjee 2020). This thesis focuses on SECISBP2 p.Arg540Gln and SECISBP2 p.Cys691Arg mutations, which will be discussed in more detail. Since various studies use either human, murine or rat SECISBP2, in the following SECISBP2^{RQ} will be used as abbreviation for SECISBP2 protein that has a mutation which represents the SECISBP2 p.Arg540Gln mutation in humans. SECISBP2^{CR} will be used as abbreviation in the same way concerning SECISBP2 p.Cys691Arg.

1.5.1 The R540Q mutation

The R540Q mutation, which targets the SID domain of SECISBP2, was identified in a

Bedouin family in which three of seven siblings had abnormal levels of thyroid hormone (Dumitrescu et al., 2005). All three affected siblings showed elevated levels of thyroid stimulating hormone (TSH), free thyroxine (fT₄), as well as total reverse-triiodothyronine (rT₃), but low levels of free triiodothyronine (fT₃). Measurement of *DIO2* mRNA levels and activity from cultured skin-fibroblasts showed that activity of DIO2 is reduced in affected individuals although mRNA levels are normal. Furthermore, GPX activity in both serum and cultured fibroblasts was reduced and SELENOP levels in serum were also reduced. A homozygous R540Q mutation in *SECISBP2* was identified in all three siblings as the cause of these findings.

Since the phenotype was rather mild the authors proposed that the R540Q mutation might not completely abolish the function of *SECISBP2*. However, since the affected individuals were not yet fully grown at the date of study, further defects that might show later in life could not be evaluated. (Dumitrescu et al., 2005)

Binding of *SECISBP2*^{RQ} to *Gpx4* and *Txnrd1* SECIS elements was observed by RNA-electrophoretic-mobility-shift-assay (rEMSA). However, *SECISBP2*^{RQ} did not bind to *Gpx1*, *Dio1* and *Dio2* SECIS elements. On the contrary *in-vitro* Sec-incorporation into a modified luciferase occurred when the luciferase mRNA sequence contained either a *Gpx4*, *Gpx1* or *Dio1* SECIS element (Bubenik and Driscoll, 2007).

Ribosomal profiling (RiboSeq) data (Fig. 5) showed that the ribosome coverage 3' of the UGA codon in brain of conditional-mutant mice is reduced regarding the *Gpx4* mRNA when comparing *SECISBP2*^{RQ} to *SECISBP2*^{WT}. Regarding the *Gpx1* mRNA it could be observed that there are overall less reads when *SECISBP2*^{RQ} was present, but no apparent change in the ribosome coverage 3' of the UGA codon relative to 5'. (Zhao et al., 2019)

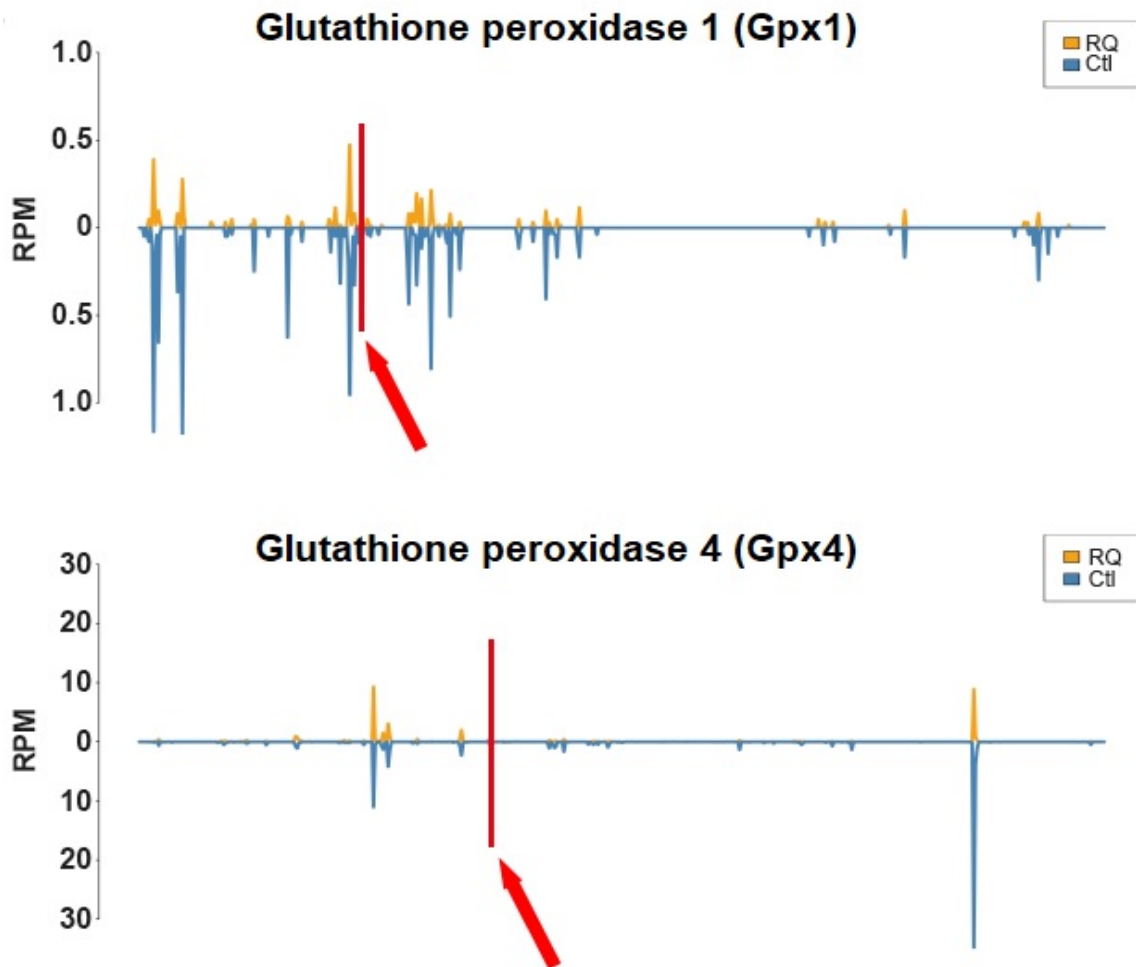


Fig. 5: Plots of ribosome coverage of Gpx1 and Gpx4 mRNAs from mice brain of either control mice or CamK-Cre; Secisbp2^{RQ/fl}. Y-axis shows the reads per million mapped reads. X-axis shows the open reading frame of the corresponding mRNA. The red line marked with a red arrow indicates the position of the UGA codon, modified after Zhao et al., (2019).

1.5.2 The C691R mutation

The C691R mutation, which targets the L7Ae domain of SECISBP2, was identified in a male child showing various symptoms (Schoenmakers et al., 2010). These symptoms included abnormal levels of thyroid hormone (elevated fT_4 , low fT_3 , normal TSH), mild, global development delay, muscle weakness, mild bilateral hearing loss of high frequencies and the tendency to develop hypoglycaemia when fasting for longer periods

(e.g. overnight). The child showed a compound heterozygous genotype with the C691R mutation in one allele and a splicing-defect leading to either lack of exons 2-4 or 3-4 in the other allele. The muscle weakness was similar to that of patients with SEPN1-related myopathies and a Western blot of the child's fibroblasts showed reduced levels of SELENON. In addition, cultured fibroblasts did show increased levels of reactive-oxygen-species (ROS) and DNA-damage after exposure to oxidative stress. Western blot analysis of further selenoproteins showed reduced levels of SELENOP, GPX3 and SEPHS2. ⁷⁵Se labeling showed reduced levels of SELENOW (Schoenmakers et al., 2010).

1.6 Selenoproteins in viruses

In 1994 it was first suggested that the genome of the HI-virus-1 might encode selenoproteins via a frameshift-mechanism. The authors proposed a frameshift-mechanism in which the ribosome “slips” at slippery sequences that are located upstream of an RNA pseudoknot. Supporting arguments towards the existence of these alternative selenoprotein encoding open reading frames were the conservation of the sequence in the -1 reading frame and some clinical data that showed improvement in AIDS patients when they were treated with Se. The authors reasoned that Se-availability in the body might be decreased in AIDS patients, if the HI-virus uses some Se for its own selenoproteins (Taylor et al., 1994).

In 1997 a homology between the potential protein that would result from a -1 frameshift in the HIV envelope (env)-gene, which encodes the glycoprotein 120 (gp120), and a Gpx was found (Taylor et al., 1997b). The potential gp120-Gpx fusion protein that would result from this frameshift was then further analysed by the authors. A protease-site was predicted just N-terminal of the Gpx sequence and the potential Gpx sequence was cloned with an additional start-codon and SECIS element. Gpx-activity was increased in cells transfected with this construct (Zhao et al., 2000).

This still left the problem of the viral mRNA having no own SECIS element to promote a potential Sec-incorporation. To propose a possible solution to this problem Taylor et al. (2016) published a hypothetical antisense-tethering-interaction (ATI) mechanism.

Interaction between viral mRNAs and human selenoprotein mRNAs would lead to a “hijacking” of the human SECIS element by the virus (see Fig. 6). Thus the virus would use the human SECIS element to recode its own UGA codon. In detail Taylor et al. (2016) found that certain sequences of viral mRNAs are in part complementary to mRNA sequences of human selenoproteins. These ATIs were proposed to take place between HIV-mRNAs and *TXNRD1* mRNA and Ebola-virus-mRNAs and *TXNRD3* mRNA. To further validate this hypothesis the authors showed results of a DNA-gel-shift assay using the sequences that are supposed to take part in the ATI in which a shift of DNA bands can be observed (see Fig. 7).

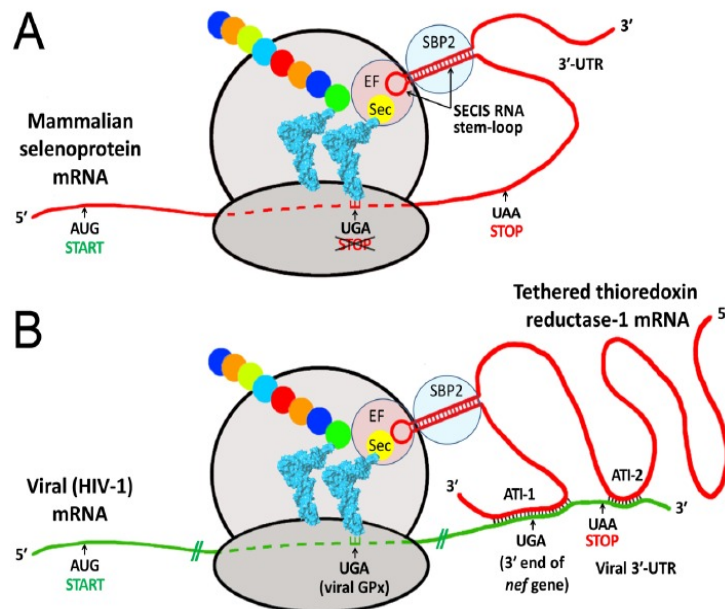


Fig. 6: A: scheme of Sec-incorporation in eukaryotes showing the selenoprotein mRNA with its SECIS element (red), SECISBP2 (light blue), eEFSec (orange) and tRNA[Ser]Sec (teal with Sec in yellow) B: Scheme of potential viral SECIS element recruitment showing viral (HIV) mRNA (green) with its ATI to human *TXNRD1* mRNA (red), SECISBP2 (light blue), eEFSec (light red) and tRNA[Ser]Sec (teal with Sec in yellow), modified after Taylor et al. (2016).

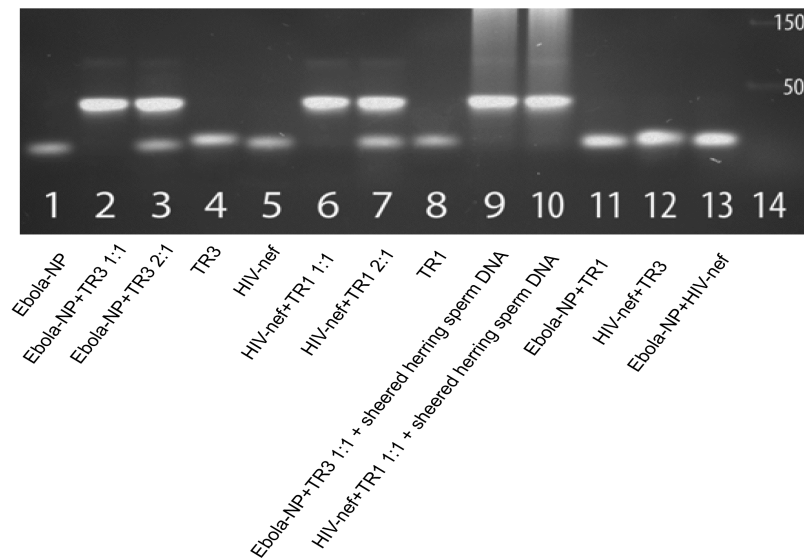


Fig. 7: Results of DNA-gel-shift assay with sequences from Ebola-nucleoprotein-gene (Ebola-NP), human TXNRD3-gene (TR3), HIV-nef-gene (HIV-nef) and human TXNRD1-gene (TR1), modified after Taylor et al. (2016).

1.7 *In-vitro* assay to measure Sec-incorporation

An *in-vitro* assay to measure Sec-incorporation is used in this thesis. Sec-incorporation is monitored by the luminescence produced by a luciferase. Since the luciferase is not a selenoprotein, the cysteine codon at position 258 of the luciferase was mutated to a UGA/Sec codon. In addition, the sequence of the rat *Gpx4* SECIS element was added in the 3' UTR downstream of the luciferase gene (see figure 8) and the whole sequence was cloned into a plasmid. This method was first used by Mehta et al. (2004) and the described plasmid was a gift to our lab from Paul Copeland.

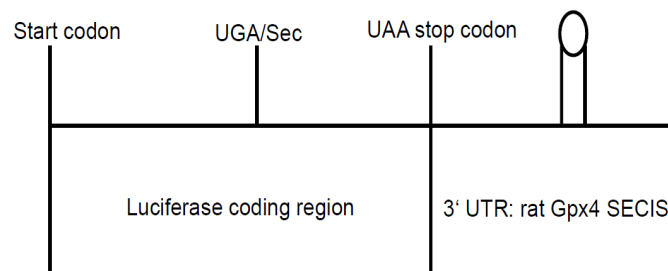


Fig. 8: Scheme of luciferase reporter showing the luciferase coding region containing the UGA codon and the rat *Gpx4* SECIS element within the 3' UTR.

This reporter plasmid can be transcribed and translated *in-vitro* so that luciferase will be produced if Sec-incorporation takes place successfully. The produced luciferase can then be quantified by adding a luciferase substrate and measuring luminescence (see figure 9). Overall the measured luminescence is therefore a correlate for Sec-incorporation and allows a direct assessment of the Sec-incorporation efficiency.

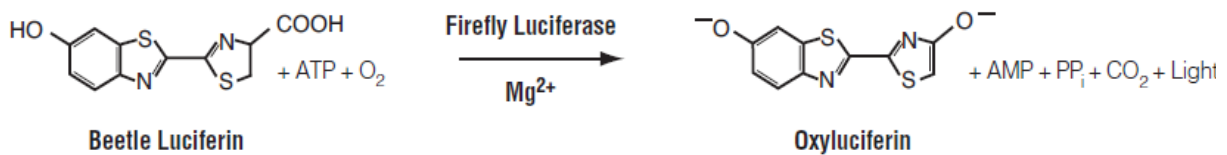


Fig. 9: Oxidation reaction of luciferin to oxyluciferin which is catalysed by the luciferase using ATP•Mg²⁺ as a cosubstrate. The reaction produces light, which can be measured as luminescence, from Promega Luciferase Assay System technical bulletin.

1.8 Aims of the thesis

1.8.1 Effects of SECISBP2 mutations in regard to different SECIS elements

Both the R540Q and C691R mutation have been found in humans (Dumitrescu et al., 2015; Schoenmakers et al., 2010). Previous experiments from other research groups (Bubenik and Driscoll, 2007) and data from our research group led to the idea that SECISBP2^{RQ} might have different effects on Sec-incorporation depending on the SECIS element. A ribo-seq analysis from a neuron-specific SECISBP2^{RQ} mutation showed that SECISBP2^{RQ} leads to a reduced amount of ribosomes that can be found 3' of the UGA codon compared to SECISBP2^{WT} on a *Gpx4* mRNA (Fig. 5). Concerning the *Gpx1* mRNA the overall amount of ribosomes that could be found on the mRNA was reduced but there was no apparent difference between the ribosome amount 5' or 3' of the UGA codon. For that reason I proposed that SECISBP2^{RQ} would lead to reduced Sec-incorporation when the SECIS element is a *Gpx4* SECIS element but would have no effect when a *Gpx1* SECIS element is used.

Since the C691R mutation likely disrupts the hydrophobic core of the RNA-binding domain of SECISBP2 I hypothesised that the C691R mutated protein is not functional, independent of the SECIS element used.

The first aim of the thesis was to show that SECISBP2^{RQ} affects the efficiency of Sec-incorporation *in-vitro* differently depending on the SECIS element. I also hoped to get insights into the hierarchy of selenoproteins by observing that some SECIS elements are impaired more severely by the RQ mutation than others. In addition, I wanted to show that SECISBP2^{CR} leads to a loss of Sec-incorporation-activity independent of the SECIS element.

1.8.2 Viral SECIS element recruitment

Another aim of the thesis was to provide the first evidence of a successful Sec-incorporation by an antisense-tethering-interaction between viral and human mRNAs that leads to an in-trans recruitment of a SECIS element. Since the sequence of the Ebola-virus from 1976 is less matching to the TXNRD3 sequence than the sequence of the Ebola-virus from 2014 I also wanted to show that the Sec-incorporation is less effective when the Ebola-virus sequence from 1976 is used compared to when the sequence of 2014 is used. Furthermore, I wanted to express the HIV-encoded Gpx *in-vitro* using the proposed mechanism of an in-trans SECIS element recruitment by antisense-tethering-interaction.

1.9. Experimental outlines

1.9.1 Investigation of SECISBP2 mutations

A luciferase assay was performed to show that SECISBP2^{RQ} affects the efficiency of Sec-incorporation differently depending on the SECIS element and SECISBP2^{CR} abolishes Sec-incorporation completely. The murine SECIS elements of *Gpx1*, *Gpx4*, *Txnrd1*, *Dio1*, *Dio2* and *Dio3* were cloned into the 3' UTR of the luciferase reporter. Subsequently, the reporters were transcribed *in-vitro*. Since SECISBP2 was shown to

be the only limiting factor for Sec incorporation in RRL (Mehta et al., 2004) the C-terminal part of murine SECISBP2 (CSECISBP2) was cloned as CSECISBP2^{WT}, CSECISBP2^{R543Q} and CSECISBP2^{C696R}. These two mutations are the equivalent to the human R540Q and C691R mutations in murine SECISBP2. The proteins were then expressed heterologously and purified. Afterwards, *in-vitro* translation of the transcribed reporters was performed using RRL adding one of the three different types of CSECISBP2. Finally, luminescence was measured as a correlate for Sec-incorporation.

1.9.2 Investigation of potential viral SECIS element recruitment

In order to show an in-trans SECIS element recruitment by means of an antisense-tethering-interaction between viral and human mRNA sequences a different luciferase assay was performed.

The viral sequences to which the ATIs were proposed were cloned into the 3' UTR of the luciferase reporter instead of a SECIS element (see Fig. 10)

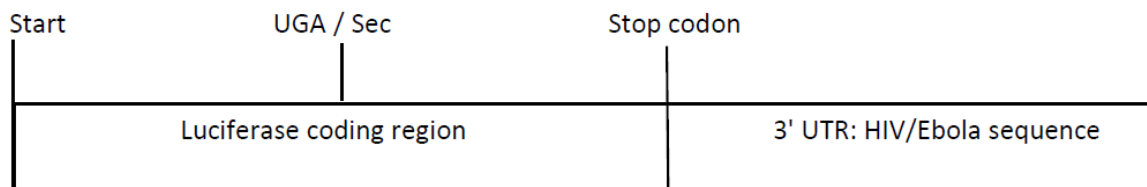


Fig. 10: Scheme of the luciferase reporter with viral sequences cloned into the 3' UTR instead of a SECIS element

Plasmids encoding the full-length mRNA sequences of human TXNRD1 and TXNRD3 were acquired commercially from BaseClear B.V.

Both the luciferase reporters and the TXNRD mRNA sequences were transcribed *in-vitro* and then incubated together in an *in-vitro* translation reaction with added murine CSECISBP2. The results of the *in-vitro* translation reaction were then checked for luciferase activity that would indicate a successful Sec-incorporation.

2. Materials and Methods

2.1 Supplementary list

2.1.1 Technical equipment

Tab. 1: Pipettes and disposable materials

| Equipment | Manufacturer |
|---|--|
| Pipettes | Eppendorf (Hamburg) |
| Pipette tips | Sarstedt (Nümbrecht) |
| Microcentrifuge tubes 1.5 and 2 ml | Sarstedt (Nümbrecht) |
| PCR tubes 0.2 ml | Biozym (Hessisch Oldendorf) |
| Falcons 15 and 50 ml | Sarstedt (Nümbrecht) |
| Round bottom tubes with ventilation cap 13 ml | Sarstedt (Nümbrecht) |
| 96-well-plate, "cellstar" white | Greiner Bio-One (Kremsmünster, Austria) |
| Centrifuge tubes 500 ml | Beckman Coulter (Brea, CA, USA) |
| Econo-Pac [®] Chromatography Columns | Bio-Rad Laboratories (Hercules, CA, USA) |

Tab. 2: Technical equipment – This list only contains technical equipment that may have been critical for the success of the experiments and does not contain general laboratory equipment

| Device | Name | Manufacturer |
|--|---------------------------|---|
| Refrigerated benchtop centrifuge | 5417-R | Eppendorf (Hamburg) |
| Refrigerated benchtop centrifuge | 5430-R | Eppendorf (Hamburg) |
| Benchtop centrifuge | 5430 | Eppendorf (Hamburg) |
| Refrigerated centrifuge, Rotor F-34-6-38, Rotor A-4-62 | 5810-R | Eppendorf (Hamburg) |
| Refrigerated centrifuge, Rotor JA-10 | Avanti J-E | Beckman Coulter (Brea, CA, USA) |
| Thermocycler | Mastercycler, Nexus GSX1e | Eppendorf (Hamburg) |
| Thermocycler | TGradient | Biometra (Göttingen) |
| Sonicator | Sonifier 250 | Branson (Danbury, CT, USA) |
| Spectrophotometer | NanoDrop 2000 | Thermo Fisher Scientific (Waltham, MA, USA) |
| Gel documentation | Gel iX Imager | Intas (Göttingen) |
| Incubator | Function Line | Heraeus (Hanau) |
| Luminometer/plate reader | Infinite M200 Pro | Tecan, Männedorf (Switzerland) |
| Ultrapure water system | GenPure Standard | Thermo Fisher Scientific (Waltham, MA, USA) |

| | | |
|--|--|---|
| Gel electrophoresis system used for SDS-PAGE (large scale) | PerfectBlue™ Doppelgelsystem | Peqlab Biotechnologie (Erlangen) |
| Gel electrophoresis system used for SDS-PAGE (small scale) | SE 250 | Hofer (Holliston, MA, USA) |
| Blotting System | PerfectBlue™ Semi-Dry Electroblotter Sedec M | Peqlab Biotechnologie (Erlangen) |
| Gel electrophoresis system used for agarose-gels | Owl™ Easy-Cast™ Electrophoresis System | Thermo Fisher Scientific (Waltham, MA, USA) |

2.1.2 Chemicals

Most chemicals were purchased from AppliChem (Darmstadt). Exceptions are listed in the following or later tables.

Tab. 3: Chemicals not purchased from AppliChem

| Chemical | Manufacturer |
|-----------------------------------|---|
| Bromophenolblue | Merck (Darmstadt) |
| Xylenecyanol | Merck (Darmstadt) |
| peqGold Universal Agarose | Peqlab Biotechnologie (Erlangen) |
| LB-Agar | Invitrogen (Carlsbad, CA, USA) |
| LB Broth (Miller) | SigmaAldrich (St. Louis, MO USA) |
| Brillant Blau R 250 (Coomassie) | Carl Roth (Karlsruhe) |
| Glycogen, molecular biology grade | Thermo Fisher Scientific (Waltham, MA, USA) |

| | |
|--|---|
| HD-Green DNA-Dye | Intas (Göttingen) |
| Acrylamide-solutions | Carl Roth (Karlsruhe) |
| β-Mercaptoethanol | Carl Roth (Karlsruhe) |
| cOmplete™ EDTA-free protease inhibitor | Roche (Basel, Switzerland) |
| Ni-NTA Agarose | Qiagen (Venlo, Netherlands) |
| RNase A | Qiagen (Venlo, Netherlands, Cat. No.:19101) |
| GeneRuler 100 bp plus DNA ladder | Thermo Fisher Scientific (Waltham, MA, USA) |
| GeneRuler 1 kb DNA ladder | Thermo Fisher Scientific (Waltham, MA, USA) |
| dNTPs (dATP, dCTP, dGTP, dTTP) | Thermo Fisher Scientific (Waltham, MA, USA) |

2.1.3 Primers used in different experiments

All primers were purchased from Eurogentec (Seraing, Belgium)

Tab. 4: Primers used for generating recombinant DNA sequences

| Species | Primer name | Sequence (5' to 3') |
|---------|--------------------|--|
| mouse | SECIS_Gpx1_Pacl_Fw | AGT-CTT-AAT-TAA-TCT-GGG-GGG-CGG-TTC-TTC-C |
| | SECIS_Gpx1_NotI_Rv | GAC-GGC-GGC-CGC-TCT-GAG-GGG-ATT-TTC-CTG-GA |
| | SECIS_Gpx4_Pacl_Fw | AGT-CTT-AAT-TAA-TGA-CCC-CTG-GAG-CCT-TCC-AC |
| | SECIS_Gpx4_NotI_Rv | GAC-GGC-GGC-CGC-CGG-CAG-GGA-TGC-ACG-CCA-GG |

| | | |
|-------------|----------------------|--|
| mouse | SECIS_Txnrd1_Pacl_Fw | AGT-CTT-AAT-TAA-CAT-CTG-GCA-GAG-CAT-CAC-AG |
| | SECIS_Txnrd1_NotI_Rv | GAC-GGC-GGC-CGC-TGA-GCT-CAA-CAG-ACC-CGG-CA |
| | Dio1_SECIS_Fw_Pacl | ATG-TTT-AAT-TAA-TTT-TAT-ATT-TGT-GTA-TGA-TGG-TCA-CA |
| | Dio1_SECIS_Rv_NotI | TTG-CGC-GGC-CGC-CCG-ACA-TTT-TTA-AAA-ATC-AAG-TCA |
| | Fw_Primer_mDio2 | ATG-TTT-AAT-TAA-CAC-TGG-TGT-GCG-AAT-GAT-AA |
| | Rv_Primer_mDio2 | TGC-AGC-GGC-CGC-GAC-TCG-TGT-GAC-TAC-ATC-CAA-CC |
| | Dio3_Seq_Fw_Primer | TAA-GCC-CTG-GCT-GCT-GAT-GAC-GAA-CCG-CCT-CTA-ACT-GGG-CTT-GAC-CAC-GGG-TCG-GCT-CTG-AAT-TGC-AGA-GAG-GCT-GC |
| | Dio3_Seq_Rv_Primer | GGC-CGC-AGC-CTC-TCT-GCA-ATT-CAG-AGC-CGA-CCC-GTG-GTC-AAG-CCC-AGT-TAG-AGG-CGG-TTC-GTC-ATC-AGC-AGC-CAG-GGC-TTA-AT |
| Ebola virus | Ebo_2014_Fw | TAA-AAC-AAC-AAG-ATC-AGG-ACC-ACA-TTC-AAG-AGG-CCA-GGA-ACC-AAG-ACA-GTG-ACA-ACA-CCC-AGG-C |
| | Ebo_2014_Rv | GGC-CGC-CTG-GGT-GTT-GTC-ACT-GTC-TTG-GTT-CCT-GGC-CTC-TTG-AAT-GTG-GTC-CTG-ATC-TTG-TTG-TTT-TAA-T |

| | | |
|-------------|-------------|---|
| Ebola-virus | Ebo_1976_Fw | TAA-AGC-AAC-AAG-ATC-AGG-ACC- ACA-CTC-AAG-AGG-CCA-GGA-ACC- AGG-ACA-GTG-ACA-ACA-CCC-AGG- C |
| | Ebo_1976_Rv | GGC-CGC-CTG-GGT-GTT-GTC-ACT- GTC-CTG-GTT-CCT-GGC-CTC-TTG- AGT-GTG-GTC-CTG-ATC-TTG-TTG- CTT-TAA-T |
| HI-virus | Fw_HIV_seq | ATG-CTT-AAT-TAA-AGC-TGC-ATC- CGG-AGT-ACT-TCA-AGA-ACT-GCT- GAC-ATC-GAG-CTT-GCT-ACA-AGG- GAC-TTT-CCG-CTG-GGG-ACT-TTC- CAG-GGA-GGC-GTG-GCC-T |
| | Rv_HIV_seq | CGA-TGC-GGC-CGC-CCA-GTA-CAG- GCA-AAA-AGC-AGC-TGC-TTA-TAT- GCA-GCA-TCT-GAG-GGC-TCG-CCA- CTC-CCC-AGT-CCC-GCC-CAG-GCC- ACG-CCT-CCC-TGG-AAA-GTC |
| | HIV_Fw_PCR | ATG-CTT-AAT-TAA-AGC-TGC-ATC-C |
| | HIV_Rv_PCR | CGA-TGC-GGC-CGC-CCA-GTA |

Tab. 5: Primers used for sequencing

| Target plasmid/sequence | Primer name | Sequence (5' to 3') |
|---------------------------------------|----------------|------------------------------------|
| pTrcHis2 | pTrcHis_Fw_seq | GAG-GTA-TAT-ATT-AAT-GTA-TCG |
| | pTrcHis_Rv_seq | GAT-TTA-ATC-TGT-ATC-AGG |
| pcDNA3.1 and pBluescript II KS+ | T7 | TAA-TAC-GAC-TCA-CTA-TAG-GG |
| pcDNA3.1 | BGH_rv_Primer | TAG-AAG-GCA-CAG-TCG-AGG |
| pBluescript II KS+ with Txnrd1 insert | Txnrd1_seq_2 | CGA-TCT-GCC-CGT-TGT-GTT |
| | Txnrd1_seq_3 | TTC-TTA-GAG-GAT-TTG-ACC-AGG-ACA-T |
| | Txnrd1_seq_4 | ACA-ACA-TTG-TCT-GTG-ACC-AAG-C |
| | Txnrd1_seq_5 | AAG-TTT-TTC-TGG-TAG-CTT-TAG-CTT-TA |
| pBluescript II KS+ with Txnrd3 insert | Txnrd3_seq_2 | GGC-TGG-GAA-TAT-AAT-CAA-CAA-G |
| | Txnrd3_seq_3 | CAC-TTG-TTA-CGC-AAA-GAT-AAT-CTG-C |
| | Txnrd3_seq_4 | TAG-TGC-GTG-GGC-CTA-GAA |

Tab. 6: Primers used for site-directed mutagenesis

| Target plasmid | Primer name | Sequence (5' to 3') |
|----------------|-------------------|--|
| pTrcHis2-CSbp2 | CSbp2R543Qforward | CTG-CTG-CAT-CCT-CTC-TTG-CTG-TTC-TTT-CAA-AAT-TAT-CTT-CT |
| | CSbp2R543Qreverse | AGA-AGA-TAA-TTT-TGA-AAG-AAC-AGC-AAG-AGA-GGA-TGC-AGC-AG |
| | SBP2_C696R_fwd | GCT-CAG-GAA-GCT-GAA-GCG-CAT-CAT-CAT-CTC-TCC |
| | SBP2_C696R_rev | GGA-GAG-ATG-ATG-ATG-CGC-TTC-AGC-TTC-CTG-AGC |

2.2 Cloning and amplification of recombinant DNA plasmids

The free software APE was used to plan all cloning procedures. Special reagents and kits used in the cloning process are listed in Tab. 11.

2.2.1 Cloning and amplification of pTrcHis2 with *CSecisbp2* inserts

In order to express the C-terminal part of mouse SECISBP2 (AA 408-858) both as wildtype and mutated protein in bacteria, the pTrcHis2 vector with the insert coding for the named amino acids plus a C-terminal His-tag of 6 histidine residues was transformed into E.coli BL21 star. The R543Q and C696R mutations were previously introduced to the pTrcHis2-CSBP2 vector using site directed mutagenesis. The mutated plasmids were subsequently transformed into E.coli DH5 α , plasmid-DNA was isolated and sent for Sanger-sequencing to confirm the identity of the mutations.

Tab. 7: pTrcHis2 plasmids with CSecisbp2 inserts

| Plasmid name | Origin | Antibiotic resistance |
|----------------------|--|-----------------------|
| pTrcHis2-CSBP2 | Previously cloned by Magdalena Antes in our laboratory | Amp |
| pTrcHis2-CSBP2_R543Q | Cloned after site directed mutagenesis | Amp |
| pTrcHis2-CSBP2_C696R | Cloned after site directed mutagenesis | Amp |

2.2.1.1 Site-directed mutagenesis

Site-directed mutagenesis was performed using the QuikChange Lightning Site-directed mutagenesis kit. Primers which were designed using the QuikChange primer design program on the Agilent website are listed in table 6. The reaction was assembled and performed according to the manufacturer's protocol with 50 ng of template and 1 μ l of each primer (10 μ M).

2.2.1.2 Transformation of plasmids into E.coli DH5 α bacteria

7,5 μ l of the site-directed mutagenesis PCR reaction or 10 ng of plasmid were added to competent bacteria with careful mixing, incubated for 20 min on ice, then a "heat-shock" of 45 s at 42 °C followed. Afterwards, the bacteria were placed on ice again for 2 min before 500 μ l of LB-medium were added and incubated for 1 h at 37 °C and 550 rpm. Finally, the transformed bacteria were centrifuged at 4000 g for 5 min at 4 °C, the supernatant was poured off and the bacteria pellet resuspended in the rest of the medium. This resuspension was then plated on LB agar plates with ampicillin (100 μ g/ml), which were incubated at 37 °C overnight. The centrifugation step was only

performed for the transformations with the mutated plasmids, otherwise 150 μ l were directly plated.

2.2.1.3 Plasmid isolation through alkaline lysis (Mini-Prep and Midi-Prep)

Single colonies from the overnight incubated bacteria were picked from the plate and incubated overnight at 37 °C, 200 rpm in 5 ml LB medium with Ampicillin added to a concentration of 100 μ g/ml. Of each bacterial culture 3 ml were centrifuged at 8000 rpm and room temperature for 1 min and the supernatant was removed. The bacteria pellet was then resuspended by pipetting up and down in 400 μ l P1-buffer (Tab.12). Afterwards 400 μ l P2-buffer (Tab. 12) was added, the tubes were carefully mixed by inverting and incubated 2-3 min at room temperature (RT) until 400 μ l P3-buffer (Tab. 12) was added. Once more the tubes were carefully mixed by inverting until a white precipitate formed and incubated at room temperature for around 30 min. Subsequently, the samples were centrifuged at 14000 rpm, RT and the clear supernatant was transferred into a new tube. 840 μ l Isopropanol was added and after thorough mixing the samples were centrifuged again (14000 rpm, RT, 10 min). The supernatant was removed, 500 μ l of 70 % ethanol (EtOH) added and after thorough mixing centrifugation followed once more (14000 rpm, RT, 2 min). The supernatant was then removed completely and the DNA pellet left to air-dry for 5-10 min before it was resuspended in 20-30 μ l nuclease-free water. DNA concentrations were afterwards measured using the NanoDrop 2000.

To confirm the integrity of the transformed DNA the isolated plasmid DNA was sequenced (GATC Biotech, Konstanz) using the primers as specified in Tab. 5. After identifying a clone with positive sequencing result, 100 μ l of the original culture were incubated overnight at 37 °C, 190 rpm in 100 ml LB medium with ampicillin added to a concentration of 100 μ g/ml. On the following day plasmid DNA from this culture was isolated using the NucleoBond Xtra MIDI Kit following the manufacturer's protocol. The isolated DNA was quantified using the NanoDrop 2000.

2.2.2 Cloning and amplification of pcDNA3.1_Luciferase with SECIS element inserts

Table 8 gives an overview of all pcDNA3.1 plasmids that were used.

The pcDNA3.1_Luciferase_1 plasmid contains a luciferase coding region in which the codon 258 was changed from a normal cysteine codon to a UGA codon and a rat *Gpx4* SECIS element in the 3' UTR. The pcDNA3.1_Luciferase_2 and pcDNA3.1_Luciferase_3 plasmids are identical to the pcDNA3.1_Luciferase_1 but contain a rat *Gpx4* SECIS element with the AUGA core of the SECIS element deleted or a UAA stop codon at position 258, respectively. All these plasmids were kindly provided to our research group from Paul Copeland. The pcDNA3.1_Luc_5 plasmid contains the original UGU Cys codon at position 258 and was created by Magdalena Antes in our research group using site directed mutagenesis.

In order to create plasmids with different SECIS elements downstream of the luciferase coding region for later usage as templates for *in-vitro* transcription, different murine SECIS elements were PCR-amplified from mouse cDNA (or gDNA in case of Dio2 SECIS element), and cloned into the pcDNA3.1_Luc_1 plasmid. When PCR-amplification failed for the Dio3 SECIS element, the sense sequence and its complementary were purchased as single stranded DNA and aligned.

Tab. 8: pcDNA3.1_Luciferase plasmids with SECIS element inserts

| Plasmid name | Origin | Antibiotic resistance |
|--------------------------------------|---|-----------------------|
| pcDNA3.1_Luc_1 (Luc C258U/rat_Gpx4) | Gift from Paul Copeland | Amp |
| pcDNA3.1_Luc_2 (Luc C258U/AUGA_del) | Gift from Paul Copeland | Amp |
| pcDNA3.1_Luc_3 (Luc C258UAA/ratGpx4) | Gift from Paul Copeland | Amp |
| pcDNA3.1_Luc_5 (Luc C258/rat_Gpx4) | Created by Magdalena Antes | Amp |
| pcDNA3.1_Luc_mGpx1 | Cloned from mouse cDNA | Amp |
| pcDNA3.1_Luc_mGpx4 | Cloned from mouse cDNA | Amp |
| pcDNA3.1_Luc_mTxnrd1 | Cloned from mouse cDNA | Amp |
| pcDNA3.1_Luc_mDio1 | Cloned from mouse cDNA | Amp |
| pcDNA3.1_Luc_mDio2 | Cloned from mouse gDNA | Amp |
| pcDNA3.1_Luc_mDio3 | Cloned after alignment of bought sequence | Amp |

2.2.2.1 RNA extraction from mouse liver

In order to extract RNA from mouse liver, 50 mg of tissue were added to 1 ml of TRIzol and homogenised. After 5 min incubation at RT 200 µl chloroform were added, the sample incubated at RT again for 2-3 min and then centrifuged for 15 min at 12000 x g, 4 °C. The aqueous phase was then transferred into a new tube, 500 µl Isopropanol were added and the sample centrifuged again for 10 min at 12000 x g, 4 °C. The supernatant was subsequently removed and 1 ml of 75 % EtOH was added. After mixing the sample

was centrifuged once more at 7500 x g, 4 °C. Again, the supernatant was removed and the pellet air-dried for around 10 min. Finally, the RNA pellet was resuspended in 30 µl of nuclease-free water, incubated for 10 min at 60 °C and the RNA concentration measured using the NanoDrop 2000.

2.2.2.2 cDNA synthesis

cDNA was synthesised using the Superscript III Reverse Transcriptase kit with the extracted RNA as template. The reaction was assembled according to the manufacturer's protocol using around 1 µg of extracted RNA, 200 ng of random primers and 1 µl RiboLock (40 U/µl) as RNase Inhibitor. After the incubation step at 70 °C the sample was frozen at -20 °C without previous removal of RNA or measurement of the yield of cDNA.

2.2.2.3 Genomic DNA extraction from mouse liver

In order to extract genomic DNA from mouse liver, 50 mg of tissue were dissolved in 500 µl lysis buffer (table 15) and incubated at 55 °C, 550 rpm overnight. The following morning 500 µl of phenol:chloroform:isoamylalcohol (25:24:1) were added, the sample mixed, centrifuged for 5 min at 14000 rpm, RT and the upper aqueous phase transferred to a new tube. Subsequently, 0.6 volumes of isopropanol were added and the sample was inverted until white fibres appeared followed by centrifugation for 10 min, 14000 rpm at RT. Afterwards the supernatant was removed and the pellet washed with 500 µl of 70 % ethanol followed once more by centrifugation (10 min, 14000 rpm, RT). Finally, the ethanol was removed, the pellet air-dried and resuspended in 150 µl nuclease-free water. The concentration of the DNA was measured using the NanoDrop 2000.

2.2.2.4 PCR amplification of *Gpx1*-, *Gpx4*-, *Txnrd1*-, *Dio1* SECIS elements from mouse cDNA and *Dio2* SECIS element from mouse genomic DNA.

In order to amplify the named SECIS elements from mouse cDNA, PCR was performed.

The primers flanking the site of interest were designed to introduce a *PacI* and *NotI* restriction site using the free Primer3Plus software and are listed in table 4. The PCR reaction was assembled using 1 μ l of the synthesised cDNA, 1 μ l of $MgCl_2$ (50 mM), 0.5 μ l dNTPs (10 mM) 0.5 μ l of Fw- and Rv-primer each (10 μ M), 2.5 μ l 10 x buffer and 0.3 μ l of Taq polymerase (5U/ μ l) in a total volume of 25 μ l. The PCR cycles were performed as specified in table 9.

Subsequently, the PCR products were purified using the QIAquick Gel Extraction Kit following the manufacturer's protocol. In order to increase the yield of the amplified PCR fragments, the PCR and subsequent purification were performed multiple times, the purified products pooled, and then quantified using the NanoDrop 2000.

The same protocol was used for the amplification of the *Dio2* SECIS element from mouse genomic DNA, using 0.15 μ g of genomic DNA instead of cDNA.

Tab. 9: TaqPolymerase PCR program

| Step | | Temperature | Duration |
|----------------------|-----|-------------|----------|
| Initial Denaturation | | 95 °C | 5 min |
| Denaturation | 30x | 95 °C | 30 s |
| Annealing | | 58 °C | 30s |
| Extension | | 72 °C | 30s |
| Final extension | | 72 °C | 5 min |

2.2.2.5 Preparation of *Dio3* SECIS element from primer sequences

Since PCR amplification of the *Dio3* SECIS element did neither work from cDNA nor from genomic DNA a different approach was taken. The sense and antisense strand of the SECIS element were purchased as "primers", with a *PacI* and *NotI* restriction site designed in such a way that after the annealing of the two primers there would be overhangs as if there had been a digestion with the restriction enzymes (Fig. 11). 1 μ g of

each fw- and rv-primer each were mixed in 20 μ l TE-buffer (table 16), incubated at 95 °C for 5 min and then left to cool down at RT for around 2 h. 1 μ l of this sample was then diluted 1:10 and used for later ligation.

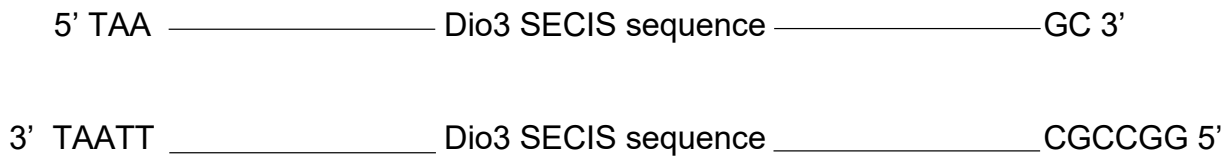


Fig. 11: Dio3 Primer scheme. The forward and reverse primers annealed with the overhanging restriction sites

2.2.2.6 Restriction digest of *Gpx1*, *Gpx4*, *Txnrd1*, *Dio1* and *Dio2* SECIS element fragments, gel electrophoresis and gel-extraction

The cleaned PCR fragments and the pcDNA3.1_Luc_1 vector were digested with PaeI and NotI restriction enzymes. 5 μ g of the vector was mixed with 5 μ l of Buffer G (10x) and 1 μ l of PaeI and NotI enzymes each in a total volume of 50 μ l. Between 0.55 and 1.6 μ g of the cleaned PCR fragments were mixed with 6 μ l of Buffer G (10x), 1 μ l of PaeI and NotI enzymes each in a total volume of 60 μ l. All of these samples were incubated at 37 °C overnight.

The digestions of the SECIS elements were then loaded onto a 2 % agarose gel with a 100 bp ladder as size control. The digested vector was loaded onto a 1 % agarose gel with a 1 kb ladder as size control. Both gels were run at 100 V for 1 h in TAE buffer (table 17), the bands corresponding to the correct size cut out and the DNA extracted using the QIAquick Gel extraction kit (table 11) following the manufacturer's protocol. The resulting DNA concentration was measured using the NanoDrop 2000.

2.2.2.7 Dephosphorylation of the digested pcDNA3.1_Luc_1 vector and ligation of the vector with the SECIS element inserts

The digested pcDNA3.1_Luc_1 vector was dephosphorylated using the FastAP

thermosensitive alkaline phosphatase (table 11) following the manufacturer's protocol. Subsequently, the dephosphorylated vector was ligated with 20-35 ng of the extracted SECIS element inserts or 10 ng in case of the annealed Dio3 insert using the buffer and ligase of the pGEM-T Easy Vector Systems (table 11). The reaction was assembled according to the manufacturer's protocol and incubated at 4 °C overnight.

2.2.2.8 Transformation of the ligated plasmids into E.coli DH5 α

The ligated plasmids were transformed into competent E.coli DH5 α bacteria following the protocol as described in 2.2.1.2 performing the centrifugation step.

2.2.2.9 Plasmid isolation of transformed bacteria

Plasmid DNA was isolated from the transformed bacteria following the protocol as described in 2.2.1.3. The integrity of the sequence was confirmed by Sanger-sequencing using the BGH rv primer.

2.2.3 Cloning and amplification of pcDNA3.1_Luc_1 with viral inserts

In order to create plasmids with a luciferase coding region containing a UGA Sec codon and a viral insert instead of a SECIS element, different viral inserts (Tab. 10) were cloned into the pcDNA3.1_Luc_1 (Tab. 8) vector.

Tab. 10: Viral inserts used for cloning

| Origin of viral insert | Accession number | Bases |
|------------------------|------------------|-----------|
| HIV-1, isolate BRU | K02013.1 | 8979-9133 |
| Zaire 1976 ebolavirus | NC_002549.1 | 2340-2398 |
| Zaire 2014 ebolavirus | KJ660346.2 | 2340-2398 |

The used HIV sequence covers both regions of the described antisense-tethering-interactions (ATI-1 and ATI-2) plus additional 10 bases on both 3' and 5' end of the

sequence. Both Ebola sequences only cover the larger region of both described antisense-tethering-interactions (ATI-1) plus 10 additional bases on both 3' and 5' end of the sequence.

2.2.3.1 Preparation of Ebola_1976 and Ebola_2014 sequences

The sense and antisense strand of both Ebola sequences were purchased as “primers”. *PacI* and *NotI* restriction sites were designed in such a way that after the annealing of the two primers there would be overhangs as if there had been a digestion with the restriction enzymes (Fig. 12). 1 µg of each fw- and rv-primer each were mixed in 20 µl TE-buffer (table 16), incubated at 95 °C for 5 min and then left to cool down at RT for around 2 h. 1 µl of this sample was then diluted 1:10 and used for later ligation.

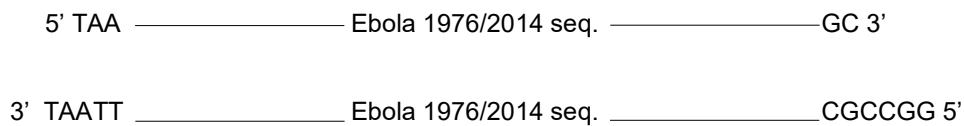


Fig. 12: Primer scheme for Ebola sequence alignments. Forward and reverse primers annealed with the overhanging restriction sites

Ligation was then performed using 10 ng of the annealed inserts following the protocol from 2.2.2.7.

Transformation was performed following the protocol from 2.2.1.2 omitting the centrifugation step.

2.2.3.2 Preparation of the HIV sequence

Since the HIV sequence was too long to be obtained completely by complementary primers, a slightly different approach was taken. Primers were designed so that each primer contained parts of the HIV sequence but both primers overlapped in their 3' sequence. Also, the primers contained the *PacI* and *NotI* restriction sites plus 4 extra nucleotides as a 5' overhang (figure 13). 2 µl of these primers in 10 µM concentration

were then mixed with 10 μ l of 10 x NEBuffer 2, 1 μ l of 100 x BSA in a total volume of 100 μ l. This sample was then incubated at 95 °C for 5 min and left to cool down at RT for around 2 hours. Afterwards 1 μ l of dNTPs (0,25 mM) and 1 μ l Klenow Fragment were added and the sample incubated for 1 h at 37 °C and then 10 min at 75 °C.

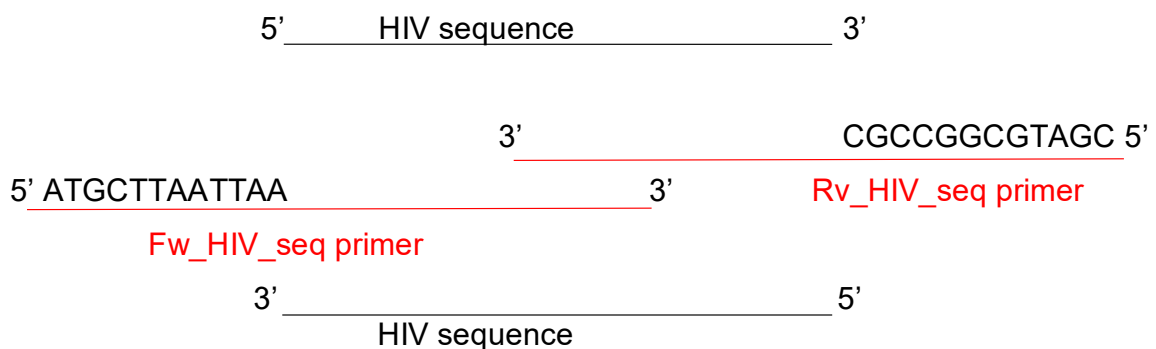


Fig. 13: Primer scheme for HIV sequence primer alignments. This shows the forward- and reverse-primer schematically in red with the overhanging restriction sites plus 4 extra nucleotides.

1 μ l of this sample was then used as a template for PCR following the same protocol as in 2.2.2.4. In order to increase the yield, the PCR was performed fourfold. Subsequently, the PCR product was purified using the QIAquick Gel Extraction Kit (table 11) following the manufacturer's protocol.

29 μ l of the purified PCR product were then digested in a total volume of 60 μ l, loaded onto a 2 % agarose gel and extracted from the gel following the protocol from 2.2.2.6.

1 μ l of the resulting HIV insert (31.4 ng/ μ l) was then ligated following the protocol from 2.2.2.7.

Transformation was performed following the protocol from 2.2.1.2 omitting the centrifugation step.

2.2.3.3 Plasmid DNA isolation from transformed bacteria

The three newly created plasmid DNAs were isolated from the transformed bacteria

following the protocol as described in 2.2.1.3. The integrity of the sequence was confirmed by Sanger sequencing using the BGH rv primer and for each SECIS element the plasmid was isolated as Midi-Prep following the already described protocol.

2.2.4 Acquisition of human Txnrd1 and Txnrd3 full length sequences

The full-length sequences of Txnrd1 and Txnrd3 were purchased as gene synthesis from BaseClear B.V. (Leiden, Netherlands) in the pBluescript II KS+ vector, using a NotI restriction site at the 5' end and a Sall restriction site at the 3' end. The integrity of the sequence was verified by Sanger sequencing using the primers listed in table 5.

Tab. 11: Kits or special reagents used in the cloning process

| Kit/reagent | Manufacturer | Catalogue number |
|--|---|------------------|
| QuikChange Lightning | Agilent (Santa Clara, CA, USA) | 210519 |
| NucleoBond® Xtra Midi | Macherey-Nagel (Düren) | 740410.100 |
| TRizol™ Reagent | Thermo Fisher Scientific (Waltham, MA, USA) | 15596026 |
| Superscript™ III Reverse Transcriptase | Thermo Fisher Scientific (Waltham, MA, USA) | 18080044 |
| Random Hexamer Primer | Thermo Fisher Scientific (Waltham, MA, USA) | SO142 |
| RiboLock (40 U/μl) | Thermo Fisher Scientific (Waltham, MA, USA) | EO0381 |
| Phenol:chloroform:isoamylalcohol 25:24:1 | SigmaAldrich (St. Louis, MO USA) | P3803 |
| BioTherm™ Taq Polymerase (5 U/μl) | GeneCraft (Köln) | GC-002 |

| Kit/reagent | Manufacturer | Catalogue number |
|---|---|-----------------------------------|
| 10x buffer BioTherm™ | GeneCraft (Köln) | Supplied with GC-002 |
| QIAquick Gel Extraction Kit | Qiagen (Venlo, Netherlands) | 28706 |
| Restriction enzymes PacI (10U/ μ l) and NotI (10U/ μ l) | Thermo Fisher Scientific (Waltham, MA, USA) | ER2201 and ER0591 |
| Buffer G (green) 10x | Thermo Fisher Scientific (Waltham, MA, USA) | Supplied with restriction enzymes |
| FastAP Thermosensitive Alkaline Phosphatase | Thermo Fisher Scientific (Waltham, MA, USA) | EF0654 |
| pGEM®-T Easy Vector Systems | Promega (Madison, WI, USA) | A1360 |
| NEBuffer™ 2 | New England Biolabs (Ipswich, MA, USA) | B7002S |
| 100 x BSA | New England Biolabs (Ipswich, MA, USA) | B9001S |
| Klenow Fragment (Large) | New England Biolabs (Ipswich, MA, USA) | M0210S |

Tab. 12: Buffers for MiniPrep

| Buffer | Component | Concentration |
|--------|-----------------------------|---------------|
| P1 | Tris-HCl pH 8 | 50 mM |
| | EDTA | 10 mM |
| | RNase A (fresh) | 100 µg/ml |
| P2 | NaOH | 200 mM |
| | SDS | 1 % |
| P3 | KCH ₃ COO pH 5,5 | 3 M |

Tab. 13: Bacteria used for DNA amplification or protein expression

| Name | Manufacturer/preparation |
|---|---|
| Chemically competent E.coli DH5 α and E.coli BL21 star | Made chemically competent by Inoue method |

Tab. 14: Preparation of LB medium and LB Agar

| Name | Preparation |
|--------------------------------|--|
| LB medium | 25 g LB broth was dissolved in 1 l purified water and autoclaved |
| LB agar plates with ampicillin | 25.6 g of LB-Agar was dissolved in 0.8 l purified water, autoclaved, left to cool to 50 °C, ampicillin was added to a final concentration of 20 µg/ml, the solution poured into sterile plates and then stored at 4 °C |
| Ampicillin | Ampicillin was dissolved to a final concentration of 100 mg/ml in 0.1 M Tris-HCl pH 8 |

Tab. 15: Lysis buffer for genomic DNA extraction

| Buffer | Components | Final concentration |
|--------------|----------------------|---------------------|
| Lysis buffer | Tris-HCl pH 8 | 10 mM |
| | EDTA | 0.1 mM |
| | NaCl | 0.15 mM |
| | SDS | 0.5% |
| | Proteinase K (fresh) | 0.5 mg/ml |
| | RNAse A | 0.5 mg/ml |

Tab. 16: TE-buffer

| Buffer | Components | Final concentration |
|----------------|------------|---------------------|
| TE-buffer pH 8 | Tris | 10 mM |
| | EDTA | 0.1 mM |

Tab. 17: TAE-buffer

| Buffer | Components | Final concentration |
|------------|-------------|---------------------|
| TAE buffer | Tris | 40 mM |
| | Acetic acid | 20 mM |
| | EDTA | 1 mM |

2.3 Expression and purification of recombinant CSECISBP2^{WT}, CSECISBP2^{RQ} and CSECISBP2^{CR} from bacterial culture

In order to purify recombinant protein, E.coli BL21 star bacteria were transformed with the previously obtained plasmids pTrcHis2-CSBP2, pTrcHis2-CSBP2_R543Q and

pTrcHis2-CSBP2_C696R. The bacteria were then grown in culture and the protein was later purified by Ni-NTA-affinity-chromatography.

2.3.1 Expression of recombinant CSECISBP2 in E.coli BL21 star

E.coli BL21 star bacteria were retransformed with 10 ng of the previously purified plasmids pTrcHis2-CSBP2, pTrcHis2-CSBP2_R543Q or pTrcHis2-CSBP2_C696R, which were obtained by Midi-Prep, following the protocol as described in 2.2.1.2 omitting the centrifugation step with direct plating of 150 μ l. A single colony of this retransformation was then dissolved in a preculture of 8 ml LB-medium with Ampicillin added to a final concentration of 100 μ g/ml and incubated at 37 °C 200 rpm overnight. The next morning, 1 ml of the preculture was inoculated in 400 ml of LB-medium with ampicillin added to a final concentration of 100 μ g/ml. This was done twice to obtain a total culture volume of 800 ml. When the cultures reached an OD₆₀₀ of around 0.6, 400 μ l IPTG (1M) were added to each culture and the cultures were further incubated at 30 °C 160 rpm for 1.5 h. Subsequently, the cultures were centrifuged for 15 min at 6000 x g and 4 °C, the supernatant was removed, the bacteria pellet air-dried, frozen in liquid nitrogen and then stored at -80 °C.

2.3.2 Ni-NTA-affinity-chromatography of recombinant CSECISBP2

All steps were performed on ice or at 4 °C in the cold room.

At first the frozen bacteria pellets were resuspended in 10 ml buffer XH1 (table 18) followed by sonication (4 x 50 s, duty cycle 50 %, output control 3.5). Then the samples were centrifuged at 4 °C, 15000 x g for 15 min. Meanwhile, 2 ml Ni-NTA agarose slurry were filled into a chromatography column. After the ethanol had dribbled out of the column, the Ni-NTA agarose beads were washed twice with 10 ml of buffer XH1. Afterwards, the supernatant from the centrifugation step was incubated with the Ni-NTA agarose beads for 2 h on a shaker before the supernatant was allowed to run through the column and was collected as flow-through. Subsequently, the beads were washed 3 times with 5 ml of buffer XH1, once with 5 ml buffer XH2 and these fractions were

collected as washing fractions W1.1, W1.2, W1.3 and W2. Then the protein was eluted with 2 ml of buffer XH3, which was collected in 2 separate fractions of 1 ml, E1.1 and E1.2. Finally, the column was closed, 1 ml of buffer XH3 was added and after 10-15 min incubation time the column was opened again and the last elution fraction collected, E1.3.

Tab. 18: Buffers for purification of bacterially expressed protein

| Buffer | Components | Final concentration |
|------------|---|---------------------|
| Buffer XH1 | Sodium phosphate pH 8 (94.7 % Na ₂ HPO ₄ , 5.3 % NaH ₂ PO ₄) | 50 mM |
| | NaCl | 1 M |
| | Tween 20 | 1 % |
| | Imidazole | 20 mM |
| | 25x cOmplete EDTA-free protease inhibitor | 1x |
| Buffer XH2 | Same as buffer XH1 but with 50 mM imidazole | |
| Buffer XH3 | Same as buffer XH1 but with 500 mM imidazole | |

2.3.3 SDS-PAGE and Coomassie Staining

SDS-PAGE and Coomassie staining was performed for all three purified proteins.

45 µl aliquots were taken from each purification fraction in order to be analysed by SDS-Page. Polyacrylamide (PA) gels were prepared using a 12.5 % PA-gel as resolving gel with an upper stacking-gel of 5 % PA following the recipe in table 19. Each 45 µl aliquot was mixed with 22.5 µl 3 x Laemmli buffer and incubated for 10 min at 95 °C before it was loaded onto the gel. The first well of the gel was loaded with a protein ladder (PageRuler™ Prestained Protein Ladder, 10 to 180 kDa, Thermo Fisher Scientific

#26616). Gel electrophoresis was then performed in running buffer at first at 90 V until the front reached the resolving gel and afterwards at 120 V until the front reached the bottom. The gel was then stained for 20 min with Coomassie Blue solution (table 20) and destained overnight.

Tab. 19: Recipes for PA-gels

| Resolving Gel (12.5 %, 20 ml) | |
|--|-------------|
| Water | 2.5 ml |
| 1.5 M Tris, 0.4 % SDS | 5 ml |
| 20 % PA Gel-solution (37.5:1 Acrylamide:Bisacrylamide) | 12.5 ml |
| TEMED | 20 μ l |
| APS | 200 μ l |
| Stacking Gel (5 %, 12 ml) | |
| Water | 6 ml |
| 1.5 M Tris, 0.4 % SDS | 3 ml |
| 20 % PA Gel-solution (37.5:1 Acrylamide:Bisacrylamide) | 3 ml |
| TEMED | 12 μ l |
| APS | 120 μ l |

Tab. 20: Buffers for SDS-PAGE and Coomassie staining

| 3 x Laemmli buffer | |
|---|----------|
| Tris-HCl pH 6.8 | 192.9 mM |
| SDS | 6 % |
| Glycerol | 30 % |
| Bromophenol blue | 0.01 % |
| β -Mercaptoethanol | 0.05 % |
| Running Buffer for SDS-PAGE | |
| Tris | 25 mM |
| Glycine | 192 mM |
| SDS | 0.1 % |
| Coomassie Blue Staining Solution (in water) | |
| Methanol | 45 % |
| Acetic acid | 10 % |
| Coomassie [®] Brilliant Blue G-250 | 0.25 % |
| Destaining solution (in water) | |
| Methanol | 40 % |
| Acetic acid | 10 % |

2.3.4 Western-Blot analysis

Western-Blot analysis was only performed for the purification of CSECISBP2^{RQ} and CSECISBP2^{CR}.

After separation by SDS-Page the proteins were transferred onto a 0.2 μ m nitrocellulose membrane (Amersham Protran 0.2 μ m NC, GE Healthcare Life Sciences, #10600001)

using a semi-dry blotter at 23 V for 1 h. Afterwards the membrane was shortly stained with Ponceau Red solution, to check if the transfer had worked. The membrane was then incubated in the blocking solution for 1 h at RT, washed with TBST-buffer and afterwards incubated with the primary antibody solution at 4 °C overnight on a shaker. On the next day the membrane was washed 3 times for 10 min with TBST-buffer at RT before it was incubated with the secondary antibody solution for 1 h at RT on a shaker. Subsequently, the membrane was washed again 3 times for 10 min with TBST-buffer at RT. Finally, the proteins were detected by chemiluminescence using the SuperSignal™ West Dura Extended Duration Substrate (Thermo Fisher Scientific, #34075) and the Fusion Solo detector (Vilber Lourmat).

Tab. 21: Buffers and Solutions for Western-Blot

| | |
|---|---------|
| Transfer Buffer | |
| Tris | 48 mM |
| Glycine | 39 mM |
| SDS | 0.033 % |
| Methanol | 20 % |
| Ponceau Red solution | |
| Ponceau S | 0.5 % |
| Acetic acid | 1 % |
| TBST-buffer | |
| Tris-HCl pH 8 | 25 mM |
| NaCl | 150 mM |
| Tween® 20 | 0.1 % |
| Blocking Solution | |
| 5 % semi-skimmed milk powder in TBST-buffer | |

| Primary Antibody solution |
|---|
| SECISBP2 rabbit antibody, polyclonal (Proteintech, 12798-1-AP) 1:1000 in TBST-buffer with 1% semi-skimmed milk powder |
| Secondary Antibody solution |
| Horseradish peroxidase-goat anti-rabbit (Jackson ImmunoResearch 111-035-003), diluted 1:15000 in TBST-buffer with 1% semi-skimmed milk powder |

2.3.5 Concentration and quantification of purified CSECISBP2

To concentrate the purified protein, the elution fractions were loaded into an Amicon[®] Ultra 2 centrifugal filter unit (Merck, UFC 803008) and centrifuged at 7000 x g for 10 min at 4 °C. The flow-through was discarded and afterwards a buffer exchange to the protein storage buffer (Tab. 22) was performed using the same filter.

The amount of protein was then quantified using the Pierce[™] BCA Protein Assay Kit (Thermo Fisher Scientific, #23225) following the manufacturer's instructions. Subsequently, 10 µl aliquots were made, frozen in liquid nitrogen and stored at -80 °C.

Tab. 22: Protein storage buffer

| Components | Final concentration |
|-------------------------------|---------------------|
| Sodiumphosphate buffer pH 7.2 | 50 mM |
| NaCl | 200 mM |
| Glycerol | 10 % |
| DTT | 1 mM |

2.4 *In-vitro* transcription from plasmid DNA

In-vitro transcription was performed for all plasmids from table 8 and the pBluescript II KS+ plasmids with both the Txnrd1 and Txnrd3 insert. Special reagents used in the process are listed in table 23.

2.4.1 Plasmid linearisation

For the pcDNA3.1 plasmids with the Gpx1, Gpx4 and Txnrd1 SECIS inserts and the pcDNA3.1_Luc_1 plasmid around 11 µg was used, for the pcDNA3.1 plasmids with the HIV and Ebola inserts around 20 µg was used and for the pcDNA3.1 with the Dio1, Dio2 and Dio3 SECIS inserts around 15 µg was used. For the pcDNA3.1_Luc plasmids 2, 3 and 5 around 5 µg was used. All these plasmids were linearised using 1.5-2 µl of XhoI (10U/µl) and 10 x buffer Red in a total volume of 30-40 µl.

For the pBluescript II KS+ vectors with the Txnrd1 and Txnrd3 inserts around 15 µg were digested using 3 and 2.5 µl of Sall, respectively, (10U/µl) and 10 x buffer Orange in a total volume of 60 and 50 µl, respectively.

All digestions took place at 37 °C overnight.

2.4.2 Phenol-chloroform extraction of digested plasmids

After checking for the success of the digestion using agarose gel electrophoresis, the digestions were filled up with water to 100 µl before 1 volume of Phenol-Chloroform-Isoamylalcohol (25:24:1) was added. The samples were mixed and cooled on ice for 10 min and afterwards centrifuged for 5 min at 12000 rpm, 4 °C. The upper aqueous phase was then transferred into a new tube and 0.5 volumes of 7.5 M ammonium acetate and 1 µl glycogen (20 mg/ml) were added. The samples were mixed and then 3 volumes of 100 % ethanol were added, before the samples were mixed again and stored at -80 °C for 30 min. Subsequently, the samples were centrifuged for 15 min at 4 °C, 13700 rpm, the supernatant discarded and 200 µl of -20 °C cold 80% ethanol were added, the samples mixed and centrifuged once more for 5 min at 12000 rpm, 4 °C. The

supernatant was then removed and after a final centrifugation step (12000 rpm, 4 °C, 5 min) all the remaining supernatant was removed before the pellet was air-dried and resuspended in 20 µl of nuclease-free water. The resulting DNA concentration was measured using the NanoDrop 2000.

2.4.3 *In-vitro* transcription reaction

All *in-vitro* transcription reactions were performed using the mMESSAGE mMACHINE T7 ULTRA Transcription kit following the manufacturer's instructions but omitting the poly-A-tailing step.

2.4.4 Phenol-chloroform extraction of mRNA

The resulting samples from the *in-vitro* transcription reactions were filled up with nuclease-free water to 100 µl before 1 volume of phenol:chloroform (5:1, pH 4.5) was added. The aqueous phase was transferred into a new tube after centrifugation for 10 min at 4 °C, 15000 rpm. 1 µl of glycogen (20mg/ml) and 0.5 volumes of ammonium acetate (7,5M) were added and the samples were mixed. Subsequently, 3 volumes of 100 % ethanol were added and the samples were mixed again. After 30 min of centrifugation at 4°C, 16400 rpm, the supernatant was discarded and 600 µl of 75 % ethanol were added before the sample was centrifuged again at 16400 rpm, 4 °C for 5 min. Afterwards the supernatant was removed again and the pellet air-dried. Finally, the pellet was resuspended in 20 µl of nuclease-free water and incubated at 62 °C for 7 min. The concentration of the RNA was measured using the NanoDrop 2000, keeping the samples on ice all the time before the samples were stored at -80 °C.

Tab. 23: Reagents used in the process of in-vitro transcription

| Reagent | Manufacturer | Catalogue number |
|--|--|--------------------------------------|
| XhoI | Thermo Fisher Scientific (Waltham, MA, USA) | ER0691 |
| Sall | Thermo Fisher Scientific (Waltham, MA, USA) | ER0645 |
| 10 x buffer Red | Thermo Fisher Scientific (Waltham, MA, USA) | Supplied with restriction enzymes |
| 10 x buffer Orange | Thermo Fisher Scientific (Waltham, MA, USA) | Supplied with restriction enzymes |
| Phenol:chloroform:isoamylalcohol 25:24:1 | SigmaAldrich (St. Louis, MO USA) | P3803 |
| mMESSAGE mMACHINE™ T7 ULTRA Transcription Kit | Thermo Fisher Scientific (Waltham, MA, USA) | AM1345 |
| Acid-Phenol:Chloroform 5:1 pH 4.5 | Thermo Fisher Scientific (Waltham, MA, USA) | AM9720 |

2.5 Luciferase assay comparing mouse SECIS elements using different SECISBP2 proteins

In-vitro translation of the *in-vitro* transcribed mRNAs was performed using rabbit-reticulocyte-lysate (RRL, table 24). The amount of translated luciferase was then quantified by measuring luminescence after adding luciferase-assay-reagent (LAR).

The *in-vitro* translation reaction was assembled in a total volume of 12.5 μ l using 6.5 μ l of rabbit reticulocyte lysate, 1.25 μ l of amino acid mixture minus leucine (0.1 mM, supplied with RRL), 1.25 μ l of amino acid mixture minus methionine (0.1 mM, supplied with RRL), 0.5 μ l RiboLock (40 U/ μ l), 2 μ l of recombinant CSECISBP2 (final concentration 160 nM or 40 nM) and 100 ng of luciferase reporter mRNA (final

concentration about 13.5 nM). The recombinant protein was diluted in Tris Acetate pH 7.2. The samples were then incubated at 30 °C for 60 min. During the incubation time the luciferase assay reagent was equilibrated to room temperature and 50 µl of 1 x PBS (table 25) was given into the wells of a 96-well plate. After the incubation 2 µl of the translation reactions were given into the wells with 50 µl 1 x PBS, 50 µl of LAR were added and the luminescence was measured at 23 °C with a wait-time of 2 seconds and a measuring-time of 10 s using the Infinite M200 Pro plate reader (table 2). For both the luciferase reporter mRNAs with murine Gpx1, Gpx4 and Txnrd1 SECIS elements and the luciferase reporter mRNAs from the plasmids pcDNA3.1_Luc_1-5 (table 8) this assay was performed using a concentration of 160 nM CSECISBP2 (a concentration previously established in our laboratory). For the luciferase reporter mRNAs with murine Dio1, Dio2 and Dio3 SECIS elements a concentration of 40 nM CSECISBP2 was used. Every SECIS element was tested using CSECISBP2^{WT}, CSECISBP2^{RQ} and CSECISBP2^{CR} in triplicates.

Tab. 24: Reagents used for luciferase assays

| Reagent | Manufacturer | Catalogue number |
|---|---|------------------|
| Rabbit Reticulocyte Lysate Nuclease Treated | Promega (Madison, WI, USA) | L4960 |
| Luciferase Assay System | Promega (Madison, WI, USA) | E1500 |
| RiboLock (40 U/µl) | Thermo Fisher Scientific (Waltham, MA, USA) | EO0381 |

Tab. 25: PBS buffer, pH 7.4

| Component | Final Concentration |
|----------------------------------|---------------------|
| NaCl | 137 mM |
| KCl | 2.7 mM |
| Na ₂ HPO ₄ | 10 mM |
| KH ₂ PO ₄ | 2 mM |

2.6 Luciferase assay comparing CSECISBP2^{WT} and CSECISBP2^{RQ} by titrating luciferase reporter mRNA

Another set of luciferase assays was performed to further compare CSECISBP2^{WT} with CSECISBP2^{RQ}. 9 different dilutions of luciferase reporter mRNAs were made and 1 μ l of these was added to a mixture of 6.5 μ l of RRL, 2.5 μ l of amino acid mixtures (0.1 mM), 2 μ l of diluted CSECISBP2 protein (final concentration 80 nM) and 0,5 μ l of RiboLock (40 U/ μ l). The samples were then incubated at 30 °C for 60 min. During the incubation time the luciferase assay reagent was equilibrated to room temperature and 50 μ l of 1 x PBS was given into the wells of a 96-well plate. After the incubation time 6 μ l of the translation reactions were given into the wells with 50 μ l 1 x PBS, 50 μ l of LAR were added and the luminescence was measured at 23 °C with a wait-time of 2 seconds and a measuring-time of 10 s using the Infinite M200 Pro plate reader (table 2). Every SECIS element was tested with the concentrations as specified in Tab. 26 in triplicates.

Tab. 26: mRNA concentrations used for the luciferase titration assays. Data points 1-9 show the mRNA concentrations used for each reporter mRNA. For the luciferase reporter with the mGpx4 SECIS, different mRNA concentrations were used in regard to CSECISBP2^{WT} and CSECISBP2^{RQ} (they differ from data point 6-9)

| Data Point | mGpx1 SECIS (nM) | mGpx4 SECIS with CSECISBP2 ^{WT} (nM) | mGpx4 SECIS with CSECISBP2 ^{RQ} (nM) | mTxnrd1 SECIS (nM) | mDio1 SECIS (nM) | mDio2 SECIS (nM) | mDio3 SECIS (nM) |
|------------|------------------|---|---|--------------------|------------------|------------------|------------------|
| 1 | 0.11 | 0.11 | 0.11 | 0.11 | 0.11 | 0.2 | 0.11 |
| 2 | 0.44 | 0.44 | 0.44 | 0.43 | 0.42 | 0.39 | 0.43 |
| 3 | 0.88 | 0.88 | 0.88 | 0.86 | 0.85 | 0.79 | 0.85 |
| 4 | 1.76 | 1.75 | 1.75 | 1.72 | 1.7 | 1.58 | 1.71 |
| 5 | 3.51 | 3.51 | 3.51 | 3.44 | 3.39 | 3.16 | 3.41 |
| 6 | 7.03 | 7.02 | 4.68 | 6.88 | 6.79 | 6.31 | 6.82 |
| 7 | 10.54 | 10.52 | 7.02 | 10.32 | 10.18 | 9.47 | 10.23 |
| 8 | 14.06 | 14.03 | 10.52 | 13.76 | 13.58 | 12.62 | 13.64 |
| 9 | 21.08 | 21.05 | 14.03 | 20.64 | 20.37 | 18.94 | 20.47 |

2.7 Luciferase assay comparing the temperature stability of CSECISBP2^{WT} and CSECISBP2^{RQ}

In order to compare the temperature stability of CSECISBP2^{WT} and CSECISBP2^{RQ}, both proteins were diluted in Tris Acetate pH 7.2 to a concentration of 0.05665 $\mu\text{g}/\mu\text{l}$ (final concentration 160 nM). 2 μl of these diluted proteins were then incubated for 30 min either on ice or at 37 °C. After this incubation 6.5 μl RRL, 2.5 μl of amino acid mixtures (0.1 mM), 0.5 μl RiboLock (40 U/ μl) and 1 μl of luciferase reporter mRNA carrying a

murine Gpx4 SECIS element (94.3 ng/ μ l) were added. The samples were then incubated at 30 °C for 1 hour. During the incubation time the luciferase assay reagent was equilibrated to room temperature and 50 μ l of 1 x PBS was given into the wells of a 96-well plate. After the incubation time 2 μ l of the translation reactions were given into the wells with 50 μ l 1 x PBS, 50 μ l of LAR were added and the luminescence was measured at 23 °C with a wait-time of 2 seconds and a measuring-time of 10 s using the Infinite M200 Pro plate reader (table 2).

The experiment was repeated with a 30 min incubation of the proteins at 40.5 °C. Both experiments were performed in triplicates.

2.8 Luciferase assays investigating potential viral SECIS element recruitment

To test a viral in-trans SECIS element recruitment a luciferase assay was performed using luciferase reporter mRNA with the viral sequences in the 3' UTR and the full length Txnrd1 and Txnrd3 mRNAs. 6.5 μ l RRL, 2.5 μ l of amino acid mixtures (0.1 mM), 0.5 μ l RiboLock (40 U/ μ l) and 1 μ l CSECISBP2^{WT} (final concentration 160 nM) were each pipetted into 11 tubes in triplicates. Then mRNAs were added following the scheme in Tab. 27.

The samples were then incubated at 30 °C for 1 hour. During the incubation time the luciferase assay reagent was equilibrated to room temperature and 50 μ l of 1 x PBS was given into the wells of a 96-well plate. After the incubation time 2 μ l of the translation reactions were given into the wells with 50 μ l 1 x PBS. 50 μ l of LAR were added and the luminescence was measured at 23 °C with a wait-time of 2 seconds and a measuring-time of 10 s using the Infinite M200 Pro plate reader (Tab. 2).

The assay was repeated on a smaller scale with the mRNAs being previously incubated at 95 °C. The mRNAs were mixed as specified in Tab. 28, then incubated at 95 °C for 5 min and left to cool down at RT for 30 min. Two tubes were filled with 6.5 μ l RRL, 2.5 μ l of amino acid mixtures (0.1 mM), 0.5 μ l RiboLock (40 U/ μ l) and 1 μ l CSECISBP2^{WT} (final concentration 160 nM) in triplicates. 2 μ l of the mRNA mixtures were added and two tubes of the same mRNA sample were then incubated at 30 °C for 1 hour, the other tube at 37 °C for 1 hour. During the incubation time the luciferase assay reagent was

equilibrated to room temperature and 50 μl of 1 x PBS was given into the wells of a 96-well plate. After the incubation time 6 μl of the translation reactions were given into the wells with 50 μl 1 x PBS, 50 μl of LAR were added and the luminescence was measured at 23 °C with a wait-time of 2 seconds and a measuring-time of 10 s using the Infinite M200 Pro plate reader (table 2).

Tab. 27: Scheme for mRNA addition for viral luciferase assay

| Sample | Added mRNAs |
|--------|---|
| 1 | 2 μl H ₂ O |
| 2 | 1 μl Luciferase_mGpx1 SECIS mRNA (100 ng/ μl) + 1 μl H ₂ O |
| 3 | 1 μl Luciferase_HIV mRNA (93.9 ng/ μl) + 1 μl full length Txnrd1 mRNA (84,3 ng/ μl) |
| 4 | 1 μl Luciferase_HIV mRNA (93.9 ng/ μl) + 1 μl full length Txnrd3 mRNA (107.7 ng/ μl) |
| 5 | 1 μl Luciferase_Ebola_2014 mRNA (95.4 ng/ μl) + 1 μl full length Txnrd1 mRNA (84,3 ng/ μl) |
| 6 | 1 μl Luciferase_Ebola_2014 mRNA (95.4 ng/ μl) + 1 μl full length Txnrd3 mRNA (107.7 ng/ μl) |
| 7 | 1 μl Luciferase_Ebola_1976 mRNA (90.1 ng/ μl) + 1 μl full length Txnrd1 mRNA (84,3 ng/ μl) |
| 8 | 1 μl Luciferase_Ebola_1976 mRNA (90.1 ng/ μl) + 1 μl full length Txnrd3 mRNA (107.7 ng/ μl) |
| 9 | 1 μl Luciferase_HIV mRNA (93.9 ng/ μl) + 1 μl H ₂ O |
| 10 | 1 μl Luciferase_Ebola_2014 mRNA (95.4 ng/ μl) + 1 μl H ₂ O |
| 11 | 1 μl Luciferase_Ebola_1976 mRNA (90.1 ng/ μl) + 1 μl H ₂ O |

Tab. 28: Scheme for mRNA mixtures for luciferase assay with 95 °C incubation

| Sample | Added mRNAs |
|--------|---|
| 1 | 5 μ l Luciferase_HIV mRNA (93.9 ng/ μ l) + 10 μ l full length Txnrd1 mRNA (84.3 ng/ μ l) |
| 2 | 5 μ l Luciferase_Ebola_2014 (95.4 ng/ μ l) + 10 μ l full length Txnrd3 mRNA (107.9 ng/ μ l) |

2.9 Agarose gel-shift assay with luciferase mRNAs with viral inserts and full length Txnrd1 and Txnrd3 mRNAs

In order to detect a possible base-pairing and therefore gel-shifting of the luciferase mRNAs with the viral inserts and the full length Txnrd1 and Txnrd3 mRNAs an agarose gel-shift assay was performed.

The mRNAs were diluted in water after the scheme in table 29, incubated at 95 °C for 2 or 5 min, left to cool down at RT for around 25 min, mixed with 3 μ l 6 x loading buffer (table 30), loaded onto a 70 ml 1 % agarose gel with 6 μ l Ethidium bromide (5 mg/ml) and then run in TAE buffer (table 17) at 100 V for 1 hour. 7 μ l of the GeneRuler 1 kb DNA ladder (table 3) was run in the first well. In total 3 gels were run with different mRNAs.

Tab. 29: Scheme for mRNA mixing for gel-shift assay

| Gel 1 | | |
|-------------|---|--------------------------|
| Well number | Added mRNAs | Incubation time at 95 °C |
| 2 | 1.5 µl Luciferase_Ebola_2014 mRNA (1300.7 ng/µl) + 13.5 µl H ₂ O | 2 min |
| 3 | 1.5 µl full length Txnrd3 mRNA (1034.3 ng/µl) + 13.5 µl H ₂ O | |
| 4 | 1.5 µl Luciferase_Ebola_2014 mRNA (1300.7 ng/µl) + 1.5 µl full length Txnrd3 mRNA (1034.3 ng/µl) + 12 µl H ₂ O | |
| Gel 2 | | |
| Well number | Added mRNAs | Incubation time at 95 °C |
| 2 | 3 µl Luciferase_HIV mRNA (635 ng/µl) + 12 µl H ₂ O | 5 min |
| 3 | 3 µl Luciferase_HIV mRNA (635 ng/µl) + 2 µl full length Txnrd1 mRNA (627.4 ng/µl) + 10 µl H ₂ O | |
| 4 | 1.5 µl Luciferase_Ebola_2014 mRNA (1300.7 ng/µl) + 13.5 µl H ₂ O | |
| 5 | 1.5 µl full length Txnrd3 mRNA (1034.3 ng/µl) + 13.5 µl H ₂ O | |
| 6 | 1.5 µl Luciferase_Ebola_2014 mRNA (1300.7 ng/µl) + 1.5 µl full length Txnrd3 mRNA (1034,3 ng/µl) + 12 µl H ₂ O | |
| Gel 3 | | |
| Well number | Added mRNAs | Incubation time at 95 °C |
| 2 | 3 µl Luciferase_HIV mRNA (635 ng/µl) + 12 µl H ₂ O | 5 min |
| 3 | 3 µl full length Txnrd1 mRNA (497.3 ng/µl) + 12 µl H ₂ O | |
| 4 | 3 µl Luciferase_HIV mRNA (635 ng/µl) + 3 µl full length Txnrd1 mRNA (497.3 ng/µl) + 9 µl H ₂ O | |

Tab. 30: 6 x loading buffer

| Components | Final concentration |
|------------------|---------------------|
| Glycerol | 30 % |
| Bromophenol blue | 0.3 % |
| Xylene Cyanol | 0.3 % |

3. Results

3.1 Results of protein purification

Murine CSECISBP2^{WT}, CSECISBP2^{RQ} and CSECIBSP2^{CR} were recombinantly expressed in bacteria and purified via Ni-NTA-chromatography. The collected fractions were then analysed by SDS-PAGE and in case of CSECISBP2^{RQ} and CSECISBP2^{CR} also by Western blot. The elution fractions were then concentrated and the protein concentration measured.

3.1.1 Results for purification of CSECISBP2^{RQ}

Figure 14 shows the different protein fractions collected after chromatography that were electrophoresed in a PA-gel, transferred to a membrane and stained with Ponceau S. The proteins on the membrane were then further analysed by Western blot using an anti-SECISBP2 antibody. The results are shown in figure 15.

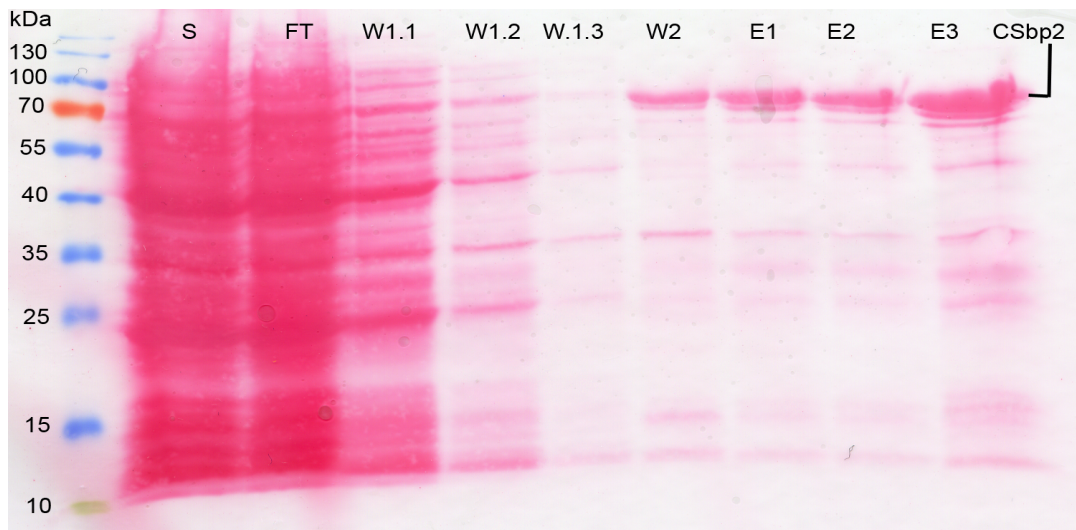


Fig. 14: Ponceau staining of membrane after transfer from PA gel for CSECISBP2^{RQ} purification. The columns represent the different fractions that were collected from the Ni-NTA-purification. S = supernatant fraction, FT = flow-through fraction, W1.1-1.3 = washing fractions 1.1-1.3, W2 = washing fraction 2, E1-3 = elution fractions 1-3, CSbp2 = band that corresponds to CSECISBP2. The outmost left column shows protein marker with the sizes of the proteins in kDa

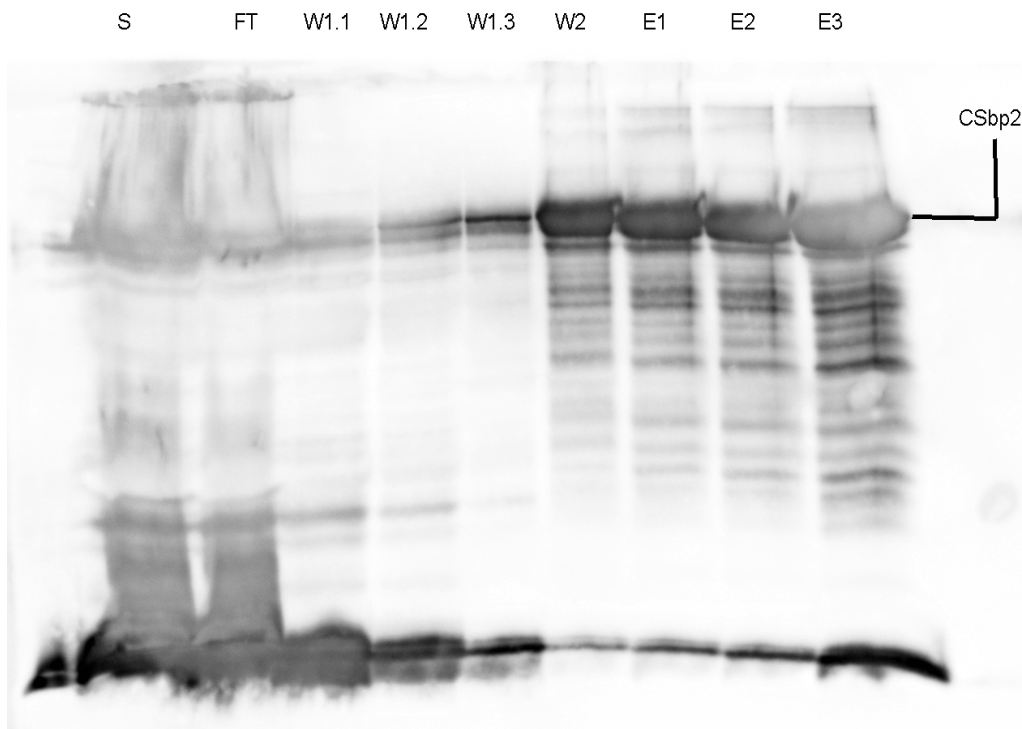


Fig. 15: Western blot results from the purification of CSECISBP2^{RQ}. The columns represent the same fractions as in figure 14.

Figure 14 shows a thick band that correlates to CSECISBP2, which also yields a very intense band in the Western blot. The signal is so intense that the band starts to become white due to a burning of the membrane. Both the ponceau staining and the Western blot show proteins that are smaller than CSECISBP2. Also, there seem to be some bands around 15 kDa in the ponceau staining that do not appear in the Western blot. The lower protein bands that do appear in the Western blot could be truncated parts of CSECISBP2 and are therefore smaller than the full-length CSECISBP2 but are recognised by the anti-CSECISBP2 antibody. However, it is also possible that the antibody does unspecifically bind to other proteins and for that reason other proteins, smaller than CSECISBP2 appear in the Western blot. The bands lower than the CSECISBP2 band that do not appear in the Western blot could be either other proteins that are to a small extent present in the elution fractions or truncated fragments of CSECISBP2 that do no longer carry the epitope that is recognised by the anti-CSECISBP2 antibody.

3.1.2 Results for purification of CSECISBP2^{CR}

Figure 16 shows once more the membrane to which the proteins were transferred from the PA gel, this time for CSECISBP2^{CR}. Western blot was performed for further analysis using an anti-SECISBP2 antibody. The results are shown in figure 17.

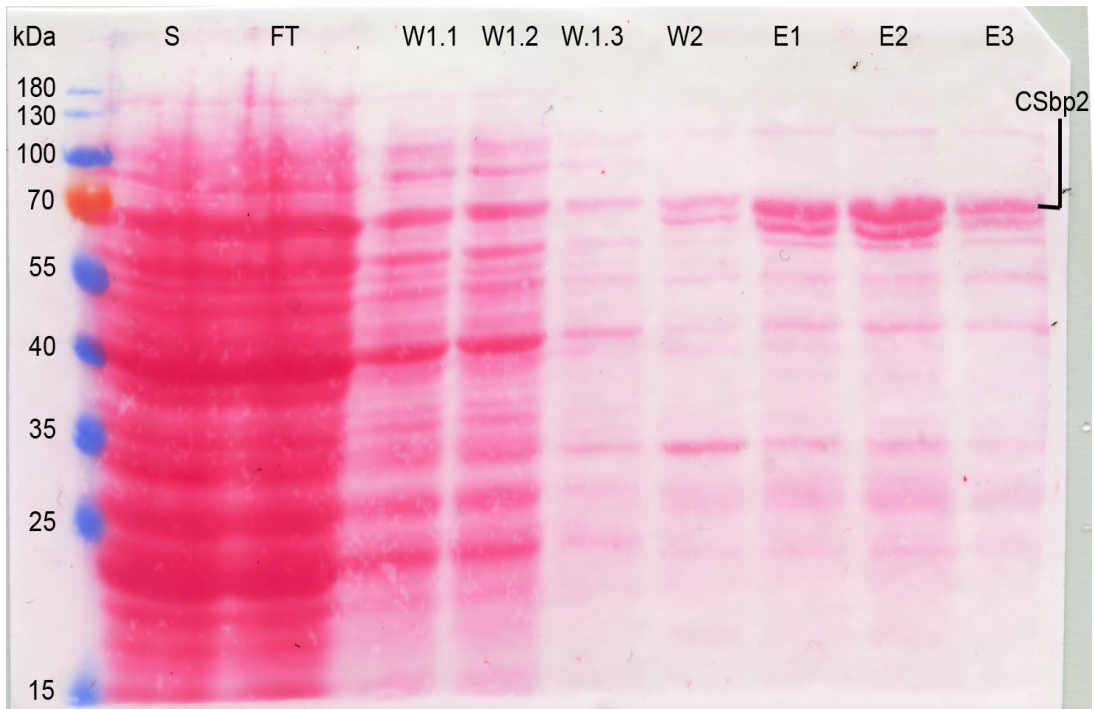


Fig. 16: Ponceau staining of membrane after transfer of the proteins from PA gel for CSECISBP2^{CR} purification. The columns represent the different fractions that were collected from the Ni-NTA-purification. S = supernatant fraction, FT = flow-through fraction, W1.1-1.3 = washing fractions 1.1-1.3, W2 = washing fraction 2, E1-3 = elution fractions 1-3, CSbp2 = band that corresponds to CSECISBP2. The outmost left column shows protein marker with the sizes in kDa

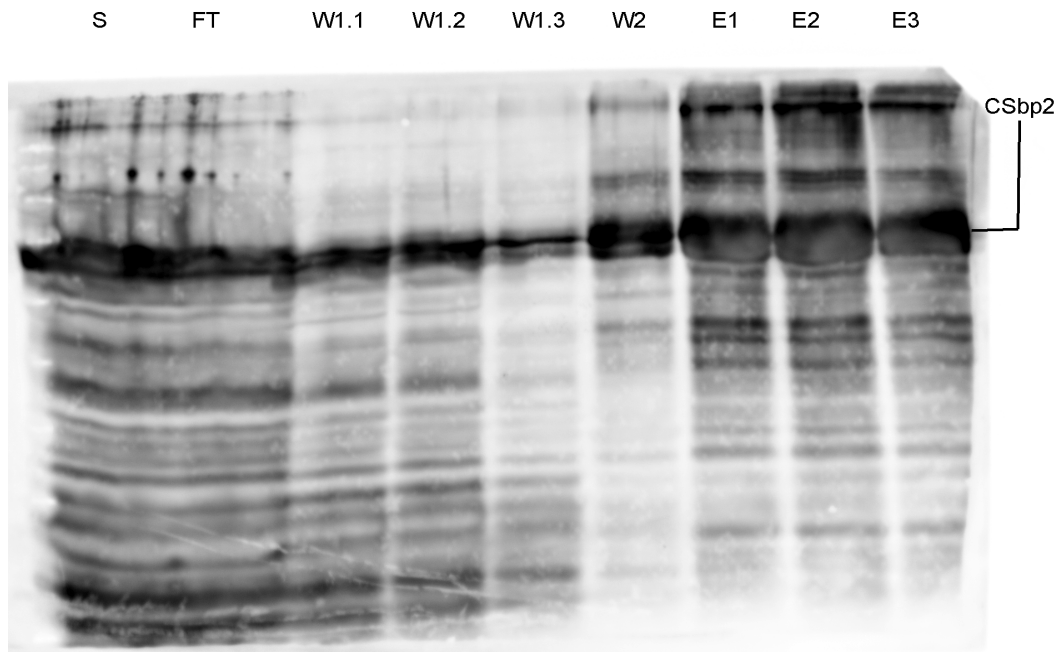


Fig. 17: Western blot results from the purification of CSECISBP2^{CR}. The columns represent the same fractions as in figure 16.

Again, it can be seen that there is a thick band corresponding to CSECISBP2 in both the ponceau staining and the Western blot. In the Western blot this band can be seen in all fractions but is most prominent in the elution fractions. The band that correlates to CSECISBP2 in the elution fractions is also turning a bit white due to a burning of the membrane. In the elution fractions there are also a lot of bands visible both higher and lower than the CSECISBP2 band but these bands are less prominent than the band for CSECISBP2. Similar to the results from the purification of CSECISBP2^{RQ} the bands that are lower than the full-length CSECISBP2 band but do appear in the Western blot are likely products of proteolytic digestion. The bands that are higher than the full-length CSECISBP2 band could be either proteins that are unspecifically recognised by the anti-CSECISBP2 antibody or an aggregation-product of CSECISBP2 protein parts which are specifically recognised by the antibody.

3.1.3 Results for purification of CSECISBP2^{WT}

After the initial Coomassie staining of the PA gel with all fractions (picture not shown) the

elution fractions were concentrated. SDS-PAGE of the concentrated protein was performed and stained with Coomassie. The result can be seen in figure 18.

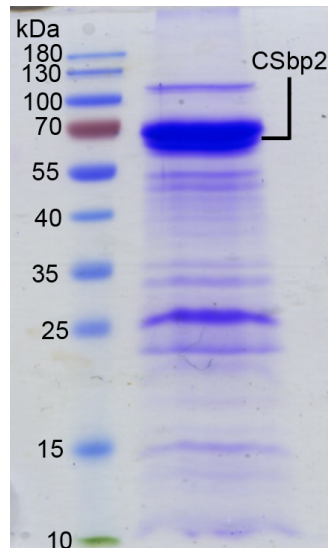


Fig. 18: Result from SDS-PAGE with Coomassie staining of the concentrated CSECISBP2^{WT} elution. The band that correlates to CSECISBP2 is marked CSbp2. The outmost left column shows protein marker with the sizes in kDa.

Similar to the results for the purification for CSECISBP2^{RQ} and CSECISBP2^{CR} a thick band can be seen that corresponds to the size of CSECISBP2 from earlier experiments. Also, one band which is higher than the CSECISBP2 and lots of bands lower than CSECISBP2 can be seen. Western blot analysis was not performed. Similar to the purifications of CSECISBP2^{RQ} and CSECISBP2^{CR} the bands that are smaller than the CSECISBP2 band could be either truncated parts of full-length CSECISBP2 or other proteins that are present as impurities. The band which is higher than the CSECISBP2 band could be caused by an aggregation of CSECISBP2 parts or by another protein which is bigger than CSECISBP2.

3.2 Results from luciferase assay comparing CSECISBP2^{WT}, CSECISBP2^{RQ} and CSECISBP2^{CR} in regard to different SECIS elements

Tab. 31: Schematic pictures of different luciferase reporters. This table shows a scheme for the mRNAs that were used for the luciferase assays of Fig. 19 and 20 and their corresponding abbreviations.

| mRNA name | Abbreviation in graphs | Schematic picture |
|-------------|------------------------|-------------------|
| Luc_mGpx1 | Gpx1 | |
| Luc_mGpx4 | Gpx4 | |
| Luc_mTxnrd1 | Txnrd1 | |
| Luc_2 | AUGA del | |
| Luc_1 | No CSbp2 | |
| Luc_3 | Luc_UAA | |

| mRNA name | Abbreviation in graphs | Schematic picture |
|-----------|------------------------|-------------------|
| Luc_mDio1 | Dio1 | |
| Luc_mDio2 | Dio2 | |
| Luc_mDio3 | Dio3 | |

Luciferase Assay CSbp2 WT vs CR and RQ mutant

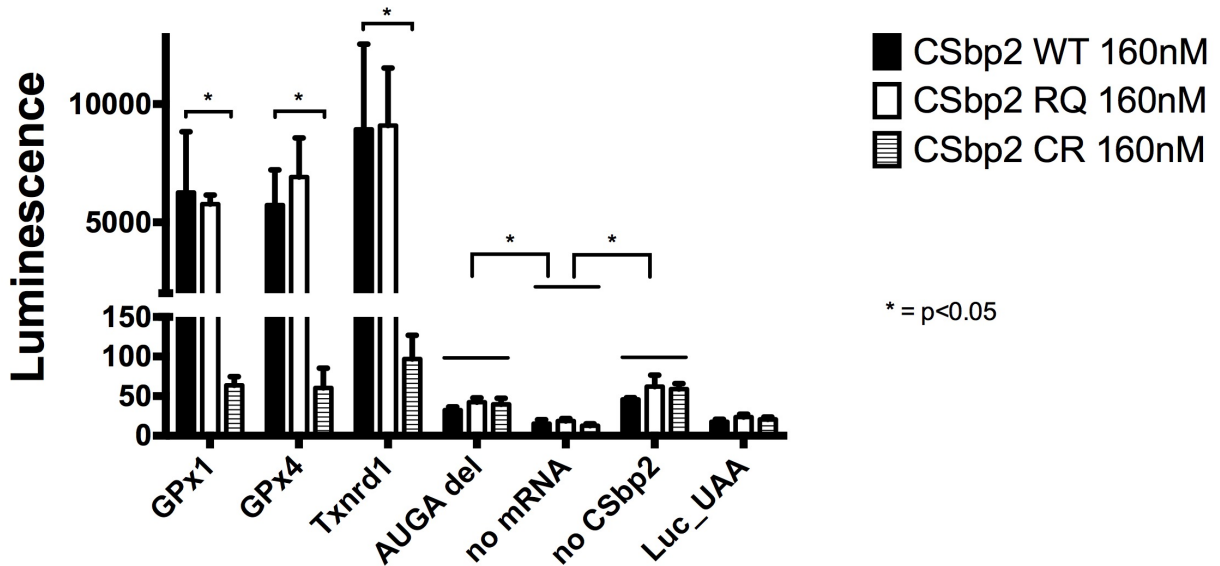


Fig. 19: Luciferase Assay comparing the mouse *Gpx1*, *Gpx4* and *Txnrd1* SECIS elements in regard to CSECISBP2^{WT}, CSECISBP2^{RQ} and CSECISBP2^{CR}. The y-axis shows the measured luminescence and is broken in order to show all the data. The x-axis shows which mRNAs were used (for explanation of names see table 31). No CSECISBP2 was added in the column named “no CSbp2” and no mRNA was added in the column named “no mRNA”. CSECISBP2 concentration was 160 nM, 100 ng of reporter mRNA was used (around 13.5 nM). The graph shows the mean value of triplicates, the error bar shows one SD.

Figure 19 shows the data from the luciferase assay comparing CSECISBP2^{WT}, CSECISBP2^{RQ} and CSECISBP2^{CR} in regard to different SECIS elements. No CSECISBP2 was added in the column named “no CSbp2”. It can be seen that all negative controls (AUGA del, no mRNA, no CSbp2, Luc_UAA) show low luminescence values below 100. Within this group of negative controls, the highest luminescence can be seen for the Luc_1 without CSECISBP2. All three reporter mRNAs with functional SECIS elements (*Gpx1*, *Gpx4*, *Txnrd1*) show luminescence values between 5000 and 10000 for both CSECISBP2^{WT} and CSECISBP2^{RQ} with the highest luminescence values at the *Txnrd1* SECIS reporter. For CSECISBP2^{CR} the same reporters show only luminescence values between 50 and 100.

The difference between the values for CSECISBP2^{WT} and CSECISBP2^{CR} for the *Gpx1*, *Gpx4* and *Txnrd1* reporters was calculated to be significant by a two-tailed unpaired student's t-test. The differences between CSECISBP2^{RQ} and CSECISBP2^{WT} were analysed by the same test, but no significant difference was found.

The differences within the group of negative control were analysed by paired two-tailed student's t-test. It can be seen that both the luciferase reporter with the AUGA deletion within the SECIS element and the Luc_1 reporter without CSECISBP2 show significantly higher luminescence values than the background (no mRNA). However, compared to the luminescence values of the complete SECIS elements these values are very low. Therefore, it can be said that very low but significant readthrough of the UGA codon takes place with both the AUGA deletion within the SECIS element and without CSECISBP2.

Figure 20 shows the results of the luciferase assay comparing the *Dio1*, *Dio2* and *Dio3* SECIS elements in regard to the different CSECISBP2 proteins.

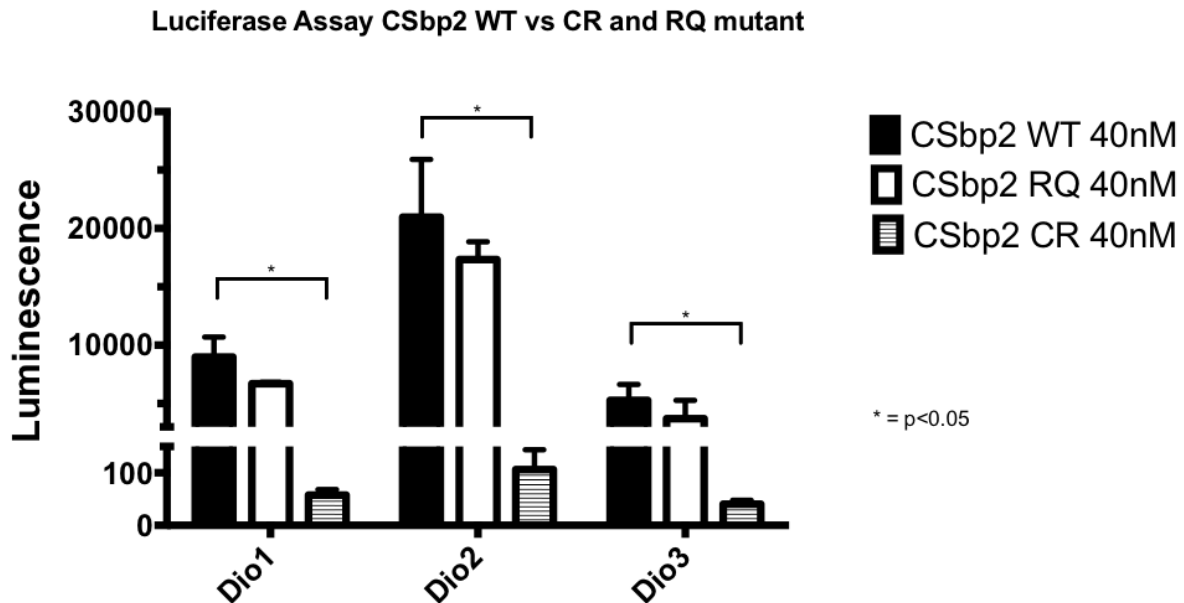


Fig. 20: Results from the luciferase assay comparing CSECISBP2^{WT}, CSECISBP2^{RQ} and CSECISBP2^{CR} for the luciferase reporters carrying a Dio1, Dio2 or Dio3 SECIS element (see table 31 for explanation of the used reporters). The y-axis shows the measured luminescence and is broken in order to show all the data. CSECISBP2 concentration was 40 nM, 100 ng of reporter mRNA was used (around 13.5 nM). Values shown are the mean of triplicates, error bars show one SD.

It can be seen that similar to the results from *Gpx1*, *Gpx4* and *Txnrd1* very low luminescence was measured for CSECISBP2^{CR}. CSECISBP2^{WT} and CSECISBP2^{RQ} show much higher luminescence values with the values of CSECISBP2^{RQ} always a little lower than CSECISBP2^{WT}. The highest luminescence was measured when the reporter contained a *Dio2* SECIS element, the least when the reporter contained a *Dio3* SECIS element. The differences between CSECISBP2^{WT} and CSECISBP2^{CR} were calculated to be significant by a two-tailed unpaired student's t-test. The same test was used to analyse the differences between CSECISBP2^{WT} and CSECISBP2^{RQ} but no significant difference was found. The fact that the concentration of CSECISBP2 was reduced to 40 nM as compared to 160 nM in the previous experiment is discussed later.

3.3 Results from luciferase assays comparing CSECISBP2^{WT} and CSECISBP2^{RQ} by titration of mRNA reporters

Figures 21 and 22 show the results for the comparison of CSECISBP2^{WT} and CSECISBP2^{RQ} with titrated Luc_mGpx1, Luc_mGpx4 and Luc_mTxnrd1 mRNA as well as Luc_mDio1, Luc_mDio2 and Luc_mDio3 mRNA. It can be seen that the luminescence values are considerably lower for the RQ mutant when the Gpx1, Gpx4 or Txnrd1 SECIS elements were used. Similarly, luminescence was also reduced for CSECISBP2^{RQ} using the Dio1, Dio2 and Dio3 SECIS elements, but the reduction in luminescence was not as evident. This result seems to be in contrast to the results of the luciferase assay without titration, since this experiment shows a considerable difference between the absolute luminescence values comparing CSECISBP2^{RQ} and CSECISBP2^{WT} that was not observable beforehand (compare fig. 19 and 20). However, this may be explained by the lower concentration of CSECISBP2 that was used (80 nM instead of 160 nM regarding Luc_mGpx1, Luc_mGpx4 and Luc_mTxnrd1).

To see if there are differences for CSECISBP2^{WT} and CSECISBP2^{RQ} in their ability to both bind to the SECIS element and then promote Sec incorporation, Michaelis-Menten kinetic was assumed to calculate and compare a K_m value. This K_m value was then compared so that any differences in the amount of active protein within the samples of CSECISBP2^{WT} and CSECISBP2^{RQ} could be eliminated. In order to compare the K_m values an extra sum of squares F test was performed with H_0 being that the K_m is the same for both data sets and H_1 being that the K_m is different for both data sets. Significant differences were found for the Txnrd1 and Dio1 SECIS element for which the K_m is significantly higher in the CSECISBP2^{RQ}-samples.

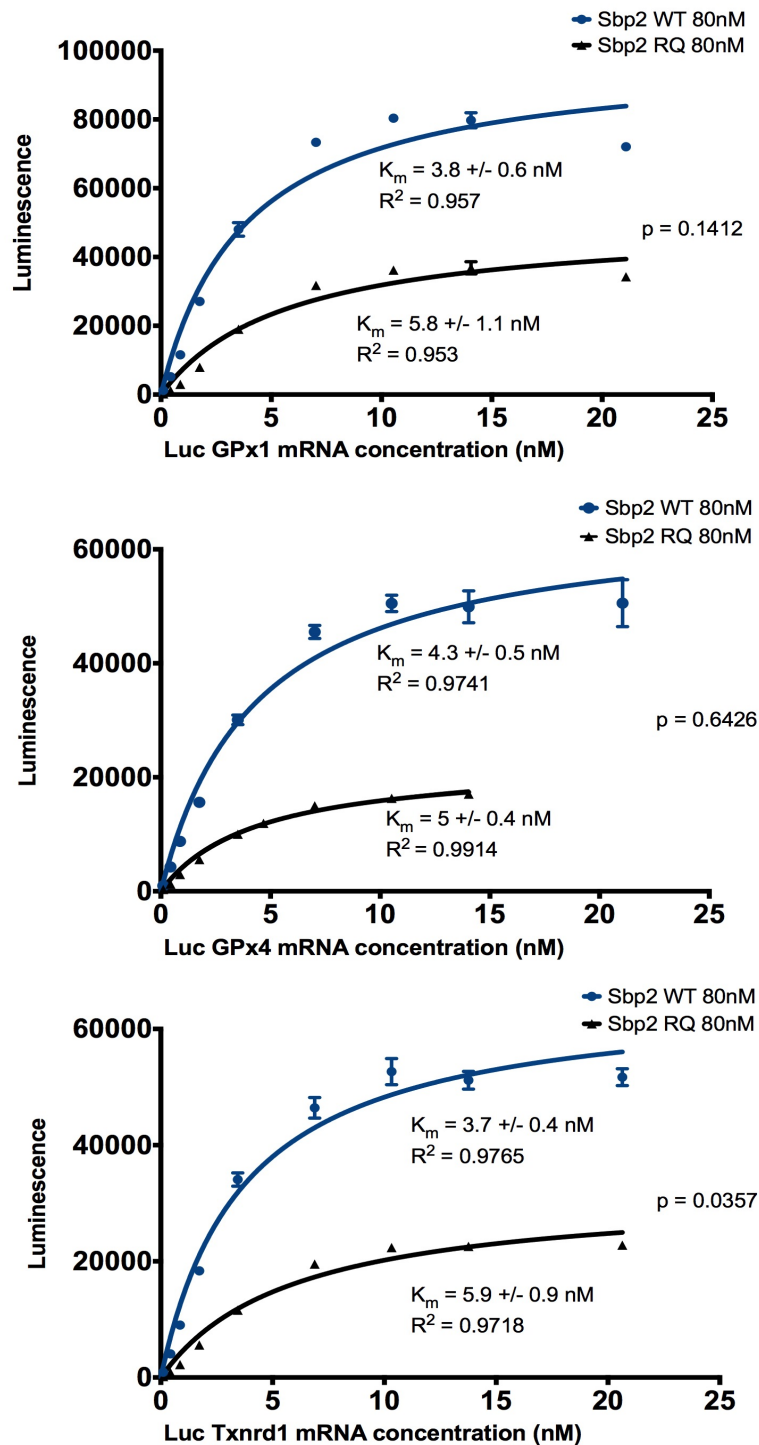


Fig. 21: Results for the comparison of CSECISBP2^{WT} and CSECISBP2^{RQ} with titrated Luc_mGpx1, Luc_mGpx4 and Luc_mTxnrd1 mRNA reporter. Values are shown as mean of triplicates, the error bars show one SD. The interpolated lines were made with the Michaelis-Menten least-squares function of GraphPad Prism 6. K_m and R^2 were calculated by the software and are written beneath or above the respective lines. P values were calculated by Extra Sum of Squares F Test. Modified after Zhao et al., (2019).

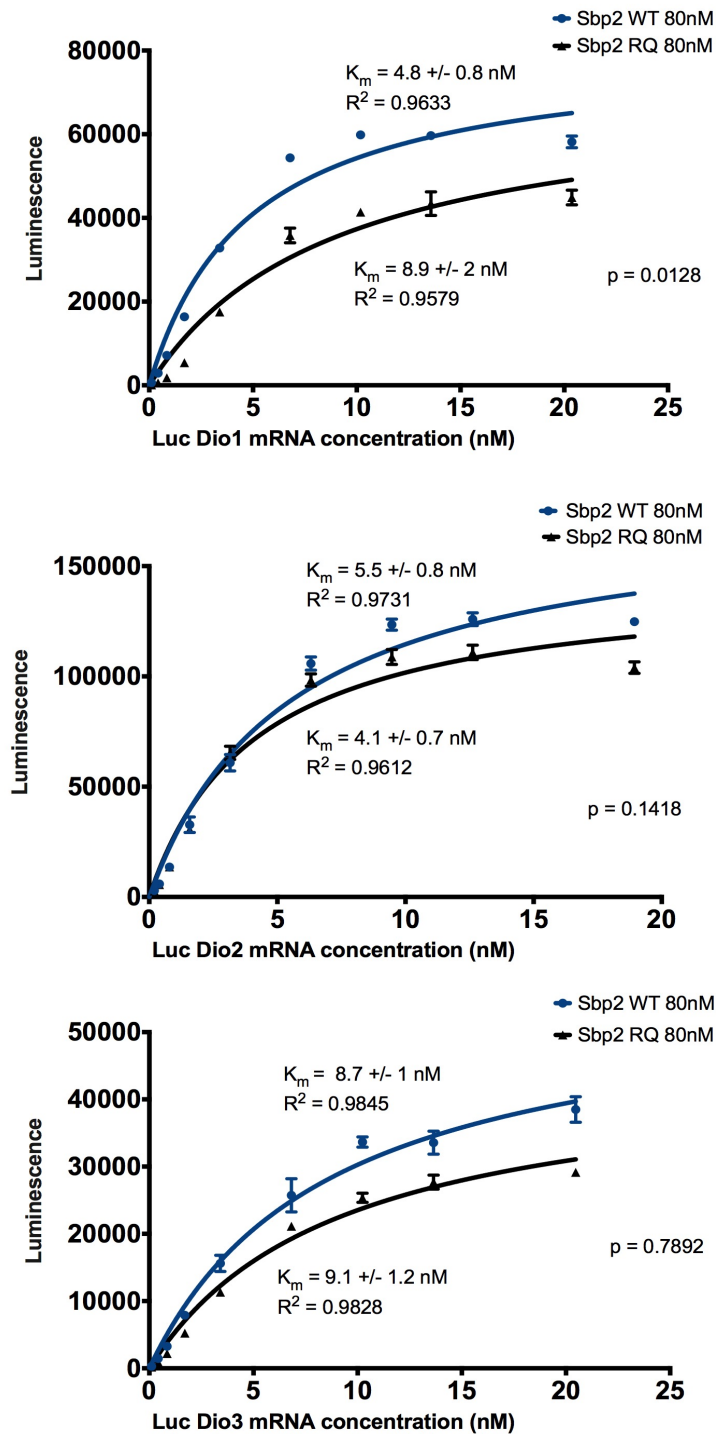


Fig. 22: Results for the comparison of CSECISBP2^{WT} and CSECISBP2^{RQ} with titrated Luc_mDio1, Luc_mDio2 and Luc_mDio3 mRNA reporter. Values are shown as mean of triplicates, the error bars show one SD. The interpolated lines were made with the Michaelis-Menten least-squares function of GraphPad Prism 6. K_m and R^2 were calculated by the software and are written beneath or above the respective lines. P values were calculated by Extra Sum of Squares F Test. Modified after Zhao et al., (2019).

3.4 Results from luciferase assays comparing thermostability of CSECISBP2^{WT} and CSECISBP2^{RQ}

Figure 23 shows the results of comparisons of the thermostability of CSECISBP2^{WT} and CSECISBP2^{RQ}. It can be seen that when the proteins were kept on ice the luminescence values of CSECISBP2^{WT} and CSECISBP2^{RQ} are similar with the CSECISBP2^{RQ} value being slightly higher. When the proteins were incubated at 37 or 40.5 °C the luminescence values for both the wild-type and the mutated protein decrease. However, the luminescence values of the CSECISBP2^{RQ}-samples diminish more than those of the CSECISBP2^{WT}-samples. This difference in decrease of Sec-incorporation-activity is even more evident in the relative data. CSECISBP2^{WT} retains about twice as much percentage activity as CSECISBP2^{RQ} when incubated at 37 or 40.5 °C and this difference was tested to be significant by an unpaired, two-tailed student's t-test. This seems to indicate that CSECISBP2^{RQ} is thermally less stable than CSECISBP2^{WT}.

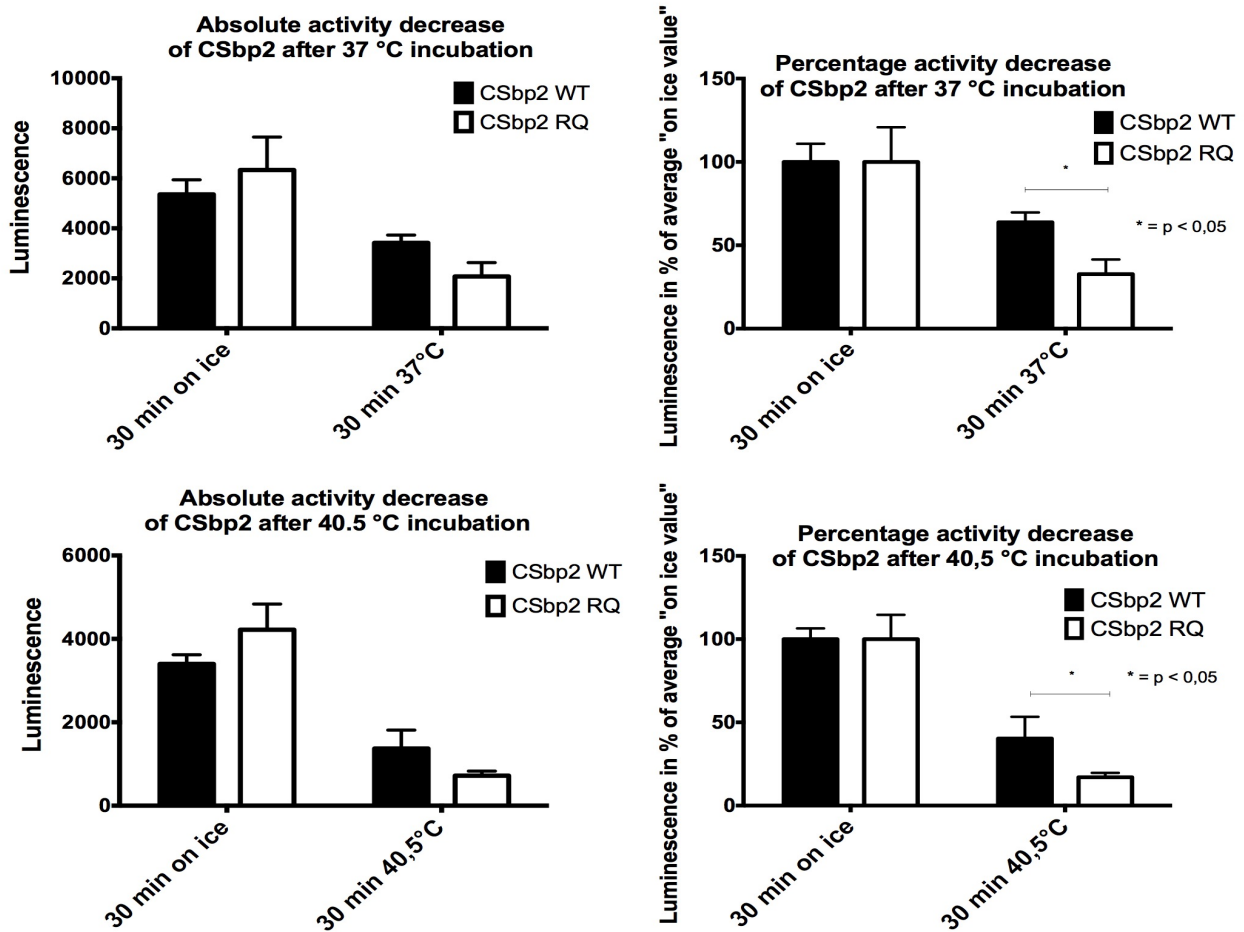


Fig. 23: Luciferase assays comparing the temperature stability of CSECISBP2^{WT} and CSECISBP2^{RQ}. The first line shows the results for 30 min incubation at 37 °C, the second line shows the results for 30 min incubation at 40.5 °C. The second column shows the calculated relative values of the first column. Values are shown as mean of triplicates, error bars show one SD. P value was calculated by unpaired, two-tailed student's t-test.

3.5 Results of luciferase assay investigating possible viral SECIS recruitment

Different luciferase assays were performed to investigate a possible viral SECIS element recruitment (compare paragraph 2.8).

The first assay without incubation of the mRNAs at 95 °C did not show any luminescence values above the level of the negative control except for the positive control (data not shown). Figure 24 shows the results of the luciferase assay after the

mRNAs were incubated at 95 °C. The luminescence values of the tested mRNAs are around the level of the negative control of an earlier experiment. In contrast, the positive control of an earlier experiment shows a much higher luminescence value.

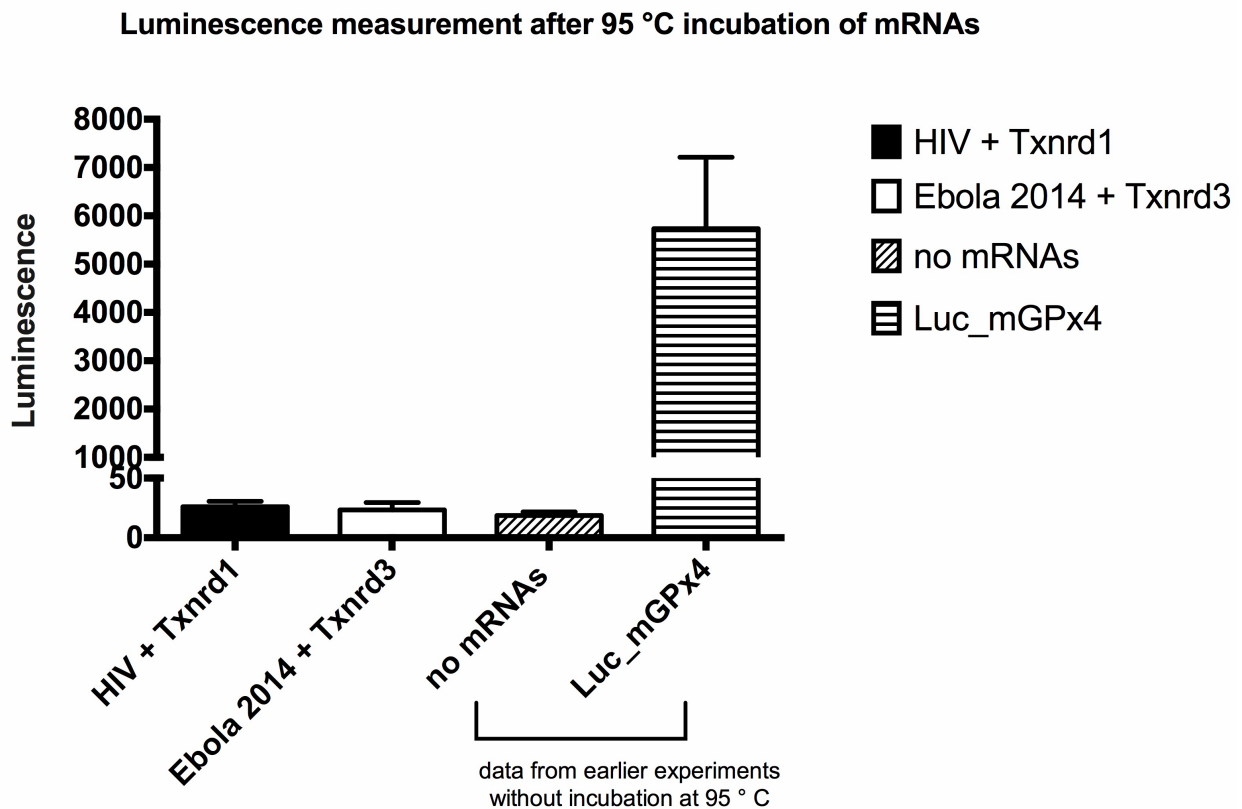


Fig. 24: Luciferase assay comparing the luminescence values of Luciferase_HIV mRNA + Txnrd1 mRNA and Luciferase_Ebola_2014 mRNA + Txnrd3 mRNA after mRNAs were incubated at 95 °C. Data from earlier experiments without incubation of mRNAs is added for comparison. “no mRNAs” is a negative control from an assay without added mRNA. “Luc_mGPx4” is a positive control in which a luciferase reporter with a murine GPX4 SECIS element was used.

3.6 Results of agarose gel-shift assays with luciferase reporters with viral inserts and Txnrd1 and Txnrd3 mRNAs

Figures 25, 26 and 27 show the results of the three performed gel shift assays. It can be seen that no new band appears that would indicate a shift of these mRNAs due to an

antisense-tethering interaction both after incubation for 2 min (fig. 25) or 5 min (fig.26 and 27) at 95 °C. Since there was not enough mRNA left for a sample with only Txnrd1 mRNA in the experiment shown in figure 26, this was repeated and the results can be seen in figure 27. The mRNAs do not run to the expected sizes but this is due to the fact that a DNA ladder was used.

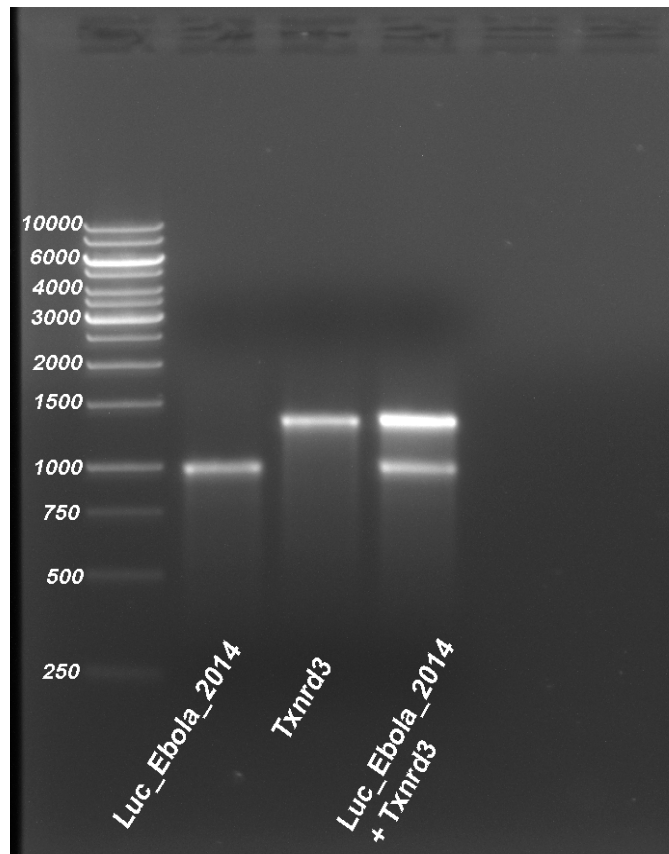


Fig. 25: Agarose gel shift assay to detect interaction between viral and selenoprotein mRNAs. Luciferase mRNA containing viral sequences and selenoprotein mRNA were either loaded alone or in combination. mRNAs were previously incubated at 95 °C for 2 min. Wells were loaded with mRNAs as written beneath each lane.

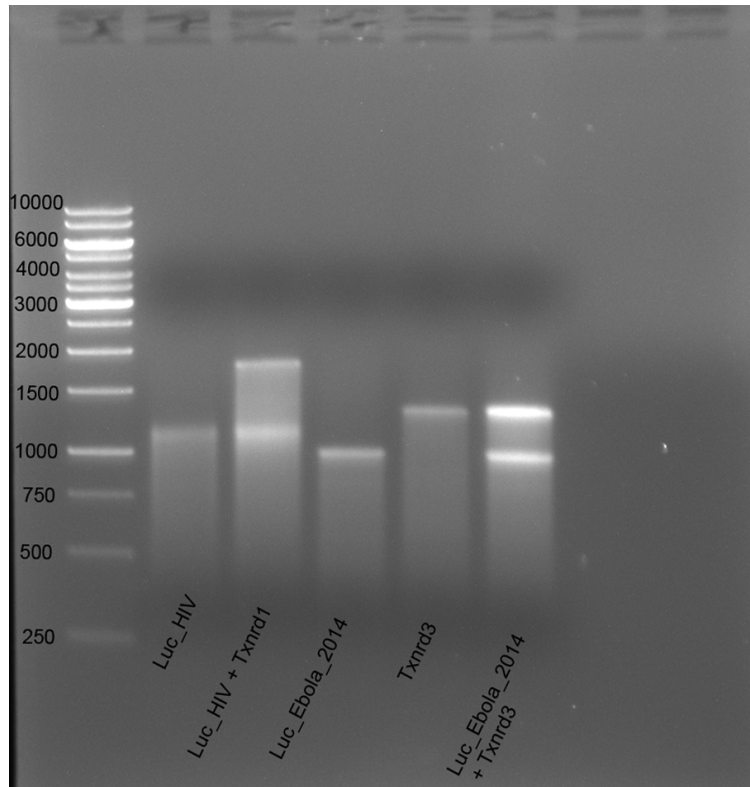


Fig. 26: Agarose gel shift assay to detect interaction between viral and selenoprotein mRNAs. Luciferase mRNAs containing viral sequences and selenoprotein mRNAs were either loaded alone or in combination. mRNAs were previously incubated at 95 °C for 5 min. Wells were loaded with mRNAs as written beneath each lane. Txnrd1 mRNAs was not loaded alone due to insufficient amount.

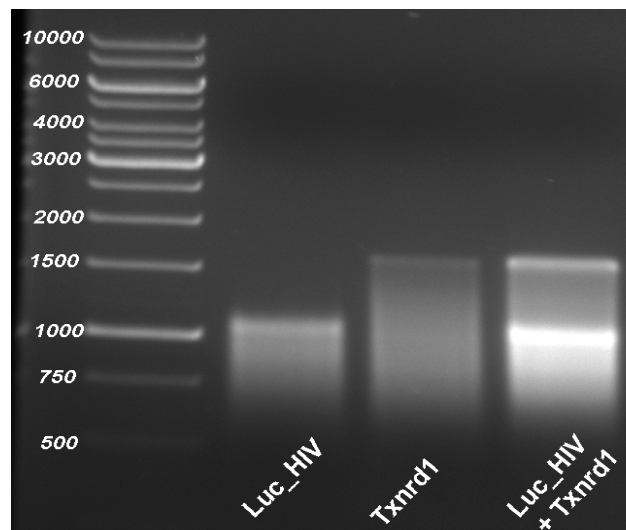


Fig. 27: Agarose gel shift assay to detect interaction between viral and selenoprotein mRNAs. Luciferase mRNAs containing viral sequences and selenoprotein mRNAs were either loaded alone or in combination. mRNAs were previously incubated at 95 °C for 5 min. Wells were loaded with mRNAs as written beneath each lane

4. Discussion

4.1 Purification and quantification of heterologously expressed CSECISBP2

Recombinant CSECISBP2 was expressed in *E. coli* and then purified by Ni-NTA-affinity-chromatography. The results of the analysis of the elution fractions by SDS-PAGE and Western blot are shown in figures 14-18.

The SDS-PAGE results clearly show a thick band that corresponds to the CSECISBP2 protein at a size of around 70 kDa. The calculated mass of the recombinant protein should actually be 53,4 kDa (calculated using the ExPASy translate tool, Artimo et al., 2012), but the band at around 70 kDa is known to correlate to CSECISBP2 from earlier experiments in our research group. This is probably due to the fact that RNA-binding proteins are often basic and therefore less mobile in SDS-PAGE.

As already mentioned in the results part there are many other bands visible in both the Coomassie staining and the Western-Blot, many lower than the CSECISBP2 band but some also higher. In general these other bands could all be impurities but it is likely that at least some of the lower bands are truncated parts of the full-length CSECISBP2. This is supported by the results of the Western-Blot in which many of these smaller bands are recognised by the anti-CSECISBP2 antibody, therefore suggesting that they carry the CSECISBP2 epitope that is recognised by the antibody.

The amount of protein in the concentrated elution fractions was quantified by comparing it to a protein standard. The resulting concentrations were then used to calculate the amount of protein used in subsequent experiments. However, this approach of quantification has some drawbacks. Firstly, the elution fractions of the Ni-NTA-affinity chromatography were not further purified (for example by using a gel-filtration-chromatography), therefore they still contained other proteins that were not separated in the Ni-NTA-affinity chromatography. Secondly, one cannot say how much of the purified CSECISBP2 protein is active protein that can still function in Sec-incorporation. All in all, this leads to the fact that although the protein concentration within the concentrated elution fractions was measured in order to use the same amount of protein in later experiments, the amount of active CSECISBP2 protein used in subsequent experiments

cannot be assumed to be entirely equal. This fact both needs to be and was considered in the interpretation of the experimental results.

4.2 Luciferase assay comparing effects of CSECISBP2 mutations in regard to different SECIS elements

4.2.1 CSECISBP2^{CR} does not support Sec-incorporation

The original hypothesis was that CSECISBP2^{CR} would show a great impairment in Sec incorporation activity due to the location of the mutation in the RNA binding domain of SECISBP2.

This hypothesis could be confirmed by the performed luciferase assays showing that CSECISBP2^{CR} displays much and significantly less Sec-incorporation activity compared to CSECISBP2^{WT} independent of the SECIS element. The reduction in Sec-incorporation activity is so prominent that the earlier mentioned fact of possibly differing amounts of active CSECISBP2 protein can be neglected in the interpretation. Furthermore, no significant difference between the measured luminescence in samples containing CSECISBP2^{CR} compared to samples without CSECISBP2 could be found. Therefore, it is shown for the first time that the C696R mutation (corresponding to the C691R mutation in humans) leads to a severe defect of function in Sec-incorporation in an *in-vitro* assay.

This lack of function in Sec-incorporation is in keeping with the described phenotype of a patient suffering from the C691R mutation (Schoenmakers et al., 2010). This patient shows various symptoms that can be attributed to a lack of function of SECISBP2. Since the described patient is only compound heterozygous for the C691R mutation he probably has a remaining activity of SECISBP2 from his allele that is affected by a splicing defect leading to an absence of either exons 2,3 and 4 or exons 3 and 4. This can be assumed since a homozygous *SECISBP2*^{C696R/C696R} mutation in mice leads to embryonic lethality (Zhao et al., 2019) and therefore, a homozygous *SECISBP2*^{C691R/C691R} mutation, which would lead to severe impairment of SECISBP2, would probably also be fatal in humans.

The lack of Sec-incorporation activity displayed by CSECISBP2^{CR} is probably due to a defect in binding to the SECIS element. This seems likely, since the mutation lies within the RNA-binding domain of SECISBP2. However, in order to further support this hypothesis further experiments investigating the binding of SECISBP2^{CR} to the SECIS element would be necessary, for example rEMSA experiments.

4.2.2 CSECISBP2^{RQ} does not show any significant differences in Sec-incorporation activity compared to CSECISBP2^{WT}

The original hypothesis was that CSECISBP2^{RQ} would show different effects on the Sec-incorporation depending on which SECIS element was used. This hypothesis was based on RiboSeq analyses from our lab, which are shown in the introduction (Fig. 5). These show that the relative amount of ribosomes that can be found 3' of the UGA codon are reduced on the *Gpx4* mRNA when SECISBP2^{RQ} was present compared to when SECISBP2^{WT} was present. This difference could not be observed for the *Gpx1* mRNA for which the presence of SECISBP2^{RQ} compared to SECISBP2^{WT} led to an absolute reduction, but no relative reduction concerning the amount of ribosomes that can be found 3' of the UGA codon. This led to the hypothesis that the RQ mutation impairs the Sec-incorporation activity of SECISBP2 depending on which SECIS element is present. Based on the RiboSeq data the assumption was that the RQ mutation would affect Sec-incorporation when a *Gpx4* SECIS element was present but would not affect Sec-incorporation when a *Gpx1* SECIS element was present. Since the UGA codon in *Txnrd1* mRNA is the penultimate codon, RiboSeq analysis cannot be performed sensibly to compare the amount of ribosomes 3' of the UGA codon. Therefore, no hypothesis concerning the effect of the RQ mutation when a *Txnrd1* SECIS element is present could be based on RiboSeq results.

Dumitrescu et al. (2005) showed that patients suffering from a homozygous RQ mutation show decreased levels of DIO2 activity in their fibroblasts, while their *Dio2* mRNA levels are normal. This led to the hypothesis that the RQ mutation would also reduce Sec-incorporation when a *Dio2* SECIS element was present.

Another hypothesis was that CSECISBP2^{RQ} might affect the translation of selenoprotein mRNAs differently depending on the type of SECIS element present within the mRNA. This idea was supported by the above-mentioned RiboSeq data that found an impairment in the readthrough of the UGA codon for the *Gpx4* mRNA (which has a type II SECIS element) but no impairment for the *Gpx1* mRNA (which has a type I SECIS element).

All these hypotheses could not be confirmed by the performed experiments. CSECISBP2^{RQ} did not show any significant differences in *in-vitro* Sec-incorporation compared to CSECISBP2^{WT} independent of the used SECIS element.

Bubenik and Driscoll (2007) also reported that they observed no reduction of Sec-incorporation activity in luciferase assays when comparing CSECISBP2^{RQ} to CSECISBP2^{WT}. They performed this comparison for *Gpx1*, *Gpx4*, and *Dio1* SECIS elements.

Together these results seem to support the idea that the RQ mutation does not affect the *in-vitro* Sec-incorporation activity of SECISBP2, even though one must keep in mind that the amount of active protein from my experiments is not entirely comparable.

Furthermore, it appears possible that the amount of protein used in the *in-vitro* translation assay (a final concentration of 160 nM was used for *Gpx1*, *Gpx4* and *Txnrd1* SECIS elements) was too high, therefore masking differences between CSECISBP2^{RQ} and CSECISBP2^{WT} protein that might be observed when using less protein. For that reason the comparison of the *Dio1*, *Dio2* and *Dio3* SECIS elements was performed using 40 nM of CSECISBP2, but still no significant differences could be observed between CSECISBP2^{RQ} and CSECISBP2^{WT}. Unfortunately the amount of protein used in the assay cannot be compared to the results of Bubenik and Driscoll (2007), because they did not publish the amount of protein they used.

The assays investigating the *Gpx1*, *Gpx4* and *Txnrd1* SECIS elements were not repeated at a lower concentration of CSECISBP2 since any differences that might have been observed could only be interpreted cautiously due to the fact that the amount of active protein might not have been the same. However, experiments titrating the concentration of the luciferase reporters discussed below yield more insights.

4.2.3 Significant readthrough of the UGA codon occurs even without CSECISBP2 and with a mutated SECIS element

It can be observed that within the group of negative controls there are significant differences between some groups. All groups show very low luminescence values, therefore confirming the previous insights that both the SECIS element and CSECISBP2 are essential for an effective Sec-incorporation *in-vitro* (Mehta et al., 2004). However, within the group of negative controls one can observe significant differences. The group in which a luciferase reporter with a SECIS element having a mutation in its SECIS core structure was used and the group in which no CSECISBP2 was added both show significantly higher luminescence values than the group in which no luciferase reporter was present. The group in which a luciferase reporter with a UAA stop codon at position 258 was present did not show significant differences compared to the group without mRNA. Therefore, one can conclude that a low but significant readthrough of the UGA (but not UAA) codon occurs even when no CSECISBP2 is added. Since SECISBP2 was shown to be the only limiting factor for Sec-incorporation in RRL (Mehta et al., 2004), this supports the findings of Fradejas-Villar et al. (2017) that SECISBP2 does stimulate the recoding of a UGA codon to Sec but is not absolutely essential for Sec-incorporation. Furthermore, one can also conclude that a low but significant readthrough of the UGA codon occurs when a mutated SECIS element is present. This might indicate that the SECIS element is also not absolutely essential for Sec-incorporation, but it is also possible that the mutated SECIS element that was used retains a very low residual activity.

4.3 Titration experiments investigating CSECISBP2 kinetics independent of protein concentration

In order to further investigate possible effects of the RQ mutation on Sec incorporation experiments titrating the luciferase reporter mRNA were performed. This allowed to calculate a K_m -value (measuring the overall function of CSECISBP2 in both binding to the SECIS element and then promoting Sec-incorporation) that is independent of

CSECISBP2 concentration, therefore allowing a comparison of the wild-type and RQ mutated protein even though the amount of active protein might not have been exactly the same.

It can be seen that the luminescence values are lower for all the six different SECIS elements tested when CSECISBP2^{RQ} was used. This is especially noticeable for the *Gpx1*, *Gpx4* and *Txnrd1* SECIS element. These results seem to be contradictory to the previous results (Fig. 19 and 20) but may be explained by the fact that a lower amount of CSECISBP2 (80 nM final concentration) was used regarding the *Gpx1*, *Gpx4* and *Txnrd1* SECIS elements. Furthermore, one must consider that the amount of active CSECISBP2 cannot be assumed to be equal and therefore only the K_m -value (which is independent of CSECISBP2 concentration) can be compared in a sensible way.

Significant differences in the K_m -value could only be observed for the *Txnrd1* and *Dio1* SECIS elements. In both cases CSECISBP2^{RQ} showed a significantly higher K_m -value than CSECISBP2^{WT}. Therefore, the overall ability to promote Sec-incorporation (a combination of binding to the SECIS element and then promoting Sec-incorporation) of CSECISBP2^{RQ} is impaired regarding the *Txnrd1* and *Dio1* SECIS element. The differences in the K_m -values were however slight, around 2 nM for the *Txnrd1* SECIS element and around 4 nM for the *Dio1* SECIS element.

Since *Txnrd1* mRNA contains a type II SECIS element while *Dio1* mRNA contains a type I SECIS element this effect seems to be independent of the type of SECIS element.

The absolute measured K_m -values for CSECISBP2^{WT} vary between 3.7 and 8.7 nM. These values are in a similar range as the K_D -value measured by Bubenik et al. (2014) for the binding of CSECISBP2 to a *Gpx4* SECIS element.

4.4 Increased temperature impairs protein stability of CSECISBP2^{RQ}

Fig. 28 shows a Western blot by Zhao et al. (2019) detecting SECISBP2 in mouse liver. Both SECISBP2^{CR} and SECISBP2^{RQ} showed almost no detectable SECISBP2 equal to the knockout.

Furthermore, another Western blot (Fig. 29) by Zhao et al. (2019) shows that the selenoproteins GPX1, GPX4, SELENOT and SEPHS2 are either undetectable or barely

detectable in mouse liver when SECISBP2 is knocked out, or affected by the CR or RQ mutation. Liver TXNRD1 is not affected in any of these mice, possibly because Sec is the penultimate amino acid.

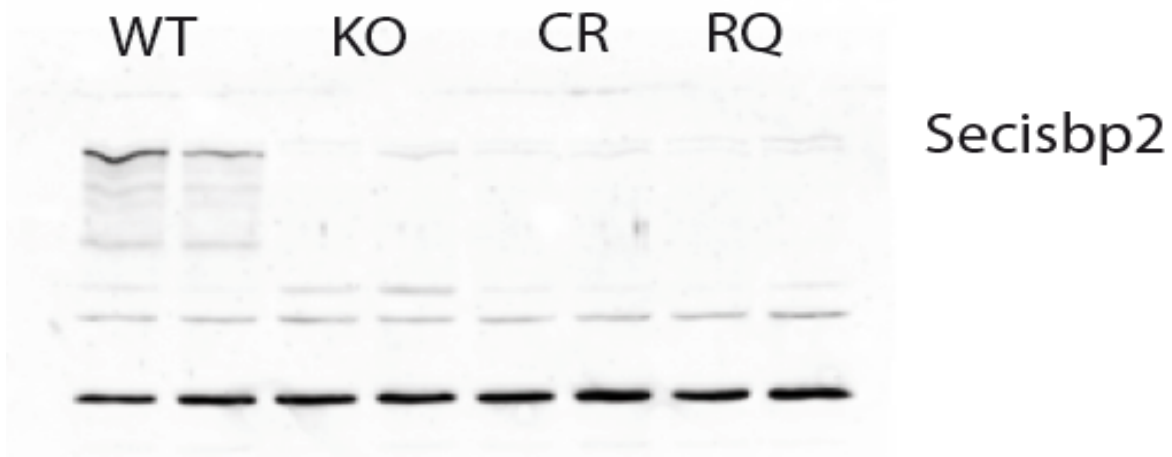


Fig. 28: Western blot of SECISBP2 in liver-specific *Secisbp2* mutant mice. Comparison of protein expression in liver of control mice (WT) with Alb-Cre; *Secisbp2*^{fl/fl} (KO), Alb-Cre; *Secisbp2*^{C696R/fl} (CR) and Alb-Cre; *Secisbp2*^{R543Q/fl} mice. The lowest band shows an unspecific band that indicates equal loading. Modified after Zhao et al. (2019)

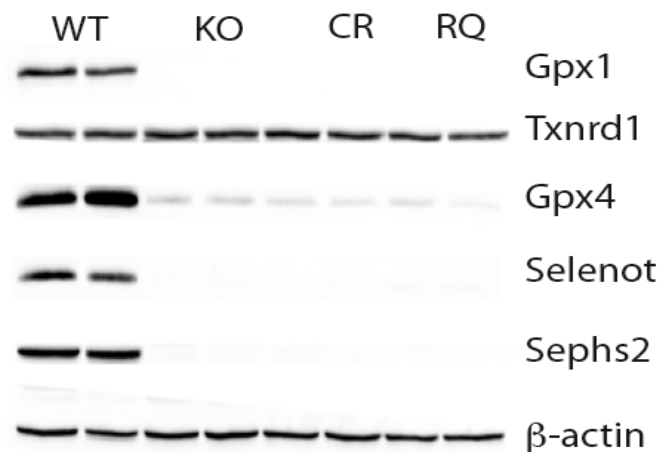


Fig. 29: Western blot of different selenoproteins in liver-specific *Secisbp2* mutant mice. Comparison of protein expression in liver of control mice (WT) with Alb-Cre; *Secisbp2*^{fl/fl} (KO), Alb-Cre; *Secisbp2*^{C696R/fl} (CR) and Alb-Cre; *Secisbp2*^{R543Q/fl} mice. β-actin bands serve as loading control. Modified after Zhao et al. (2019)

The fact that the CR mutation leads to a decrease in selenoprotein expression in liver similar to the knockout of *Secisbp2* is expected since CSECISBP2^{CR} did show a loss of Sec-incorporation activity in the luciferase assays. However, for the RQ mutation this seems contradictory to the results of the luciferase assays in which CSECISBP2^{RQ} did not show any significant differences in Sec-incorporation compared to the wild-type.

Therefore, the hypothesis came up that the RQ mutation might lead to a reduced protein stability of SECISBP2 explaining both the fact that SECISBP2^{RQ} itself and the measured selenoproteins cannot or only to a very small extent be detected in Western-blot. The fact that SECISBP2^{CR} can also not be detected in Western-Blot might also be caused by a reduced protein stability while the failing expression of selenoproteins could be explained both by absent SECISBP2^{CR} due to instability or its inability to promote efficient Sec-incorporation.

The findings that CSECISBP2^{RQ} shows a reduced thermal stability compared to CSECISBP2^{WT} supports the hypothesis that the RQ mutation reduces the protein stability of CSECISBP2. The temperatures of the assay (37 °C and 40.5°C) were chosen to reflect both physiological temperature and a stressful state for protein stability. Since significant differences in protein stability can already be observed at 37 °C it is reasonable to assume that SECISBP2^{RQ} would be less stable in the human body thereby affecting the expression of selenoproteins.

Western blots similar to the ones performed for liver were also performed for brain by Zhao et al. (2019). SECISBP2 and several selenoproteins were detected from neuron-specific *Secisbp2* knockout mice and *Secisbp2*^{RQ} and *Secisbp2*^{CR} mutant mice. (Fig. 30 and 31). It is hard to judge whether SECISBP2^{RQ} and SECISBP2^{CR} are expressed at higher levels compared to the knockout. In my opinion, it seems to be the case that in contrast to the findings in liver, both SECISBP2^{CR} and SECISBP2^{RQ} can be detected at higher levels than in mice with a knockout of *Secisbp2* (Fig. 30). The fact that SECISBP2 can be detected in the knockout mice at all is due to SECISBP2 expression from other brain cells in which the *Secisbp2* gene is not knocked out.

The observation that SECISBP2^{RQ} seems to be expressed at higher levels in neurons compared to a SECISBP2-knockout is supported by the fact that *CamK-Cre; SECISBP2*^{RQ/fl} mice showed an apparently normal phenotype. In contrast, *CamK-Cre;*

SECISBP2^{CR/fl} and *CamK-Cre; SECISBP2^{fl/fl}* mice showed the same phenotype including impaired movement and impaired growth (Seeher et al., 2014, Zhao et al., 2019). Furthermore, the expression of selenoproteins in neurons of *CamK-Cre; SECISBP2^{RQ/fl}* mice is reduced but it is still higher than in hepatocytes from *Alb-Cre; SECISBP2^{RQ/fl}* mice (Fig. 29 and 31).

This suggests that SECISBP2^{RQ} and possibly also SECISBP2^{CR} show a different protein-stability depending on the tissue or the cell-type. Therefore, it appears possible that the rather mild phenotype of patients carrying a homozygous SECISBP2^{RQ} mutation could be explained by a different protein stability of SECISBP2^{RQ} depending on the tissue. The affected patients show low activity of DIO2 in fibroblasts, low activity of GPX3 in serum and reduced levels of SELENOP in serum. GPX3 and SELENOP are expressed in the kidney and liver, respectively before they are secreted into the blood. Therefore, the reduced levels of SELENOP in affected patients can be explained by the fact that SECISBP2^{RQ} seems to be less stable in liver. Since there is no data on the stability of SECISBP2^{RQ} in kidney or fibroblasts one can only speculate that SECISBP2 might also be less stable in these tissues thereby leading to the described phenotype.

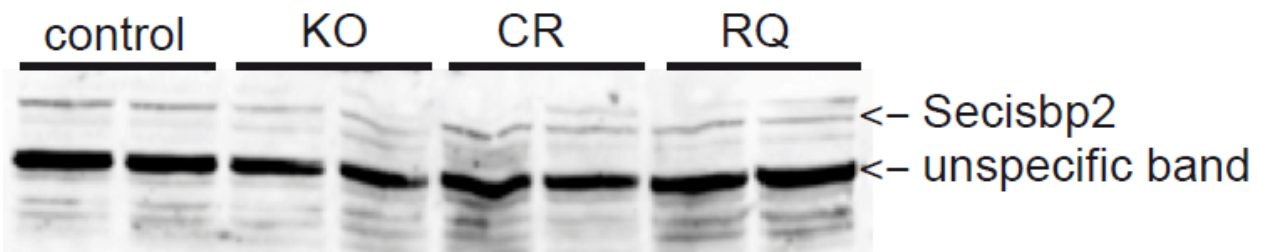


Fig. 30: Western blot of SECISBP2 in neuron-specific SECISBP2 mutant mice. Comparison of protein expression in cortex of control mice (control) with *CamK-Cre; SECISBP2^{fl/fl}* (KO), *CamK-Cre; SECISBP2^{C696R/fl}* (CR) and *CamK-Cre; SECISBP2^{R543Q/fl}* mice. The small band that corresponds to SECISBP2 is marked “Secisbp2”. Modified after Zhao et al. (2019)

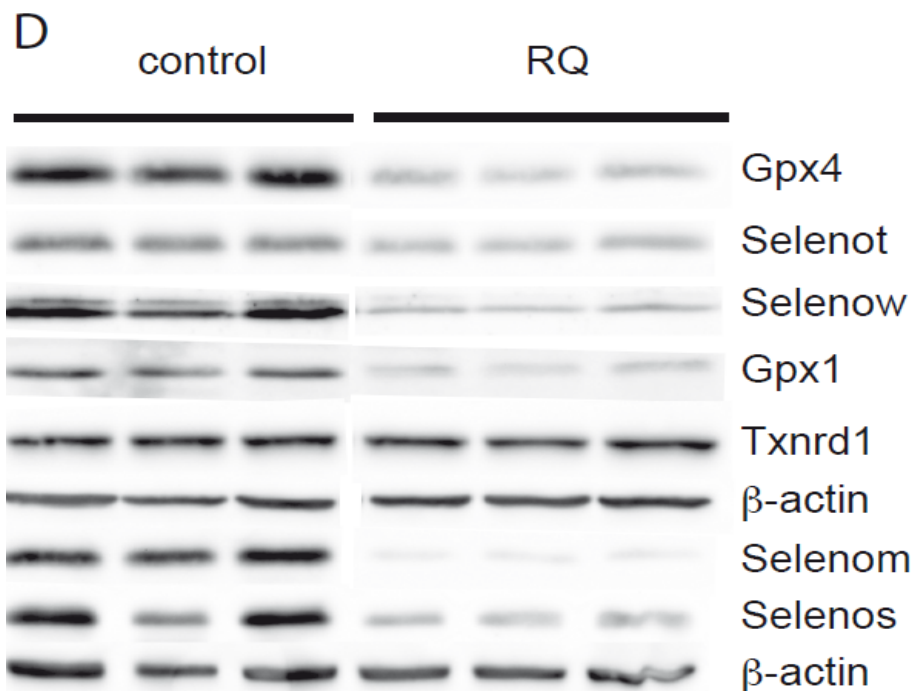


Fig. 31: Western blot of different selenoproteins in neuron-specific Secisbp2 mutant mice. Comparison of protein expression in cortex of control mice (WT) with CamK-Cre; Secisbp2R543Q/fl mice. β -actin bands serve as loading control. Modified after Zhao et al. (2019)

4.5 Conclusions to analysis of mutant SECISBP2

4.5.1 SECISBP2^{CR} shows decreased function in Sec-incorporation and might also be unstable

The C691R mutation in SECISBP2 leads to two effects. Firstly, the Sec-incorporation activity *in-vitro* of SECISBP2^{CR} is reduced to levels similar to when no SECISBP2 was added at all. This is expected since the mutation lies within the RNA-binding domain and thereby probably disrupting the binding of SECISBP2^{CR} to the SECIS element and therefore, abolishing its function in Sec-incorporation. Bubenik et al. (2014) published that an *in-vitro* translated CSECISBP2 carrying a C691S mutation does not show an impaired SECIS binding to a Gpx4 SECIS element. This seems at first glance contradictory to the hypothesis that the CR mutation disrupts the binding of SECISBP2^{CR}

to the SECIS element. However, serine is an amino acid that is very similar to cysteine in contrast to arginine and one might assume that a C691S mutation leads to effects much less severe than a C691R mutation.

Secondly, the Western-Blot from Zhao et al. (2019) (Fig. 28) suggests that the CR mutation might also lead to a reduced protein stability of SECISBP2^{CR} since the protein can hardly be detected in mouse liver. This is supported by findings from Schoenmakers et al. (2010) who could not detect full-length SECISBP2 by Western-Blot in fibroblasts from a patient suffering a compound heterozygous C691R mutation. Furthermore, they found that SECISBP2^{CR} is more susceptible to proteasomal degradation than SECISBP2^{WT}.

4.5.2 SECISBP2^{RQ} shows almost no impairment in Sec-incorporation but reduced protein stability possibly depending on the tissue

The performed luciferase assays did only show a slight impairment in Sec-incorporation efficiency affecting the *Txnrd1* and *Dio1* SECIS elements. Together with the similar results from Bubenik and Driscoll (2007) this seems to suggest that the pathogenicity of the R540Q mutation is not caused by a reduced function in Sec-incorporation.

Furthermore, Bubenik and Driscoll (2007) showed that when challenged by an environment of competing SECIS elements CSECISBP2^{RQ} does show differences in binding affinity towards different SECIS elements. They found that CSECISBP2^{RQ} shows less affinity towards the *Gpx1* and *Dio2* SECIS elements compared to CSECISBP2^{WT} while no difference could be observed for the *Gpx4* SECIS element.

The already above discussed results from our research group suggest that SECISBP2^{RQ} is less stable than SECISBP2^{WT} and that this instability might be dependent on the tissue in which SECISBP2 is expressed. This potential tissue-dependent difference in stability might contribute to the mild phenotype of patients affected by a homozygous R540Q mutation.

To sum it all up, SECISBP2^{RQ} does not show any impairment in Sec-incorporation activity in isolated *in-vitro* experiments for *Gpx1*, *Gpx4*, *Dio2*, and *Dio3* SECIS elements and only a slight impairment for *Txnrd1* and *Dio1* SECIS elements. SECISBP2^{RQ} seems

to be less stable both *in-vitro* and *in-vivo*. Due to both these reasons SECISBP2^{RQ} may lead to a reduced expression of a subset of selenoproteins in an environment where different selenoprotein mRNAs compete for SECISBP2.

4.6 Viral SECIS element recruitment cannot be shown in *in-vitro* assay despite compelling supporting evidence

4.6.1 Data that supports the hypothesis of viral selenoproteins

As already described in the introduction the idea that viruses may encode selenoproteins first came up in 1994 (Taylor et al., 1994). It then developed further to the idea of a potential Gpx being encoded in the -1 reading frame of the HIV envelope-gene (Taylor et al., 1997b).


HIV envelope gene  **RRVVQREKKS SGNRSSFVPWV LGSSRKHYGR TVNDADGTGQ TIIVWYSAAA**
EQFAEGYCGA TASVATHSLG HQAAPGKNPG CGKIPKGSTA PGDLGLLWKT
HLHHCCALEC

Fig. 32: Protein sequence of a potential protein from the -1 reading frame of the HIV envelope gene. The first part of the sequence shows a part of the 0 reading frame. Beginning with the red arrow the sequence is shown in the -1 reading frame. The underlined SFVPWV shows a potential protease cleavage site. The underlined C shows the position of a UGA codon that might be decoded as Sec. Modified after Taylor et al. (1994).

Figure 32 shows the transition from the 0 to the -1 reading frame in the HIV envelope-gene that is hypothesised to lead to the encoding of a Gpx. A potential protease cleavage site just in front of the hypothesised Gpx sequence is also shown.

Figure 33 shows the sequence of the predicted Gpx from the -1 reading frame of the env gene (named env-fs) aligned to the sequences of different glutathione peroxidases,

namely mouse, rat, human and bovine Gpx3 (rows named “P”), mouse, rat, bovine, human and rabbit Gpx1 (rows named “C”) and pig Gpx4 (row named “L”).

```

Match:  G SR  Y* *  D DG *  * Y *  F  *YUG*T*  *  ****GHQ*  PGKN  PG G *PK *  * GD*  ** W*  ** * *
env-fs  GSSRKH YGRTVNDADGTGQTIIVWYSAAAEQF..AEGYUGATAS.VATHSLGHQAAPGKN.PGCGKIPKGST.APGDL.GLLWKTHLHHCCALEC
P-P46412 GMSGTIYEYGAL TIDGEEYIPFKQYAGKYILFVN VASYUGLTD.%FPCNQFGKQE.PGEN#PGGGFV PNFQLFEKGDV~DIRWNFE.KFLVGPDG
P-P23764 GMSGTIYEYGAL TIDGEEYIPFKQYAGKYILFVN VASYUGLTD.%FPCNQFGKQE.PGEN#PGGGFV PNFQLFEKGDV~DIRWNFE.KFLVGPDG
P-P22352 GISGTIYEYGAL TIDGEEYIPFKQYAGKYILFVN VASYUGLTD.%FPCNQFGKQE.PGEN#PGGGFV PNFQLFEKGDV~DIRWNFE.KFLVGPDG
P-P37141 GVGGTIYEYGAL TIDGEEYIPFKQYAGKYILFVN VASYUGLTD.%FPCNQFGKQE.PGEN#PGGGFV PNFQLFEKGDV~DIRWNFE.KFLVGPDG
C-P11352 AAQSTVYAFSARPL TGGEPVSLGSLRGKVLLIEN VASLUGTTIR%FPCNQFGHQE.NGKN#PGGGFEPNFTLFEKCEV~DIAWNFE.KFLVGPDG
C-P04041 VAQSTVYAFSARPL AGGEPVSLGSLRGKVLLIEN VASLUGTTTR%FPCNQFGHQE.NGKN#PGGGFEPNFTLFEKCEV~DISWNFE.KFLVGPDG
C-P00435 AAPRTVYAFSARPL AGGEPFNLSLRGKVLLIEN VASLUGTTVR%FPCNQFGHQE.NAKN#PGGGFEPNFMLFEKCEV~DVSWNFE.KFLVGPDG
C-P07203 AAAQSVYAFSARPL AGGEPVSLGSLRGKVLLIEN VASLUGTTVR%FPCNQFGHQE.NAKN#PGGGFEPNFMLFEKCEV~DVAWNFE.KFLVGPDG
C-P11909 AAAQSVYFSARPL AGGEPVNLGSLRGKVLLIEN VASLUGTTVR%FPCNQFGHQE.NAKN#PGGGFEPNFMLFQKCEV~DVSWSFE.KFLVGPDG
L-P36968 RCARSMHEFSAKDIDG.HMVNLDKYRGYVCIVTN VASQUGKTEV%FPCNQFGRQE.PGSD#YNV...KDFMFSKICV~AIKWNFT.KFLIDKNG
AS 1      AS 2      AS 3

```

Fig. 33: Alignment of the potential frameshift protein from the HIV envelope gene (*env-fs*) as shown in figure 32 to different Gpx proteins named by their Swiss-Prot accession number. Rows named “P” show sequences of mouse, rat, human and bovine Gpx3. Rows named “C” show sequences of mouse, rat, bovine, human and rabbit Gpx1. The row named “L” shows a pig Gpx4 sequence. AS1, AS2 and AS3 show active site regions in red boxes with their catalytic amino acids U=selenocysteine, Q=glutamine, W=tryptophan; three areas of deletions of 19, 11 and 41 amino acids are indicated by %, # and ~ respectively; amino acids identical to at least one of the Gpx sequences are indicated by the corresponding letters in the “Match” row, similar amino acids are indicated by an asterisk. Modified after Zhao et al., (2000).

Three active site regions of the *env-fs* protein are similar to the other Gpx sequences to an extent that it seems possible that the *env-fs* protein might encode a functional Gpx. This idea is supported by the findings of Zhao et al. (2000) who cloned this potential Gpx sequence together with an additional start codon and a rat Dio1 SECIS element. Subsequent transfection of mammalian cells with this construct led to a significant increase in measured Gpx activity.

Furthermore, Cohen et al. (2004) published data showing that mammalian cells transfected with a plasmid containing this potential Gpx together with an additional start codon and a rat Dio1 SECIS element are more resistant against apoptosis when exposed to reactive oxygen species (ROS).

It has already been shown that the *Molluscum contagiosum* virus does encode a functional Gpx (Shisler et al., 1998) and until now this is the only example of a virus-encoded selenoprotein. All this evidence shows that the general idea of viral selenoproteins is not erroneous.

Another hint towards a potential Gpx encoded by HIV is the fact that HIV-infected T-cells show an increase of low molecular Se compounds as shown in figure 34 (Gladyshev et al., 1999). This could be caused by the expression of the potential Gpx protein which is predicted to have a mass of around 9 kDa (Zhao et al., 2000).

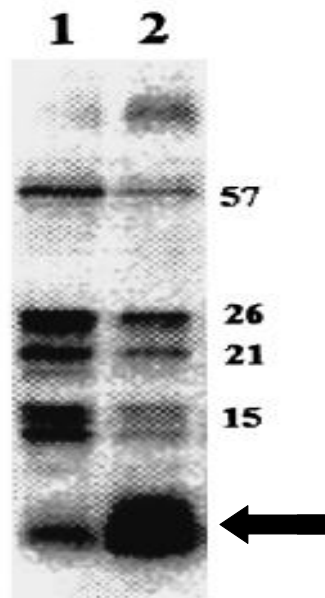


Fig. 34: PhosphorImager detection of ^{75}Se labeled proteins of HIV-infected cells (lane 2) compared to uninfected cells (lane 1) after separation by SDS/PAGE. The arrow marks low molecular weight Se compounds. Molecular masses in kDa of some selenoproteins are shown, modified after Gladyshev et al., (1999).

Molluscum contagiosum has a SECIS element within the 3' non coding region of its mRNA that allows for an efficient recoding of its UGA codon to Sec. The HI-virus, however, lacks a SECIS element and this is still an unsolved problem in the idea of an HIV encoded Gpx.

Towards this end Taylor et al. (2016) published the idea of an antisense-tethering-interaction between viral and human mRNAs that would lead to the “hijacking” of a human SECIS element in order to recode a viral UGA codon to Sec as described in the introduction.

The idea of an in-trans recruitment of a SECIS element is supported by findings from Berry et al. (1993) that showed that Sec-incorporation can be observed in cells

transfected with both a reporter plasmid lacking a SECIS element and a second plasmid carrying a SECIS element.

If the HI-virus does encode a functional Gpx, this might be a factor increasing the virulence for example by making infected cells more resistant against apoptosis. It has been shown that the expression of the HIV tat protein in HeLa cells leads to reduced levels of Mn-dependent superoxide dismutase (Mn-SOD) in turn leading to reduced levels of glutathione and a reduced ratio of reduced:oxidised glutathione (Westendorp et al., 1995). Therefore, one can speculate that an infection of a cell with HIV leads to a situation of increased oxidative stress within the cell which might be countered by an HIV-encoded Gpx. The enhanced survival of infected cells would then improve the ability of HIV to replicate.

Furthermore, ferroptosis might also be a way that could lead to the death of HIV-infected cells. A key enzyme that prevents a cell from undergoing ferroptosis is Gpx4 (Cao and Dixon, 2016). Therefore, an HIV-encoded Gpx might also prevent HIV-infected cells from undergoing ferroptosis thereby also improving the ability of HIV to replicate.

4.6.2 *In-vitro* assay fails to show Sec-incorporation by means of “hijacked” SECIS element

Despite the compelling data that supports the theory of an HIV-encoded Gpx, the performed *in-vitro* experiments trying to show a successful Sec-incorporation by means of a via antisense-tethering-interaction “hijacked” SECIS element were unsuccessful.

Furthermore, the performed gel-shift assays did also not show any band-shifting that would indicate a stable base-pairing taking place between the viral and human mRNA sequences.

Altogether, these results fail to provide evidence for a potential in-trans recruitment of a SECIS element that would lead to a successful Sec-incorporation. However, this can be interpreted in different ways.

It is possible that the hypothesised antisense-tethering-interactions simply do not take place and therefore can also not be shown in both the luciferase and the gel-shift assay. However, the above discussed data strongly suggests that the HI-virus does encode a

functional Gpx. Regarding the Ebola virus there is less supporting data indicating that it might encode a functional selenoprotein (Ramanathan and Taylor, 1997).

Since only a small part of the viral genomes of the HI- and Ebola-virus were used in the described assays it seems possible that larger parts of the viral sequences are necessary for a successful ATI that might then lead to a successful Sec-incorporation. This seems especially possible for the Ebola-virus since only one of the two regions to which the ATI has been proposed was used. Concerning the HI-virus both regions to which the ATI has been proposed were used in the luciferase assay. If other parts of the viral genome or transcriptome were necessary for an ATI this would explain the fact that the experiments do not show any successful Sec-incorporation as well as no stable base-pairing in the gel-shift assay.

Furthermore, it is also possible that additional factors that were not present in the *in-vitro* translation assay are necessary for a successful ATI between the mRNAs. These factors could be proteins or nucleic acids that are either present in the cells that are normally infected by the viruses or that are synthesised by the viruses themselves.

Although, Taylor et al. (1994) proposed several potential mRNA structures that might function as SECIS element in the HIV genome none of these have so far been shown to be able to promote Sec-incorporation (Taylor et al., 1997a; Zhao et al., 2006). This makes it less likely, yet does not completely rule out the possibility that HIV encodes a SECIS element or a similar RNA motif on its own that allows the recoding of a UGA codon to Sec.

All in all, there is a lot of compelling data that supports the idea of the HI-virus encoding a Sec-containing Gpx. However, evidence is still lacking as to how the HI-virus might recode its UGA codon. The here described *in-vitro* assay failed to provide evidence towards an antisense-tethering-interaction between viral and human selenoprotein mRNAs but further experiments possibly using a cell based model and active HI-virus might yield further insights.

5. Summary

The 21st amino acid selenocysteine (Sec) is encoded by the UGA codon. In order to recode the canonical stop codon additional factors are needed in mammals including the selenocysteine-insertion-sequence (SECIS) element and SECISBP2. Mutations of SECISBP2 have been identified in patients and this thesis investigates the R540Q and C691R mutations in an *in-vitro* luciferase assay. Moreover, it has been speculated that viruses, although lacking a SECIS element, are able to express selenoproteins by using the SECIS element of a human mRNA via an antisense-tethering-interaction (ATI). This possibility was also investigated in an *in-vitro* luciferase assay.

Murine SECISBP2 was cloned and expressed in *E. coli*. Both R543Q and C696R mutations were introduced by site-directed mutagenesis. Different murine SECIS elements were cloned into the 3' UTR of a luciferase reporter that contains a UGA instead of a cysteine codon. All reporters were transcribed *in-vitro*. *In-vitro* translation of the luciferase reporters together with SECISBP2 protein was performed and luminescence as a correlate for Sec incorporation was measured.

Furthermore, the SECIS element of the same luciferase reporter was replaced by viral sequences predicted to take part in the ATI. Full-length mRNAs of human *TXNRD1* and *TXNRD3* were transcribed *in-vitro*, as well as the luciferase reporter. Finally, an *in-vitro* luciferase assay was performed mixing the reporter and TXNRD mRNAs.

The luciferase assay comparing the mutated SECISBP2 proteins with the wildtype showed that the C696R mutation causes highly reduced Sec-incorporation. No significant difference between the wildtype and the R543Q mutation could be found.

The luciferase assay trying to show an in-trans SECIS element recruitment by viral sequences did not show any luminescence beyond background.

The present data show for the first time loss of function of the C691R mutant in an *in-vitro* assay, thereby showing that RNA binding of SECISBP2 is critical for its function. Decreased thermal stability of the R540Q mutant protein could be observed which might explain the partial loss of function.

A viral in-trans SECIS element recruitment could not be shown. Therefore, the proposed ATI may not take place or it simply could not be shown by the performed approach.

6. List of figures

| | |
|--|----|
| Fig. 1: Scheme showing the metabolism of iodotyronines..... | 15 |
| Fig. 2: Scheme of mammalian Sec incorporation..... | 19 |
| Fig. 3: Scheme of type I and type II SECIS elements..... | 21 |
| Fig. 4: Scheme of SECISBP2 domains in murine SECISBP2..... | 22 |
| Fig. 5: Plots of ribosome coverage of Gpx1 and Gpx4 mRNAs from mice brain of either control mice or CamK-Cre; Secisbp2RQ/fl..... | 26 |
| Fig. 6: Scheme of Sec-incorporation in eukaryotes and scheme of potential viral SECIS element recruitment..... | 28 |
| Fig. 7: DNA-gel-shift assay with viral and human selenoprotein sequences..... | 29 |
| Fig. 8: Scheme of luciferase reporter..... | 29 |
| Fig. 9: Oxidation reaction of luciferin to oxyluciferin..... | 30 |
| Fig. 10: Scheme of the luciferase reporter with viral sequences cloned into the 3' UTR instead of a SECIS element..... | 32 |
| Fig. 11: Dio3 Primer scheme..... | 47 |
| Fig. 12: Primer scheme for Ebola sequence alignments..... | 49 |
| Fig. 13: Primer scheme for HIV sequence primer alignments..... | 50 |
| Fig. 14: Ponceau staining of membrane after transfer from PA gel for CSECISBP2 ^{RQ} purification..... | 72 |
| Fig. 15: Western blot results from the purification of CSECISBP2 ^{RQ} | 73 |
| Fig. 16: Ponceau staining of membrane after transfer of the proteins from PA gel for CSECISBP2 ^{CR} purification..... | 74 |
| Fig. 17: Western blot results from the purification of CSECISBP2 ^{CR} | 75 |
| Fig. 18: Result from SDS-PAGE with Coomassie staining of the concentrated CSECISBP2 ^{WT} elution..... | 76 |
| Fig. 19: Luciferase Assay comparing the mouse <i>Gpx1</i> , <i>Gpx4</i> and <i>Txnrd1</i> SECIS elements in regard to CSECISBP2 ^{WT} , CSECISBP2 ^{RQ} and CSECISBP2 ^{CR} | 78 |
| Fig. 20: Results from the luciferase assay comparing CSECISBP2 ^{WT} , CSECISBP2 ^{RQ} and CSECISBP2 ^{CR} for the luciferase reporters carrying a Dio1, Dio2 or Dio3 SECIS element..... | 80 |

| | |
|--|-----|
| Fig. 21: Results for the comparison of CSECISBP2 ^{WT} and CSECISBP2 ^{RQ} with titrated Luc_mGpx1, Luc_mGpx4 and Luc_mTxnrd1 mRNA reporter..... | 82 |
| Fig. 22: Results for the comparison of CSECISBP2 ^{WT} and CSECISBP2 ^{RQ} with titrated Luc_mDio1, Luc_mDio2 and Luc_mDio3 mRNA reporter..... | 83 |
| Fig. 23: Luciferase assays comparing the temperature stability of CSECISBP2 ^{WT} and CSECISBP2 ^{RQ} | 85 |
| Fig. 24: Luciferase assay comparing the luminescence values of Luciferase_HIV mRNA + Txnrd1 mRNA and Luciferase_Ebola_2014 mRNA + Txnrd3 mRNA after mRNAs were incubated at 95 °C..... | 86 |
| Fig. 25: Agarose gel shift assay to detect interaction between viral and selenoprotein mRNAs..... | 87 |
| Fig. 26: Agarose gel shift assay to detect interaction between viral and selenoprotein mRNAs..... | 88 |
| Fig. 27: Agarose gel shift assay to detect interaction between viral and selenoprotein mRNAs..... | 88 |
| Fig. 28: Western blot of SECISBP2 in liver-specific Secisbp2 mutant mice..... | 95 |
| Fig. 29: Western blot of different selenoproteins in liver-specific Secisbp2 mutant mice..... | 95 |
| Fig. 30: Western blot of SECISBP2 in neuron-specific SECISBP2 mutant mice..... | 97 |
| Fig. 31: Western blot of different selenoproteins in neuron-specific Secisbp2 mutant mice..... | 98 |
| Fig. 32: Protein sequence of a potential protein from the -1 reading frame of the HIV envelope gene..... | 100 |
| Fig. 33: Alignment of the potential frameshift protein from the HIV envelope gene (env-fs) as shown in figure 32 to different Gpx proteins | 101 |
| Fig. 34: PhosphorImager detection of ⁷⁵ Se labeled proteins of HIV-infected cells (lane 2) compared to uninfected cells (lane 1) | 102 |

7. List of tables

| | |
|---|----|
| Tab. 1: Pipettes and disposable materials..... | 33 |
| Tab. 2: Technical equipment | 34 |
| Tab. 3: Chemicals not purchased from AppliChem..... | 35 |
| Tab. 4: Primers used for generating recombinant DNA sequences..... | 36 |
| Tab. 5: Primers used for sequencing..... | 39 |
| Tab. 6: Primers used for site-directed mutagenesis..... | 40 |
| Tab. 7: pTrcHis2 plasmids with CSecisbp2 inserts..... | 41 |
| Tab. 8: pcDNA3.1_Luciferase plasmids with SECIS element inserts..... | 44 |
| Tab. 9: TaqPolymerase PCR program..... | 46 |
| Tab. 10: Viral inserts used for cloning..... | 48 |
| Tab. 11: Kits or special reagents used in the cloning process..... | 51 |
| Tab. 12: Buffers for MiniPrep..... | 53 |
| Tab. 13: Bacteria used for DNA amplification or protein expression..... | 53 |
| Tab. 14: Preparation of LB medium and LB Agar..... | 53 |
| Tab. 15: Lysis buffer for genomic DNA extraction..... | 54 |
| Tab. 16: TE-buffer..... | 54 |
| Tab. 17: TAE-buffer..... | 54 |
| Tab. 18: Buffers for purification of bacterially expressed protein..... | 56 |
| Tab. 19: Recipes for PA-gels..... | 57 |
| Tab. 20: Buffers for SDS-PAGE and Coomassie staining..... | 58 |
| Tab. 21: Buffers and Solutions for Western-Blot..... | 59 |
| Tab. 22: Protein storage buffer..... | 60 |
| Tab. 23: Reagents used in the process of in-vitro transcription..... | 63 |
| Tab. 24: Reagents used for luciferase assays..... | 64 |
| Tab. 25: PBS buffer, pH 7.4..... | 65 |
| Tab. 26: mRNA concentrations used for the luciferase titration assays..... | 66 |
| Tab. 27: Scheme for mRNA addition for viral luciferase assay..... | 68 |
| Tab. 28: Scheme for mRNA mixtures for luciferase assay with 95 °C incubation..... | 69 |
| Tab. 29: Scheme for mRNA mixing for gel-shift assay..... | 70 |

| | |
|--|----|
| Tab. 30: 6 x loading buffer..... | 71 |
| Tab. 31: Schematic pictures of different luciferase reporters..... | 77 |

8. References

- Arbogast S, Ferreiro A. Selenoproteins and protection against oxidative stress: selenoprotein N as a novel player at the crossroads of redox signaling and calcium homeostasis. *Antioxid Redox Signal*. 2010. 12: 893–904
- Arnér ES, Holmgren A. Physiological functions of thioredoxin and thioredoxin reductase. *Eur J Biochem*. 2000. 267: 6102–6109
- Artimo P, Jonnalagedda M, Arnold K, Baratin D, Csardi G, Castro E de, Duvaud S, Flegel V, Fortier A, Gasteiger E, Grosdidier A, Hernandez C, Ioannidis V, Kuznetsov D, Liechti R, Moretti S, Mostaguir K, Redaschi N, Rossier G, Xenarios I, Stockinger H. ExpASy: SIB bioinformatics resource portal. *Nucleic Acids Res*. 2012. 40: W597-603
- Baker RD, Baker SS, LaRosa K, Whitney C, Newburger PE. Selenium regulation of glutathione peroxidase in human hepatoma cell line Hep3B. *Arch Biochem Biophys*. 1993. 304: 53–57
- Berry MJ, Banu L, Chen YY, Mandel SJ, Kieffer JD, Harney JW, Larsen PR. Recognition of UGA as a selenocysteine codon in type I deiodinase requires sequences in the 3' untranslated region. *Nature*. 1991. 353: 273–276
- Berry MJ, Banu L, Harney JW, Larsen PR. Functional characterization of the eukaryotic SECIS elements which direct selenocysteine insertion at UGA codons. *EMBO J*. 1993. 12: 3315–3322
- Bondareva AA, Capecchi MR, Iverson SV, Li Y, Lopez NI, Lucas O, Merrill GF, Prigge JR, Siders AM, Wakamiya M, Wallin SL, Schmidt EE. Effects of thioredoxin reductase-1 deletion on embryogenesis and transcriptome. *Free Radic Biol Med*. 2007. 43: 911–923
- Boukhzar L, Hamieh A, Cartier D, Tanguy Y, Alsharif I, Castex M, Arabo A, El Hajji S, Bonnet JJ, Errami M, Falluel-Morel A, Chagraoui A, Lihmann I, Anouar Y. Selenoprotein T Exerts an Essential Oxidoreductase Activity That Protects Dopaminergic Neurons in Mouse Models of Parkinson's Disease. *Antioxid Redox Signal*. 2016. 24: 557–574

- Bubenik JL, Driscoll DM. Altered RNA binding activity underlies abnormal thyroid hormone metabolism linked to a mutation in selenocysteine insertion sequence-binding protein 2. *J Biol Chem*. 2007. 282: 34653–34662
- Bubenik JL, Miniard AC, Driscoll DM. Characterization of the UGA-recoding and SECIS-binding activities of SECIS-binding protein 2. *RNA Biol*. 2014. 11: 1402–1413
- Budiman ME, Bubenik JL, Miniard AC, Middleton LM, Gerber CA, Cash A, Driscoll DM. Eukaryotic initiation factor 4a3 is a selenium-regulated RNA-binding protein that selectively inhibits selenocysteine incorporation. *Mol Cell*. 2009. 35: 479–489
- Caban K, Kinzy SA, Copeland PR. The L7Ae RNA binding motif is a multifunctional domain required for the ribosome-dependent Sec incorporation activity of Sec insertion sequence binding protein 2. *Mol Cell Biol*. 2007. 27: 6350–6360
- Cao JY, Dixon SJ. Mechanisms of ferroptosis. *Cell Mol Life Sci*. 2016. 73: 2195–2209
- Castets P, Bertrand AT, Beuvin M, Ferry A, Le Grand F, Castets M, Chazot G, Rederstorff M, Krol A, Lescure A, Romero NB, Guicheney P, Allamand V. Satellite cell loss and impaired muscle regeneration in selenoprotein N deficiency. *Hum Mol Genet*. 2011. 20: 694–704
- Chavatte L, Brown BA, Driscoll DM. Ribosomal protein L30 is a component of the UGA-selenocysteine recoding machinery in eukaryotes. *Nat Struct Mol Biol*. 2005. 12: 408–416
- Chen LL, Huang JQ, Xiao Y, Wu YY, Ren FZ, Lei XG. Knockout of Selenoprotein V Affects Regulation of Selenoprotein Expression by Dietary Selenium and Fat Intakes in Mice. *J Nutr*. 2020. 150: 483–491
- Cheng WH, Ho YS, Valentine BA, Ross DA, Combs GF, Lei XG. Cellular glutathione peroxidase is the mediator of body selenium to protect against paraquat lethality in transgenic mice. *J Nutr*. 1998. 128: 1070–1076
- Cohen I, Boya P, Zhao L, Métivier D, Andreau K, Perfettini JL, Weaver JG, Badley A, Taylor EW, Kroemer G. Anti-apoptotic activity of the glutathione peroxidase homologue encoded by HIV-1. *Apoptosis*. 2004. 9: 181–192

- Cone JE, Del Río RM, Davis JN, Stadtman TC. Chemical characterization of the selenoprotein component of clostridial glycine reductase: identification of selenocysteine as the organoselenium moiety. *Proc Natl Acad Sci U S A*. 1976. 73: 2659–2663
- Conrad M, Jakupoglu C, Moreno SG, Lippl S, Banjac A, Schneider M, Beck H, Hatzopoulos AK, Just U, Sinowatz F, Schmahl W, Chien KR, Wurst W, Bornkamm GW, Brielmeier M. Essential role for mitochondrial thioredoxin reductase in hematopoiesis, heart development, and heart function. *Mol Cell Biol*. 2004. 24: 9414–9423
- Copeland PR, Fletcher JE, Carlson BA, Hatfield DL, Driscoll DM. A novel RNA binding protein, SBP2, is required for the translation of mammalian selenoprotein mRNAs. *EMBO J*. 2000. 19: 306–314
- Copeland PR, Stepanik VA, Driscoll DM. Insight into mammalian selenocysteine insertion: domain structure and ribosome binding properties of Sec insertion sequence binding protein 2. *Mol Cell Biol*. 2001. 21: 1491–1498
- Cox AG, Tsomides A, Kim AJ, Saunders D, Hwang KL, Evason KJ, Heidel J, Brown KK, Yuan M, Lien EC, Lee BC, Nissim S, Dickinson B, Chhangawala S, Chang CJ, Asara JM, Houvras Y, Gladyshev VN, Goessling W. Selenoprotein H is an essential regulator of redox homeostasis that cooperates with p53 in development and tumorigenesis. *Proc Natl Acad Sci U S A*. 2016. 113: E5562-71
- Curran JE, Jowett JB, Elliott KS, Gao Y, Gluschenko K, Wang J, Abel Azim DM, Cai G, Mahaney MC, Comuzzie AG, Dyer TD, Walder KR, Zimmet P, MacCluer JW, Collier GR, Kissebah AH, Blangero J. Genetic variation in selenoprotein S influences inflammatory response. *Nat Genet*. 2005. 37: 1234–1241
- Dentice M, Marsili A, Zavacki A, Larsen PR, Salvatore D. The deiodinases and the control of intracellular thyroid hormone signaling during cellular differentiation. *Biochim Biophys Acta*. 2013. 1830: 3937–3945
- Dikiy A, Novoselov SV, Fomenko DE, Sengupta A, Carlson BA, Cerny RL, Ginalski K, Grishin NV, Hatfield DL, Gladyshev VN. SelT, SelW, SelH, and Rdx12: genomics and molecular insights into the functions of selenoproteins of a novel thioredoxin-like family. *Biochemistry*. 2007. 46: 6871–6882

- Donovan J, Caban K, Ranaweera R, Gonzalez-Flores JN, Copeland PR. A novel protein domain induces high affinity selenocysteine insertion sequence binding and elongation factor recruitment. *J Biol Chem*. 2008. 283: 35129–35139
- Donovan J, Copeland PR. Threading the needle: getting selenocysteine into proteins. *Antioxid Redox Signal*. 2010. 12: 881–892
- Dumitrescu AM, Liao XH, Abdullah MS, Lado-Abeal J, Majed FA, Moeller LC, Boran G, Schomburg L, Weiss RE, Refetoff S. Mutations in SECISBP2 result in abnormal thyroid hormone metabolism. *Nat Genet*. 2005. 37: 1247–1252
- Fletcher JE, Copeland PR, Driscoll DM, Krol A. The selenocysteine incorporation machinery: interactions between the SECIS RNA and the SECIS-binding protein SBP2. *RNA*. 2001. 7: 1442–1453
- Fomenko DE, Novoselov SV, Natarajan SK, Lee BC, Koc A, Carlson BA, Lee TH, Kim HY, Hatfield DL, Gladyshev VN. MsrB1 (methionine-R-sulfoxide reductase 1) knock-out mice: roles of MsrB1 in redox regulation and identification of a novel selenoprotein form. *J Biol Chem*. 2009. 284: 5986–5993
- Fradejas-Villar N. Consequences of mutations and inborn errors of selenoprotein biosynthesis and functions. *Free Radic Biol Med*. 2018. 127: 206–214
- Fradejas-Villar N, Seeher S, Anderson CB, Doengi M, Carlson BA, Hatfield DL, Schweizer U, Howard MT. The RNA-binding protein Secisbp2 differentially modulates UGA codon reassignment and RNA decay. *Nucleic Acids Res*. 2017. 45: 4094–4107
- Franke KW. A New Toxicant Occurring Naturally in Certain Samples of Plant Foodstuffs. Results Obtained in Preliminary Feeding Trials: Eight Figures. *J Nutr*. 1934. 8: 597–608
- Fu Y, Cheng WH, Porres JM, Ross DA, Lei XG. Knockout of cellular glutathione peroxidase gene renders mice susceptible to diquat-induced oxidative stress. *Free Radic Biol Med*. 1999. 27: 605–611
- Gereben B, Zavacki AM, Ribich S, Kim BW, Huang SA, Simonides WS, Zeöld A, Bianco AC. Cellular and molecular basis of deiodinase-regulated thyroid hormone signaling. *Endocr Rev*. 2008. 29: 898–938

Gladyshev VN. Eukaryotic Selenoproteomes. In: Hatfield DL, Schweizer U, Tsuji PA, Gladyshev VN, eds. *Selenium*. Cham: Springer International Publishing, 2016: 127–140

Gladyshev VN, Arnér ES, Berry MJ, Brigelius-Flohé R, Bruford EA, Burk RF, Carlson BA, Castellano S, Chavatte L, Conrad M, Copeland PR, Diamond AM, Driscoll DM, Ferreira A, Flohé L, Green FR, Guigó R, Handy DE, Hatfield DL, Hesketh J, Hoffmann PR, Holmgren A, Hondal RJ, Howard MT, Huang K, Kim HY, Kim IY, Köhrle J, Krol A, Kryukov GV, Lee BJ, Lee BC, Lei XG, Liu Q, Lescure A, Lobanov AV, Loscalzo J, Maiorino M, Mariotti M, Sandeep Prabhu K, Rayman MP, Rozovsky S, Salinas G, Schmidt EE, Schomburg L, Schweizer U, Simonović M, Sunde RA, Tsuji PA, Tweedie S, Ursini F, Whanger PD, Zhang Y. Selenoprotein Gene Nomenclature. *J Biol Chem*. 2016. 291: 24036–24040

Gladyshev VN, Stadtman TC, Hatfield DL, Jeang KT. Levels of major selenoproteins in T cells decrease during HIV infection and low molecular mass selenium compounds increase. *Proc Natl Acad Sci U S A*. 1999. 96: 835–839

Gong T, Hashimoto AC, Sasuclark AR, Khadka VS, Gurary A, Pitts MW. Selenoprotein M Promotes Hypothalamic Leptin Signaling and Thioredoxin Antioxidant Activity. *Antioxid Redox Signal*. 2019

Gonzalez-Flores JN, Gupta N, DeMong LW, Copeland PR. The selenocysteine-specific elongation factor contains a novel and multi-functional domain. *J Biol Chem*. 2012. 287: 38936–38945

Grundner-Culemann E, Martin GW, Harney JW, Berry MJ. Two distinct SECIS structures capable of directing selenocysteine incorporation in eukaryotes. *RNA*. 1999. 5: 625–635

Guimarães MJ, Peterson D, Vicari A, Cocks BG, Copeland NG, Gilbert DJ, Jenkins NA, Ferrick DA, Kastelein RA, Bazan JF, Zlotnik A. Identification of a novel selD homolog from eukaryotes, bacteria, and archaea: is there an autoregulatory mechanism in selenocysteine metabolism? *Proc Natl Acad Sci U S A*. 1996. 93: 15086–15091

Hamieh A, Cartier D, Abid H, Calas A, Burel C, Bucharles C, Jehan C, Grumolato L, Landry M, Lerouge P, Anouar Y, Lihrmann I. Selenoprotein T is a novel OST subunit that regulates UPR signaling and hormone secretion. *EMBO Rep*. 2017. 18: 1935–1946

- Han SJ, Lee BC, Yim SH, Gladyshev VN, Lee SR. Characterization of mammalian selenoprotein o: a redox-active mitochondrial protein. *PLoS One*. 2014. 9: e95518
- Hatfield DL, Gladyshev VN. How selenium has altered our understanding of the genetic code. *Mol Cell Biol*. 2002. 22: 3565–3576
- Hill KE, Lyons PR, Burk RF. Differential regulation of rat liver selenoprotein mRNAs in selenium deficiency. *Biochem Biophys Res Commun*. 1992. 185: 260–263
- Horibata Y, Elpeleg O, Eran A, Hirabayashi Y, Savitzki D, Tal G, Mandel H, Sugimoto H. EPT1 (selenoprotein I) is critical for the neural development and maintenance of plasmalogen in humans. *J Lipid Res*. 2018. 59: 1015–1026
- Horibata Y, Hirabayashi Y. Identification and characterization of human ethanolaminephosphotransferase1. *J Lipid Res*. 2007. 48: 503–508
- Imai H, Hirao F, Sakamoto T, Sekine K, Mizukura Y, Saito M, Kitamoto T, Hayasaka M, Hanaoka K, Nakagawa Y. Early embryonic lethality caused by targeted disruption of the mouse PHGPx gene. *Biochem Biophys Res Commun*. 2003. 305: 278–286
- Jurynek MJ, Xia R, Mackrill JJ, Gunther D, Crawford T, Flanigan KM, Abramson JJ, Howard MT, Grunwald DJ. Selenoprotein N is required for ryanodine receptor calcium release channel activity in human and zebrafish muscle. *Proc Natl Acad Sci U S A*. 2008. 105: 12485–12490
- Korotkov KV, Novoselov SV, Hatfield DL, Gladyshev VN. Mammalian selenoprotein in which selenocysteine (Sec) incorporation is supported by a new form of Sec insertion sequence element. *Mol Cell Biol*. 2002. 22: 1402–1411
- Kryukov GV, Castellano S, Novoselov SV, Lobanov AV, Zehtab O, Guigó R, Gladyshev VN. Characterization of mammalian selenoproteomes. *Science*. 2003. 300: 1439–1443
- Kryukov GV, Kumar RA, Koc A, Sun Z, Gladyshev VN. Selenoprotein R is a zinc-containing stereo-specific methionine sulfoxide reductase. *Proc Natl Acad Sci U S A*. 2002. 99: 4245–4250

Labunskyy VM, Hatfield DL, Gladyshev VN. The Sep15 protein family: roles in disulfide bond formation and quality control in the endoplasmic reticulum. *IUBMB Life*. 2007. 59: 1–5

Labunskyy VM, Hatfield DL, Gladyshev VN. Selenoproteins: molecular pathways and physiological roles. *Physiol Rev*. 2014. 94: 739–777

Lee BC, Péterfi Z, Hoffmann FW, Moore RE, Kaya A, Avanesov A, Tarrago L, Zhou Y, Weerapana E, Fomenko DE, Hoffmann PR, Gladyshev VN. MsrB1 and MICALs regulate actin assembly and macrophage function via reversible stereoselective methionine oxidation. *Mol Cell*. 2013. 51: 397–404

Lee BJ, Worland PJ, Davis JN, Stadtman TC, Hatfield DL. Identification of a selenocysteyl-tRNA(Ser) in mammalian cells that recognizes the nonsense codon, UGA. *J Biol Chem*. 1989. 264: 9724–9727

Lei XG, Evenson JK, Thompson KM, Sunde RA. Glutathione peroxidase and phospholipid hydroperoxide glutathione peroxidase are differentially regulated in rats by dietary selenium. *J Nutr*. 1995. 125: 1438–1446

Leinfelder W, Stadtman TC, Böck A. Occurrence in vivo of selenocysteyl-tRNA(SERUCA) in *Escherichia coli*. Effect of sel mutations. *J Biol Chem*. 1989. 264: 9720–9723

Li F, Mao A, Fu X, She Y, Wei X. Correlation between SEPS1 gene polymorphism and type 2 diabetes mellitus: A preliminary study. *J Clin Lab Anal*. 2019. 33: e22967

Lobanov AV, Hatfield DL, Gladyshev VN. Selenoproteinless animals: selenophosphate synthetase SPS1 functions in a pathway unrelated to selenocysteine biosynthesis. *Protein Sci*. 2008. 17: 176–182

Lubos E, Loscalzo J, Handy DE. Glutathione peroxidase-1 in health and disease: from molecular mechanisms to therapeutic opportunities. *Antioxid Redox Signal*. 2011. 15: 1957–1997

Maiorino M, Roveri A, Benazzi L, Bosello V, Mauri P, Toppo S, Tosatto SC, Ursini F. Functional interaction of phospholipid hydroperoxide glutathione peroxidase with sperm

- mitochondrion-associated cysteine-rich protein discloses the adjacent cysteine motif as a new substrate of the selenoperoxidase. *J Biol Chem.* 2005. 280: 38395–38402
- Marino M, Stoilova T, Giorgi C, Bachi A, Cattaneo A, Auricchio A, Pinton P, Zito E. SEP1, an endoplasmic reticulum-localized selenoprotein linked to skeletal muscle pathology, counteracts hyperoxidation by means of redox-regulating SERCA2 pump activity. *Hum Mol Genet.* 2015. 24: 1843–1855
- Matsumura S, Ikawa Y, Inoue T. Biochemical characterization of the kink-turn RNA motif. *Nucleic Acids Res.* 2003. 31: 5544–5551
- Mehta A, Rebsch CM, Kinzy SA, Fletcher JE, Copeland PR. Efficiency of mammalian selenocysteine incorporation. *J Biol Chem.* 2004. 279: 37852–37859
- Miniard AC, Middleton LM, Budiman ME, Gerber CA, Driscoll DM. Nucleolin binds to a subset of selenoprotein mRNAs and regulates their expression. *Nucleic Acids Res.* 2010. 38: 4807–4820
- Papp LV, Lu J, Striebel F, Kennedy D, Holmgren A, Khanna KK. The redox state of SECIS binding protein 2 controls its localization and selenocysteine incorporation function. *Mol Cell Biol.* 2006. 26: 4895–4910
- Petit N, Lescure A, Rederstorff M, Krol A, Moghadaszadeh B, Wewer UM, Guicheney P. Selenoprotein N: an endoplasmic reticulum glycoprotein with an early developmental expression pattern. *Hum Mol Genet.* 2003. 12: 1045–1053
- PINSENT J. The need for selenite and molybdate in the formation of formic dehydrogenase by members of the coli-aerogenes group of bacteria. *Biochem J.* 1954. 57: 10–16
- Ramanathan CS, Taylor EW. Computational genomic analysis of hemorrhagic fever viruses. Viral selenoproteins as a potential factor in pathogenesis. *Biol Trace Elem Res.* 1997. 56: 93–106
- Ren B, Liu M, Ni J, Tian J. Role of Selenoprotein F in Protein Folding and Secretion: Potential Involvement in Human Disease. *Nutrients.* 2018. 10

Saberi M, Sterling FH, Utiger RD. Reduction in extrathyroidal triiodothyronine production by propylthiouracil in man. *J Clin Invest.* 1975. 55: 218–223

Saitoh M, Nishitoh H, Fujii M, Takeda K, Tobiume K, Sawada Y, Kawabata M, Miyazono K, Ichijo H. Mammalian thioredoxin is a direct inhibitor of apoptosis signal-regulating kinase (ASK) 1. *EMBO J.* 1998. 17: 2596–2606

Schnurr K, Belkner J, Ursini F, Schewe T, Kühn H. The selenoenzyme phospholipid hydroperoxide glutathione peroxidase controls the activity of the 15-lipoxygenase with complex substrates and preserves the specificity of the oxygenation products. *J Biol Chem.* 1996. 271: 4653–4658

Schoenmakers E, Agostini M, Mitchell C, Schoenmakers N, Papp L, Rajanayagam O, Padidela R, Ceron-Gutierrez L, Doffinger R, Prevosto C, Luan J, Montano S, Lu J, Castanet M, Clemons N, Groeneveld M, Castets P, Karbaschi M, Aitken S, Dixon A, Williams J, Campi I, Blount M, Burton H, Muntoni F, O'Donovan D, Dean A, Warren A, Brierley C, Baguley D, Guicheney P, Fitzgerald R, Coles A, Gaston H, Todd P, Holmgren A, Khanna KK, Cooke M, Semple R, Halsall D, Wareham N, Schwabe J, Grasso L, Beck-Peccoz P, Ogunko A, Dattani M, Gurnell M, Chatterjee K. Mutations in the selenocysteine insertion sequence-binding protein 2 gene lead to a multisystem selenoprotein deficiency disorder in humans. *J Clin Invest.* 2010. 120: 4220–4235

Schoenmakers E, Chatterjee K. Human disorders affecting the selenocysteine incorporation pathway cause systemic selenoprotein deficiency. *Antioxid Redox Signal.* 2020

Schomburg L, Schweizer U, Holtmann B, Flohé L, Sendtner M, Köhrle J. Gene disruption discloses role of selenoprotein P in selenium delivery to target tissues. *Biochem J.* 2003. 370: 397–402

Schwarz K, Foltz CM. SELENIUM AS AN INTEGRAL PART OF FACTOR 3 AGAINST DIETARY NECROTIC LIVER DEGENERATION. *Journal of the American Chemical Society.* 1957. 79: 3292–3293

Schweizer U, Bohleber S, Fradejas-Villar N. The modified base isopentenyladenosine and its derivatives in tRNA. *RNA Biol.* 2017. 14: 1197–1208

- Schweizer U, Fradejas-Villar N. Why 21? The significance of selenoproteins for human health revealed by inborn errors of metabolism. *FASEB J*. 2016. 30: 3669–3681
- Seeher S, Atassi T, Mahdi Y, Carlson BA, Braun D, Wirth EK, Klein MO, Reix N, Miniard AC, Schomburg L, Hatfield DL, Driscoll DM, Schweizer U. Secisbp2 is essential for embryonic development and enhances selenoprotein expression. *Antioxid Redox Signal*. 2014. 21: 835–849
- Shchedrina VA, Everley RA, Zhang Y, Gygi SP, Hatfield DL, Gladyshev VN. Selenoprotein K binds multiprotein complexes and is involved in the regulation of endoplasmic reticulum homeostasis. *J Biol Chem*. 2011. 286: 42937–42948
- Shisler JL, Senkevich TG, Berry MJ, Moss B. Ultraviolet-induced cell death blocked by a selenoprotein from a human dermatotropic poxvirus. *Science*. 1998. 279: 102–105
- Squires JE, Stoytchev I, Forry EP, Berry MJ. SBP2 binding affinity is a major determinant in differential selenoprotein mRNA translation and sensitivity to nonsense-mediated decay. *Mol Cell Biol*. 2007. 27: 7848–7855
- Su D, Novoselov SV, Sun QA, Moustafa ME, Zhou Y, Oko R, Hatfield DL, Gladyshev VN. Mammalian selenoprotein thioredoxin-glutathione reductase. Roles in disulfide bond formation and sperm maturation. *J Biol Chem*. 2005. 280: 26491–26498
- Sun QA, Kirnarsky L, Sherman S, Gladyshev VN. Selenoprotein oxidoreductase with specificity for thioredoxin and glutathione systems. *Proc Natl Acad Sci U S A*. 2001. 98: 3673–3678
- Sunde RA, Raines AM. Selenium regulation of the selenoprotein and nonselenoprotein transcriptomes in rodents. *Adv Nutr*. 2011. 2: 138–150
- Sunde RA, Raines AM, Barnes KM, Evenson JK. Selenium status highly regulates selenoprotein mRNA levels for only a subset of the selenoproteins in the selenoproteome. *Biosci Rep*. 2009. 29: 329–338
- Sung YH, Baek IJ, Kim DH, Jeon J, Lee J, Lee K, Jeong D, Kim JS, Lee HW. Knockout mice created by TALEN-mediated gene targeting. *Nat Biotechnol*. 2013. 31: 23–24

Taylor EW, Bhat A, Nadimpalli RG, Zhang W, Kececioglu J. HIV-1 encodes a sequence overlapping env gp41 with highly significant similarity to selenium-dependent glutathione peroxidases. *J Acquir Immune Defic Syndr Hum Retrovirol.* 1997a. 15: 393–394

Taylor EW, Nadimpalli RG, Ramanathan CS. Genomic structures of viral agents in relation to the biosynthesis of selenoproteins. *Biol Trace Elem Res.* 1997b. 56: 63–91

Taylor EW, Ramanathan CS, Jalluri RK, Nadimpalli RG. A basis for new approaches to the chemotherapy of AIDS: novel genes in HIV-1 potentially encode selenoproteins expressed by ribosomal frameshifting and termination suppression. *J Med Chem.* 1994. 37: 2637–2654

Taylor EW, Ruzicka JA, Premadasa L, Zhao L. Cellular Selenoprotein mRNA Tethering via Antisense Interactions with Ebola and HIV-1 mRNAs May Impact Host Selenium Biochemistry. *Curr Top Med Chem.* 2016. 16: 1530–1535

Tujebajeva RM, Copeland PR, Xu XM, Carlson BA, Harney JW, Driscoll DM, Hatfield DL, Berry MJ. Decoding apparatus for eukaryotic selenocysteine insertion. *EMBO Rep.* 2000. 1: 158–163

Ursini F, Heim S, Kiess M, Maiorino M, Roveri A, Wissing J, Flohé L. Dual function of the selenoprotein PHGPx during sperm maturation. *Science.* 1999. 285: 1393–1396

Walczak R, Westhof E, Carbon P, Krol A. A novel RNA structural motif in the selenocysteine insertion element of eukaryotic selenoprotein mRNAs. *RNA.* 1996. 2: 367–379

Westendorp MO, Shatrov VA, Schulze-Osthoff K, Frank R, Kraft M, Los M, Krammer PH, Dröge W, Lehmann V. HIV-1 Tat potentiates TNF-induced NF-kappa B activation and cytotoxicity by altering the cellular redox state. *EMBO J.* 1995. 14: 546–554

Wu R, Shen Q, Newburger PE. Recognition and binding of the human selenocysteine insertion sequence by nucleolin. *J Cell Biochem.* 2000. 77: 507–516

Xu XM, Carlson BA, Mix H, Zhang Y, Saira K, Glass RS, Berry MJ, Gladyshev VN, Hatfield DL. Biosynthesis of selenocysteine on its tRNA in eukaryotes. *PLoS Biol.* 2007. 5: e4

- Xu XM, Carlson BA, Irons R, Mix H, Zhong N, Gladyshev VN, Hatfield DL. Selenophosphate synthetase 2 is essential for selenoprotein biosynthesis. *Biochem J*. 2007. 404: 115–120
- Yang GQ, Ge KY, Chen JS, Chen XS. Selenium-related endemic diseases and the daily selenium requirement of humans. *World Rev Nutr Diet*. 1988. 55: 98–152
- Yant LJ, Ran Q, Rao L, van Remmen H, Shibatani T, Belter JG, Motta L, Richardson A, Prolla TA. The selenoprotein GPX4 is essential for mouse development and protects from radiation and oxidative damage insults. *Free Radic Biol Med*. 2003. 34: 496–502
- Ye Y, Shibata Y, Yun C, Ron D, Rapoport TA. A membrane protein complex mediates retro-translocation from the ER lumen into the cytosol. *Nature*. 2004. 429: 841–847
- Zhao W, Bohleber S, Schmidt H, Seeher S, Howard MT, Braun D, Arndt S, Reuter U, Wende H, Birchmeier C, Fradejas-Villar N, Schweizer U. Ribosome profiling of selenoproteins. *J Biol Chem*. 2019. 294: 14185–14200
- Zhao L, Cox AG, Ruzicka JA, Bhat AA, Zhang W, Taylor EW. Molecular modeling and in vitro activity of an HIV-1-encoded glutathione peroxidase. *Proc Natl Acad Sci U S A*. 2000. 97: 6356–6361
- Zhao L, Olubajo B, Taylor EW. Functional studies of an HIV-1 encoded glutathione peroxidase. *Biofactors*. 2006. 27: 93–107

9. Acknowledgements

First of all, I would like to thank Ulrich Schweizer for giving me the opportunity of doing this thesis in his lab and creating such a nice atmosphere within our workgroup. Furthermore, I want to thank Noelia Fradejas Villar for teaching me a lot about laboratory work, always having a friendly ear for my questions, granting me a credit for all the times I did not have the 500 € on the spot and becoming a friend of mine.

I also want to thank all the other members of our workgroup, Simon Bohleber, Doreen Braun, Uschi Reuter, Alfonso Rodrigues Ruiz and Wenchao Zhao for all the help, the friendly chats, walks to the Mensa, funny staff outings, LAN-parties and the overall good time. I am glad that I worked in a lab with so many colleagues that became friends.

I want to thank my friends and my family for their ongoing support, all the laughter and good times together. Having you made this work a whole lot easier.

Lastly, I would like to thank the BONFOR programme for supporting me and this work.